

Contents

17 Local Moments and the Kondo effect.	<i>page</i> 2
17.1 Strongly Correlated Electrons	2
17.2 Anderson's Model of Local Moment Formation	5
17.3 The Coulomb Blockade: local moments in quantum dots	18
17.4 The Kondo Effect	20
17.5 Renormalization concept	25
17.6 Schrieffer-Wolff transformation	29
17.7 "Poor Man" Scaling	35
17.8 Nozières Fermi Liquid Theory	48
17.9 Multi-channel Kondo physics and Non-Fermi liquids	55
Exercises	56
<i>References</i>	60
<i>References</i>	63

17.1 Strongly Correlated Electrons

One of the fascinating growth areas in condensed matter physics concerns “strongly correlated systems”: states of matter in which the many body interaction energies dominate the kinetic energies, becoming large enough to qualitatively transform the macroscopic properties of the medium. Some of the growing list of strongly correlated systems include

- **Cuprate superconductors**, where interactions amongst electrons in localized 3d-shells form an antiferromagnetic “Mott” insulator, which develops high temperature superconductivity when doped.
- **Heavy electron compounds**, in which localized magnetic moments immersed within the metal give rise to electron quasiparticles with effective masses in excess of 1000 bare electron masses.
- **Fractional Quantum Hall systems**, where strong interactions in the lowest Landau level of a two-dimensional electron fluid generate an incompressible state with quasiparticles of fractional charge and statistics.
- **Quantum Dots**, which are tiny pools of electrons in semiconductors that act as artificial atoms. As the gate voltage is changed, the electron repulsion in the dot causes a “Coulomb Blockade”, whereby electrons can only be added one by one to the quantum dot.
- **Cold atomic gases**, in which the interactions between the neutral atoms governed by two-body resonances, can be magnetically tuned to create a whole new world of strongly correlated quantum fluids.

In each case, the electron system has been tuned - by electronic or nuclear chemistry, by geometry or nanofabrication, to give rise to a quantum state with novel collective properties, in which the interactions between the particles are large compared with their kinetic energies. The next two chapters will introduce one corner of this field: the physics of local moments and heavy fermion compounds. A large class of strongly correlated materials contain atoms with partially filled d, or f orbitals. Heavy electron materials are an extreme example, in which one component of the electron fluid is highly localized, usually inside f-orbitals giving rise to the formation of magnetic moments. The interaction of localized magnetic moments with the conduction sea provides the driving force for the strongly correlated electron physics in these materials.

Within the periodic table, there are broad trends that govern strongly correlated electron behavior. The most strongly interacting electrons tend to reside in partially filled orbitals that are well-localized around the nucleus. The weak overlap between orbitals of neighboring atoms promotes the formation of narrow electron bands, while the interactions between electrons in the highly localized orbitals are strong.

In order of increasing degree of localization, the unfilled electron orbitals of the central rows of the periodic table may be ordered

$$5d < 4d < 3d < 5f < 4f.$$

There are two trends operating here: first, orbitals with higher principle quantum numbers contain more radial nodes and tend to be more delocalized, so that $5d < 4d < 3d$ and $5f < 4f$. Second, as we move from d to f orbitals, or along a row of the periodic table, the increased nuclear charge pulls the orbitals towards the nucleus. These trends are summarized in the Kmetko-Smith diagram in Fig 17.1, in which the central rows of the periodic table are stacked in order of increasing localization. Moving up and to the right in this diagram leads to increasingly localized atoms. In metals lying on the bottom-left hand side of this diagram, the d-orbitals are highly itinerant giving rise to the metals exhibit conventional superconductivity at low temperatures. By contrast, in metals towards the top right hand side of the diagram, the electrons in the rare earth or actinide ions are localized, forming magnets, or more typically, antiferromagnets.

The materials that lie in the cross-over between these two regions are particularly interesting, for these materials are “on the brink of magnetism”. With some exceptions, it is in this region that the the cerium and uranium heavy fermion materials, and the iron based superconductors are found.

17.1.1 Local moments

To understand heavy electron materials, we need to understand how electrons localize to form magnetic moments, and how these local moments interact with the conduction sea of electrons. The simplest example of a localized moment is an unpaired electron bound in an isolated atom, or ion (17.2 (a)). At temperatures far below the ionization energy $|E_f|$, the only remaining degree of freedom of this localized electron is its magnetic moment, described by the operator

$$\vec{M} = \mu_B \vec{\sigma}$$

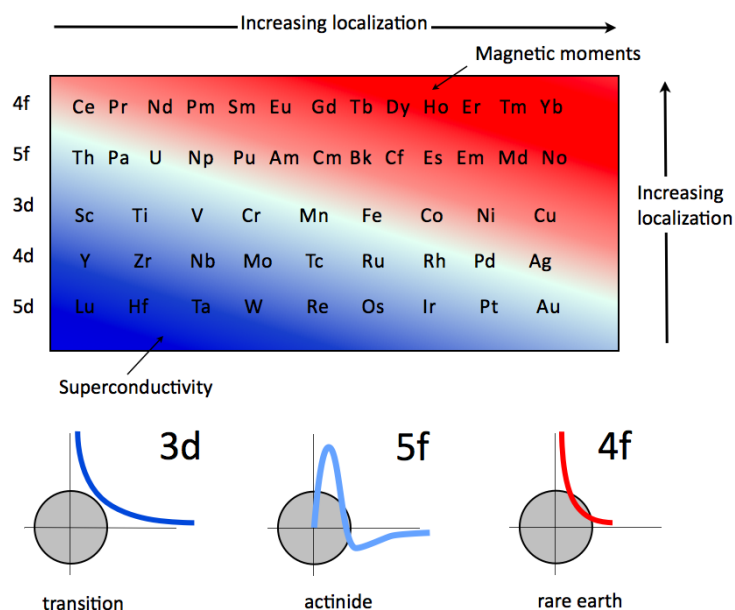


Fig. 17.1 The Kmetko-Smith diagram, showing the broad trends towards increasing electron localization in the d- and f-electron compounds.

where $\vec{\sigma}$ denotes the Pauli matrices and $\mu_B = \frac{e\hbar}{2m}$ is the Bohr magneton. In a magnetic field, the Hamiltonian describing low energy physics is simply $H = -\vec{M} \cdot \vec{B} = -\mu_B \vec{\sigma} \cdot \vec{B}$, giving rise to a “Curie” susceptibility

$$\chi(T) = \frac{\partial M}{\partial B} = -\frac{\partial^2 F}{\partial B^2} = \frac{\mu_B^2}{T}$$

The classic signature of local moments is the appearance of Curie paramagnetism with a high-temperature magnetic susceptibility of the form

$$\chi \approx n_i \frac{M^2}{3(T + \theta)} \quad M^2 = g^2 \mu_B^2 J(J + 1), \quad (17.1)$$

where, n_i is the concentration of magnetic moments while M is the magnetic moment with total angular momentum quantum number J and gyro-magnetic ratio (“g-factor”) g . θ is the “Curie Weiss” temperature, a phenomenological scale which takes account of interactions between spins¹. For a pure spin, $J = S$ is the total spin and $g = 2$, but for rare earth and actinide ions, the orbital and spin angular momentum combine into a single entity with angular momentum $\vec{J} = \vec{L} + \vec{S}$ for which g lies between one and two. For example, a Ce^{3+} ion contains a single unpaired 4f-electron in the state $4f^1$, with $l = 3$ and $s = 1/2$. Spin-orbit coupling gives rise to low-lying multiplet with $j = 3 - \frac{1}{2} = \frac{5}{2}$, consisting of $2j + 1 = 6$ degenerate orbitals $|4f^1 : Jm\rangle$, ($m_J \in [-\frac{5}{2}, \frac{5}{2}]$) with an associated magnetic moment $M = 2.64\mu_B$.

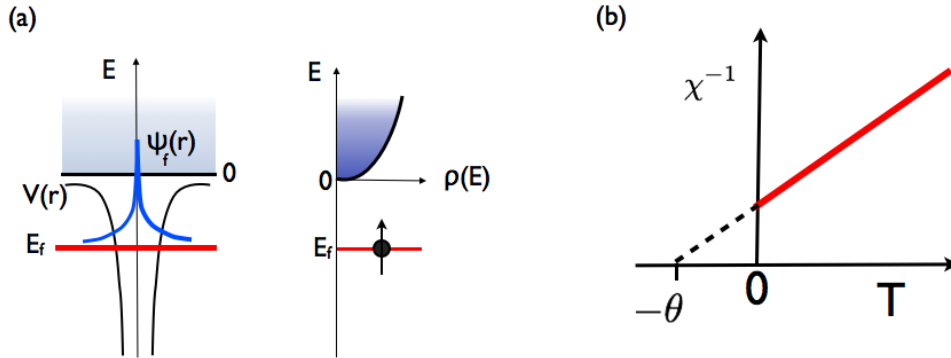


Fig. 17.2

(a) In isolation, the localized atomic states of an atom form a stable, sharp excitation lying below the continuum. (b) The inverse of the Curie-Weiss susceptibility of local moments χ^{-1} is a linear function of temperature, intersecting zero at $T = -\theta$.

Though the concept of localized moments was employed in the earliest applications of quantum theory to condensed matter², a theoretical understanding of the *mechanism* of moment formation did not develop

¹ A positive $\theta > 0$ indicates an antiferromagnetic interaction between spins, while a negative $\theta < 0$ is associated with ferromagnetic interactions, giving rise to a divergence of the susceptibility at the Curie temperature $T_c = -\theta$.

² The concept of a local moment appears in Heisenberg's original paper on ferromagnetism[1]. Landau and Néel invoked the notion of the localized moment in their 1932 papers on antiferromagnetism, and in 1933, Kramers used this idea again in his theory of magnetic superexchange.

until the early sixties, when experimentalists began to systematically study impurities in metals.³ In the early 1960s, Clogston, Mathias and collaborators[2] showed that when small concentrations n_i of magnetic ions, such as iron are added to a metallic host, they do not always form magnetic moments. For example, iron impurities in pure niobium do not develop a local moment, but they do so in the niobium-molybdenum alloy, $Nb_{1-x}Mo_x$ once the concentration of molybdenum exceeds 40% ($x > 0.4$). It was these observations that led Anderson to develop his model for local moment formation.

17.2 Anderson's Model of Local Moment Formation

Anderson's model for moment formation, proposed in 1963, combines two essential ideas[3]:

- the localizing influence of Coulomb interactions. Peierls and Mott [4, 5] had reasoned in the 1940s that strong-enough Coulomb repulsion between electrons in an atomic state would blockade the passage of electrons, converting a metal into what is now called a “Mott insulator”. These ideas were independently explored by Van Vleck and Hurvitz in an early attempt to understand magnetic ions in metals[6].
- the formation of an electronic resonance. In the 1950's Friedel and Blandin [7, 8, 9] proposed that electrons in the core states of magnetic atoms tunnel out into the conduction sea, forming a resonance.

Anderson unified these ideas in a second-quantized Hamiltonian

$$H = \sum_{\mathbf{k}, \sigma} \epsilon_{\mathbf{k}} n_{\mathbf{k}\sigma} + \overbrace{\sum_{\mathbf{k}, \sigma} [V(\mathbf{k}) c_{\mathbf{k}\sigma}^\dagger f_\sigma + V^*(\mathbf{k}) f_\sigma^\dagger c_{\mathbf{k}\sigma}]}^{H_{\text{resonance}}} \underbrace{[E_f n_f + U n_{f\uparrow} n_{f\downarrow}]}_{H_{\text{atomic}}}, \quad (17.2)$$

Anderson model.

where H_{atomic} describes the atomic limit of an isolated magnetic ion containing a Kramer's doublet of energy E_f . The engine of magnetism in the Anderson model is the Coulomb interaction

$$U = \frac{e^2}{4\pi\epsilon_0} \int_{\mathbf{r}, \mathbf{r}'} \frac{1}{|\mathbf{r} - \mathbf{r}'|} \rho_f(\mathbf{r}) \rho_f(\mathbf{r}')$$

of a doubly occupied f-state, where $\rho_f(\mathbf{r}) = |\Psi_f(\mathbf{r})|^2$ is the electron density in a single atomic orbital $\psi_f(\mathbf{r})$. The operator $c_{\mathbf{k}\sigma}^\dagger$ creates a conduction electron of momentum \mathbf{k} , spin σ and energy $\epsilon_{\mathbf{k}} = E_{\mathbf{k}} - \mu$, while

$$f_\sigma^\dagger = \int_{\mathbf{r}} \Psi_f(\mathbf{r}) \hat{\psi}_\sigma^\dagger(r), \quad (17.3)$$

creates an f-electron in the atomic f-state. Unlike the electron continuum in a vacuum, a conduction band in a metal has a finite energy width, so in the model, the energies are taken lying in the range $\epsilon_{\mathbf{k}} \in [-D, D]$.

³ It was not until the sixties that materials physicists could control the concentration of magnetic impurities in the parts per million range required for the study of individual impurities. The control of purity evolved during the 1950s, with the development of new techniques needed for semiconductor physics, such as zone refining.

$H_{resonance}$ describes the hybridization with the Bloch waves of the conduction sea that develops when the ion is immersed in a metal. The quantity

$$V(\mathbf{k}) = \langle \mathbf{k} | V_{ion} | f \rangle = \int d^3 r e^{-i\mathbf{k} \cdot \mathbf{r}} V_{ion}(r) \Psi_f(\vec{r}). \quad (17.4)$$

is the hybridization between the ionic potential and a plane wave. This term is the result of applying first order perturbation theory to the degenerate states of the conduction sea and the atomic f-orbital.

17.2.1 A competition between localization and hybridization.

To understand the formation and properties of local moments, we need to examine the two limiting types of behaviour in the Anderson model:

- Localized moment behavior, described by the limiting case where the hybridization vanishes.
- Virtual bound-state formation, described by the limiting case where the interaction is negligible.

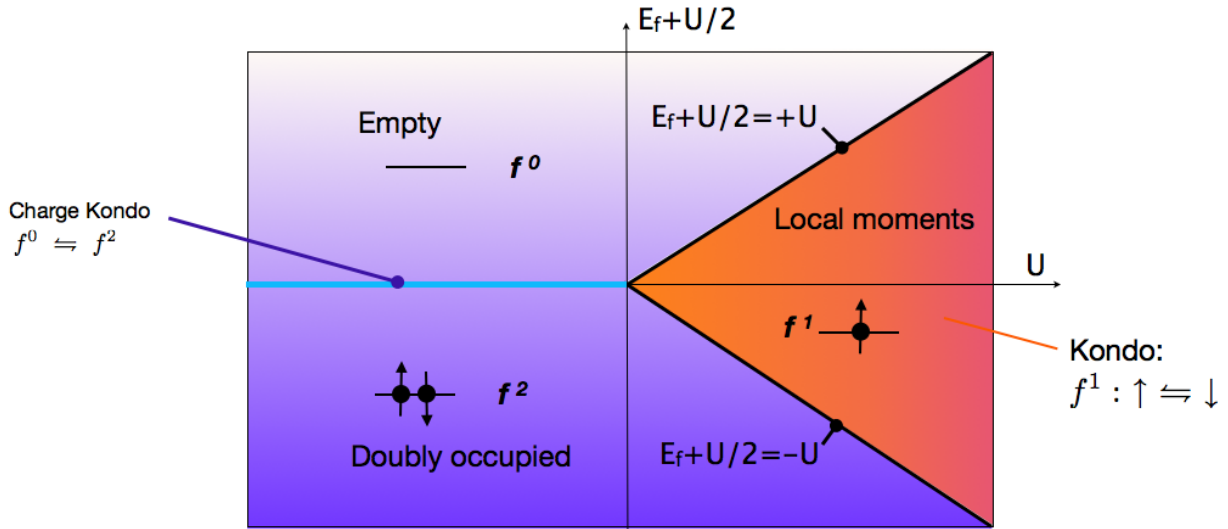


Fig. 17.3

Phase diagram for Anderson impurity model in the atomic limit. For $U > |E_f + U/2|$, the ground-state is a magnetic doublet. When $U < 0$, the ground-state is degenerate charge doublet provided $E_f + U/2 = 0$.

17.2.2 The Atomic limit.

The atomic physics of an isolated ion, described by

$$H_{atomic} = E_f n_f + U n_{f\uparrow} n_{f\downarrow}. \quad (17.5)$$

is the engine at the heart of the Anderson model that drives moment formation. The four atomic quantum states are

$$\left. \begin{array}{l} |f^2\rangle \\ |f^0\rangle \end{array} \right\} \begin{array}{l} E(f^2) = 2E_f + U \\ E(f^0) = 0 \end{array} \quad \text{non-magnetic} \quad (17.6)$$

$$|f^1 \uparrow\rangle, |f^1 \downarrow\rangle \quad E(f^1) = E_f. \quad \text{magnetic.}$$

The cost of adding or removing to the magnetic f^1 state is given by

$$\left. \begin{array}{l} \text{adding: } E(f^2) - E(f^1) = U + E_f \\ \text{removing: } E(f^0) - E(f^1) = -E_f \end{array} \right\} \Rightarrow \Delta E = \frac{U}{2} \pm (E_f + \frac{U}{2}) \quad (17.7)$$

In other words, provided (Fig. 17.3)

$$U/2 > |E_f + U/2| \quad (17.8)$$

the ground-state of the atom is a two-fold degenerate magnetic doublet. Indeed, provided it is probed at energies below the smallest charge excitation energy, $\Delta E_{\min} = U/2 - |E_f + U/2|$, only the spin degrees of freedom remain, and the system behaves as a local moment - a “quantum top”. The interaction between such a local moment and the conduction sea gives rise to the “Kondo effect” that will be the main topic of this chapter.

Although we shall be mainly interested in positive, repulsive U , we note that in the attractive region of the phase diagram ($U < 0$) the atomic ground-state can form a degenerate “charge” doublet ($|f^0\rangle, |f^2\rangle$) or “isospin”. For $U < 0$, when $E_f + U/2 = 0$ the doubly occupied state $|f^2\rangle$ and the empty state $|f^0\rangle$ become degenerate. This is the charge analog of the magnetic doublet that exists for $U > 0$, and when coupled to the sea of electrons, gives rise to an effect known as the “charge Kondo effect”. Such charge doublets are thought to be important in certain “negative U ” materials, such as *Tl* doped *PbTe*.

Example 17.1: Derivation of the non-interacting Anderson model

Consider an isolated ion, where the f-state is a solution of the one-particle Schrödinger equation

$$[-\nabla^2 + \hat{V}_{ion}] |f\rangle = E_f^{ion} |f\rangle, \quad (17.9)$$

where $V_{ion}(r)$ is the ionic potential and $E_f^{ion} < 0$ is the energy of the atomic f-level. In a metal, the positive ionic background draws the continuum downwards to become degenerate with the f-level as shown in Fig. 17.4. A convenient way to model this situation is to use “muffin tin potential”,⁴

$$V(r) = (V_{ion}(r) + W) \theta(R_0 - r) \quad (17.10)$$

equal to the ionic potential, shifted upwards by an amount W inside the muffin tin radius R_0 . The f-state is now an approximate eigenstate of $\mathcal{H} = -\nabla^2 + \hat{V}$ that is degenerate with the continuum.

Derive the non-interacting component of the Anderson model using degenerate perturbation theory, evaluating the matrix elements of \mathcal{H} between the conduction states $|\mathbf{k}\rangle$ and the local f-state $|f\rangle$. You may assume that the muffin tin R_0 is much smaller than the Fermi wavelength, so that the conduction electron matrix elements $V_{\mathbf{k},\mathbf{k}'} = \langle \mathbf{k} | V | \mathbf{k}' \rangle$ are negligible.

Solution:

To carry out degenerate perturbation theory we must first orthogonalize the f-state to the continuum

$|\tilde{f}\rangle = |f\rangle - \sum_{\mathbf{k} \in [-D, D]} |\mathbf{k}\rangle \langle \mathbf{k}|f\rangle$, where D is the conduction electron band-width. Now we need to evaluate the matrix elements of $\mathcal{H} = -\nabla^2 + V$. If we set

$$V_{\mathbf{k}, \mathbf{k}'} = \int_{r < R_0} d^3r e^{i(\mathbf{k}' - \mathbf{k}) \cdot \mathbf{r}} (V_{ion}(r) + W), \quad (17.11)$$

then the conduction electron matrix elements are

$$\langle \mathbf{k} | \mathcal{H} | \mathbf{k}' \rangle = E_{\mathbf{k}} \delta_{\mathbf{k}, \mathbf{k}'} + V_{\mathbf{k}, \mathbf{k}'} \approx E_{\mathbf{k}} \delta_{\mathbf{k}, \mathbf{k}'} \quad (17.12)$$

while $\langle \tilde{f} | \mathcal{H} | \tilde{f} \rangle \approx E_f^{ion}$ is the f-level energy.

The hybridization is given by the off-diagonal matrix element,

$$V(\mathbf{k}) = \langle \mathbf{k} | \mathcal{H} | \tilde{f} \rangle = \langle \mathbf{k} | -\nabla^2 + \hat{V} | \tilde{f} \rangle = E_{\mathbf{k}} \langle \mathbf{k} | \tilde{f} \rangle + \langle \mathbf{k} | \hat{V} | \tilde{f} \rangle = \langle \mathbf{k} | \hat{V} | \tilde{f} \rangle, \quad (17.13)$$

where we have used the orthogonality $\langle \mathbf{k} | \tilde{f} \rangle = 0$ to eliminate the kinetic energy. Infact, since the f-state is highly localized, its overlap with the conduction electron states is small $\langle \mathbf{k} | f \rangle \approx 0$, so we can now drop the tilde, approximating $\langle \mathbf{k} | \hat{V} | \tilde{f} \rangle \approx \langle \mathbf{k} | \hat{V}_{ion} + W | f \rangle \approx \langle \mathbf{k} | \hat{V}_{ion} | f \rangle$, so that

$$V(\mathbf{k}) \approx \langle \mathbf{k} | V_{ion} | f \rangle = \int d^3r e^{-i\mathbf{k} \cdot \mathbf{r}} V_{ion}(r) \psi_f(\mathbf{r}). \quad (17.14)$$

In this way, the only surviving term contributing to the hybridization is the atomic potential - only this term has the high-momentum Fourier components to create a significant overlap between the low-momentum conduction electrons and the localized f-state. Putting these results together, the non-interacting Anderson model can then be written

$$\hat{H}_{resonance} = \sum_{\mathbf{k}} \overbrace{(E_{\mathbf{k}} + W - \mu)}^{\epsilon_{\mathbf{k}}} c_{\mathbf{k}\sigma}^\dagger c_{\mathbf{k}\sigma} + \sum_{\mathbf{k}\sigma} (V(\mathbf{k}) c_{\mathbf{k}\sigma}^\dagger f_\sigma + \text{H.c.}) + \overbrace{(E_f^{ion} - \mu)}^{E_f} n_f.$$

17.2.3 Virtual bound-state formation: the non-interacting resonance.

When the magnetic ion is immersed in a sea of electrons, the f-electrons within the core of the atom can tunnel out, hybridizing with the Bloch states of surrounding electron sea [9] as shown in Fig. 17.4.

In the absence of interactions, this physics is described by

$$H_{resonance} = \sum_{\mathbf{k}, \sigma} \epsilon_{\mathbf{k}} n_{\mathbf{k}\sigma} + \sum_{\mathbf{k}\sigma} [V(\mathbf{k}) c_{\mathbf{k}\sigma}^\dagger f_\sigma + \text{H.c.}] + E_f n_f, \quad (17.15)$$

where $c_{\mathbf{k}\sigma}^\dagger$ creates an electron of momentum \mathbf{k} , spin σ and energy $\epsilon_{\mathbf{k}} = E_{\mathbf{k}} - \mu$ in the conduction band. The hybridization broadens the localized f-state, and in the absence of interactions, gives rise to a resonance of width Δ given by Fermi's Golden Rule.

$$\Delta = \pi \sum_{\vec{k}} |V(\mathbf{k})|^2 \delta(\epsilon_{\mathbf{k}} - E_f) \quad (17.16)$$

This is really an average of the density of states $\rho(\epsilon) = \sum_{\mathbf{k}} \delta(\omega - \epsilon_{\mathbf{k}})$ with the hybridization $|V(\mathbf{k})|^2$. For future reference, we shall define

$$\Delta(\epsilon) = \pi \sum_{\vec{k}} |V(\mathbf{k})|^2 \delta(\epsilon_{\mathbf{k}} - \epsilon) = \overline{\pi \rho(\epsilon) V^2(\epsilon)} \quad (17.17)$$

as the ‘‘hybridization’’ function.

Let us now examine the resonant scattering off a non-interacting f-level, using Feynman diagrams. We'll

denote the propagator of the bare f-electron by a full line, and that of the conduction electron by a dashed line, as follows:

$$\begin{aligned} G_f^{(0)}(\omega) &= \frac{1}{\omega - E_f} \\ G^{(0)}(\mathbf{k}, \omega) &= \frac{1}{\omega - \epsilon_{\mathbf{k}}}. \end{aligned} \quad (17.18)$$

For simplicity, we will ignore the momentum dependence of the hybridization, taking $V(\mathbf{k}) = V(\mathbf{k})^* \equiv V$. The hybridization is a kind of off-diagonal potential scattering which we denote by a filled dot, as follows:

$$(17.19)$$

Now the hybridization permits the f-electron to tunnel back and forth into the continuum, a process we can associate with the “self-energy” diagram

$$= \Sigma_c(\omega) = \sum_{\mathbf{k}} \frac{V^2}{\omega - \epsilon_{\mathbf{k}}}. \quad (17.20)$$

We can view this term as an effective scattering potential for the f-electrons, one that is frequency dependent and hence retarded in time, reflecting the fact that an f-electron can spend large amounts of time out in the

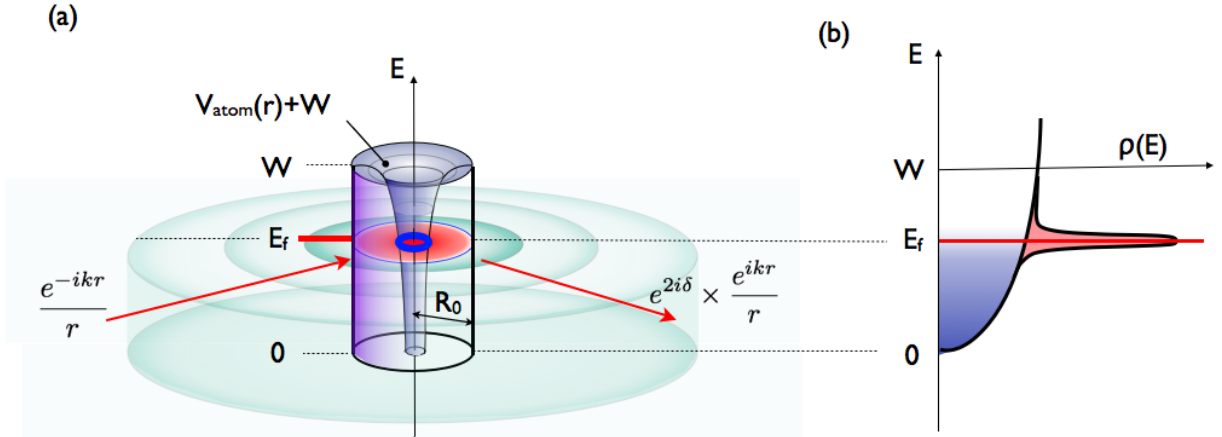


Fig. 17.4

(a) The immersion of an atomic f state in a conduction sea leads to hybridization between the localized f-state and the degenerate conduction electron continuum, forming (b) a resonance in the density of states.

conduction band. The Feynman diagrams describing the multiple scattering of the f-electron off this potential are then:

$$= \quad + \quad + \quad + \dots \quad (17.21)$$

Each time the electron tunnels into the conduction band, it does so with a different momentum, so the momenta of the conduction electrons are independently summed over in the intermediate states. As in previous chapters, we can sum these terms as a geometric series to obtain a familiar-looking self-energy correction to the f-propagator.

$$G_f(\omega) = G_f^{(0)} \left[1 + \Sigma_c G_f^{(0)} + (\Sigma_c G_f^{(0)})^2 + \dots \right] = [\omega - E_f - \Sigma_c(\omega)]^{-1} \quad (17.22)$$

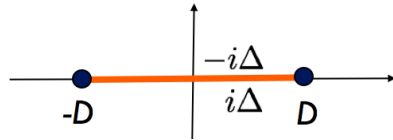
Now for a broad conduction band there is a very useful approximation for Σ_c . To derive it, we re-write the momentum sum in the self-energy as an energy integral with the density of states, replacing $\sum_{\mathbf{k}} \rightarrow \int d\epsilon \rho(\epsilon)$, so that

$$\Sigma_c(\omega) = \int \frac{d\epsilon}{\pi} \rho(\epsilon) \frac{\pi V^2}{\omega - \epsilon} = \int \frac{d\epsilon}{\pi} \frac{\Delta(\epsilon)}{\omega - \epsilon}, \quad (17.23)$$

where $\Delta(\epsilon) = \pi \rho(\epsilon) V^2$. In the complex plane, $\Sigma_c(\omega)$ has a branch cut along the real axis with a discontinuity in its imaginary part proportional to the hybridization:

$$Im \Sigma_c(\omega \pm i\delta) = \int \frac{d\epsilon}{\pi} \Delta(\epsilon) \overbrace{\text{Im} \frac{1}{\omega - \epsilon \pm i\delta}}^{\mp i\pi \delta(\omega - \epsilon)} = \mp \Delta(\omega). \quad (17.24)$$

Consider the particular case where $\Delta(\epsilon) = \Delta$ is constant for $\epsilon \in [-D, D]$, so that

$$\begin{aligned} \Sigma(\omega \pm i\delta) &= \frac{\Delta}{\pi} \int_{-D}^D \frac{d\epsilon}{\omega - \epsilon \pm i\delta} = \frac{\Delta}{\pi} \ln \left[\frac{\omega \pm i\delta + D}{\omega \pm i\delta - D} \right] \\ &= \frac{\Delta}{\pi} \overbrace{\ln \left| \frac{\omega + D}{\omega - D} \right|}^{O(\omega/D)} \mp i\Delta \theta(D - |\omega|) \end{aligned} \quad (17.25)$$


which is a function with a branch-cut stretching from $\omega = -D$ to $\omega = +D$. The frequency dependent part of $Re \Sigma_c = O(\omega/D)$ is negligible in a broad band. We can extend this observation to more general functions $\Delta(\omega)$ that vary slowly over the width of the resonance (lumping any constant part of Σ_c into a shift of E_f .) With this observation, for a broad band, we drop the real part of Σ_c , writing it in the form

$$\Sigma_c(\omega + i\omega') = -i\Delta \text{sgn}(\omega'), \quad (17.26)$$

where ω' is the imaginary part of the frequency. (at the Matsubara frequencies, $\Sigma_c(i\omega_n) = -i\Delta \text{sgn} \omega_n$). On the real axis, the f-propagator takes a particularly simple form

$$G_f(\omega - i\delta) = \frac{1}{(\omega - E_f - i\Delta)}, \quad (17.27)$$

that describes a resonance with a width Δ , centered around energy E_f , with a Lorentzian density of states

$$\rho_f(\omega) = \frac{1}{\pi} Im G_f(\omega - i\delta) = \frac{\Delta}{(\omega - E_f)^2 + \Delta^2}.$$

Now let us turn to see how the conduction electrons scatter off this resonance. Consider the repeated scattering of the conduction electrons, represented by the dashed line, off the f-level as follows:

$$= \quad + \quad + \quad + \dots$$

Now using (17.21) we see that third and higher terms can be concisely absorbed into the second term by replacing the bare f-propagator by the full (broadened) f-propagator, as follows

$$G(\mathbf{k}', \mathbf{k}, \omega) = \delta_{\mathbf{k}', \mathbf{k}} G^{(0)}(\mathbf{k}, \omega) + G^{(0)}(\mathbf{k}, \omega) V^2 G_f(\omega) G^{(0)}(\mathbf{k}', \omega) \quad (17.28)$$

We can identify

$$t(\omega) = V^2 G_f(\omega) \quad (17.29)$$

as the scattering t-matrix of the resonance. Infact, this relationship holds quite generally, even when interactions are present, because the only way conduction electrons can scatter, is by passing through the localized f-state. The full conduction electron propagator can then be written

$$G(\mathbf{k}', \mathbf{k}, \omega) = \delta_{\mathbf{k}', \mathbf{k}} G^{(0)}(\mathbf{k}, \omega) + G^{(0)}(\mathbf{k}, \omega) t(\omega) G^{(0)}(\mathbf{k}', \omega). \quad (17.30)$$

Scattering theory tells us that the t-matrix is related to the S-matrix $S(\omega) = e^{2i\delta(\omega)}$, where $\delta(\omega)$ is the scattering phase shift, by the relation $S = 1 - 2\pi i \rho t(\omega + i\eta)$ (here we use η as the infinitesimal to avoid confusion with the notation for the phase shift), or

$$t(\omega + i\eta) = \frac{1}{-2\pi i \rho} (S(\omega) - 1) = -\frac{1}{\pi \rho} \times \frac{1}{\cot \delta(\omega) - i}. \quad (17.31)$$

Substituting our explicit form of the f-Green's function,

$$t(\omega + i\delta) = V^2 G_f(\omega + i\eta) = \frac{1}{\pi \rho} \times \frac{\overbrace{\pi \rho V^2}^{\Delta}}{\omega - E_f + i\Delta} = -\frac{1}{\pi \rho} \times \frac{1}{\left(\frac{E_f - \omega}{\Delta}\right) - i} \quad (17.32)$$

Comparing (17.31) and (17.32), we see that scattering phase shift is given by

$$\delta_f(\omega) = \cot^{-1} \left(\frac{E_f - \omega}{\Delta} \right) = \tan^{-1} \left(\frac{\Delta}{E_f - \omega} \right). \quad (17.33)$$

$\delta_f(\omega)$ is a monotonically increasing function, rising from $\delta_f = 0$ at $\omega \ll 0$ to $\delta_f = \pi$ at high energies. On resonance, $\delta(E_f) = \pi/2$, corresponding to the strongest kind of “unitary scattering”.

17.2.4 The Friedel Sum Rule

Remarkably, the phase shift $\delta_f \equiv \delta_f(0)$ at the Fermi surface determines sets the amount of charge bound inside the resonance. Here, we can see this by using the f-spectral function to calculate the ground-state occupancy:

$$n_f = 2 \int_{-\infty}^0 d\omega \rho_f(\omega) = 2 \int_{-\infty}^0 \frac{d\omega}{\pi} \frac{\Delta}{(\omega - E_f)^2 + \Delta^2} = \frac{2}{\pi} \cot^{-1} \left(\frac{E_f}{\Delta} \right) \equiv 2 \times \frac{\delta_f}{\pi}, \quad (17.34)$$

Note that when $\delta(0) = \pi/2$, $n_f = 1$. This is a particular example of the “Friedel sum rule”, - a very general relation between the number of particles Δn bound in a potential well and the sum of the scattering phase shifts at the Fermi surface

$$\Delta n = \sum_{\lambda} \frac{\delta_{\lambda}}{\pi} \quad (17.35)$$

where δ_{λ} denotes the scattering phase shift in the partial wave state labelled by the orbital quantum numbers λ .⁵

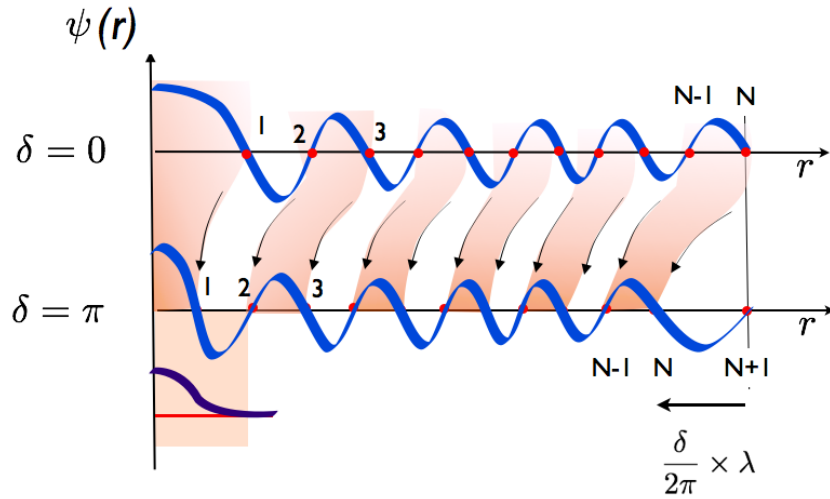


Fig. 17.5

Illustrating the Friedel sum rule. As the scattering phase shift grows, the nodes of the eigenstates at the Fermi surface are drawn into the potential well. Each time the phase shift passes through π one more node passes into the well, leading to one more bound-electron. In this illustration, one bound-state has formed as one node passes through the boundary, increasing the phase shift by π .

We can understand the Friedel sum rule by looking at the scattering wavefunction far from the impurity. The asymptotic radial wavefunctions of the incoming and the phase-shifted outgoing electrons on the Fermi surface take the form

$$\psi(r) \sim \left[\frac{e^{-ik_F r}}{r} + e^{2i\delta_f} \frac{e^{ik_F r}}{r} \right] \sim \frac{e^{i\delta} \sin(k_F r + \delta_f)}{r}$$

which corresponds to a radial wave in which the wavefunction of the electrons is shifted by an amount

$$\Delta r = -\frac{\delta_f}{k_F} = -\frac{\lambda_F}{2} \times \frac{\delta_f}{\pi}.$$

Thus for a positive phase shift, electrons are *drawn inwards* by the scattering process. Each time δ_f passes

⁵ For a spherical atom, without spin-orbit coupling $\lambda = (l, m, \sigma)$, where l , m and σ are the angular momentum and spin quantum numbers. With spin orbit coupling, $\lambda = (j, m)$ denote the quantum numbers of total angular momentum j .

through π , one more node of the wavefunction passes through the boundary at infinity, corresponding to an additional bound electron. Anderson has called Friedel's sum rule a "node counting theorem".

Example 17.2: Anderson Model as a path integral

Formulate the Anderson model as a path integral and show that the conduction electrons can be "integrated out", giving rise to an action of the following form[10]

$$S_F = \sum_{\sigma, i\omega_n} \bar{f}_{\sigma n} \left\{ -i\omega_n + E_f - i\Delta \text{sgn}(\omega_n) \right\} f_{\sigma n} + \int_0^\beta d\tau U n_\uparrow n_\downarrow. \quad (17.36)$$

where $f_{\sigma n} \equiv \beta^{-\frac{1}{2}} \int_0^\beta d\tau e^{i\omega_n \tau} f_\sigma(\tau)$ is the Fourier transform of the f-electron field.

Solution: We begin by writing the partition function of the Anderson model as a path integral

$$Z = \int \mathcal{D}[f, c] e^{-S} \quad (17.37)$$

where the action $S = S_A + S_B$ is the sum of two terms, an atomic term

$$S_A = \int_0^\beta d\tau \left[\sum_\sigma \bar{f}_\sigma (\partial_\tau + E_f) f_\sigma + U n_{f\uparrow} n_{f\downarrow} \right]$$

and a bath term

$$S_B = \int_0^\beta d\tau \left\{ \sum_{\mathbf{k}\sigma} \bar{c}_{\mathbf{k}\sigma} (\partial_\tau + \epsilon_{\mathbf{k}\sigma}) c_{\mathbf{k}\sigma} + V \left[\bar{f}_\sigma c_{\mathbf{k}\sigma} + \bar{c}_{\mathbf{k}\sigma} f_\sigma \right] \right\} \quad (17.38)$$

describing the hybridization with the surrounding sea of conduction electrons.

We can re-arrange the path integral so that the conduction electron integral is carried out first,

$$Z = \int \mathcal{D}[f] e^{-S_F} \overbrace{\int \mathcal{D}[c] e^{-S_B}}^{Z_B[\{f\}]}, \quad (17.39)$$

where $Z_B[\{f\}]$ contains the change to the f-electron induced by "integrating out" the conduction electrons. The bath action is free of interactions and can be written schematically as a quadratic form

$$S_B = \bar{c} \cdot A \cdot c + \bar{c} \cdot j + \bar{j} \cdot c \quad (17.40)$$

where $A \equiv (\partial_\tau + \epsilon_{\mathbf{k}}) \delta(\tau - \tau')$ is the matrix acting on the fields between the fields $c \equiv c_{\mathbf{k}\sigma}(\tau)$ and $\bar{c} = \bar{c}_{\mathbf{k}\sigma}(\tau)$, while $j(\tau) = V f_\sigma(\tau)$ and $\bar{j} = \bar{f}_\sigma(\tau) V$ are source terms. You may find it reassuring to recast S_B in Fourier space, where $A = (-i\omega_n + \epsilon_{\mathbf{k}})$ is explicitly diagonal.

Using the standard result for Gaussian fermion integrals,

$$Z_B = \int \mathcal{D}[c] e^{-\bar{c} A c - \bar{j} c + \bar{c} j} = \det A \times \exp[\bar{j} A^{-1} j].$$

or explicitly,

$$Z_B[\{f\}] = \overbrace{\det[\partial_\tau + \epsilon_{\mathbf{k}}]}^{Z_C = e^{-\beta F_C}} \exp \left[\int_0^\beta d\tau \bar{f}_\sigma \left(\sum_{\mathbf{k}} \frac{V^2}{\partial_\tau + \epsilon_{\mathbf{k}}} \right) f_\sigma \right] \quad (17.41)$$

The first term is the partition function Z_C of the conduction sea in the absence of the magnetic ion. Substituting $Z_B[\{f\}]$ back into the full path integral (17.39) and combining the quadratic terms then gives

$$Z = Z_C \times \int \mathcal{D}[f] \exp \left[- \int d\tau \left\{ \bar{f}_\sigma \left(\partial_\tau + E_f - \sum_{\mathbf{k}} \frac{V^2}{\partial_\tau + \epsilon_{\mathbf{k}}} \right) f_\sigma + U n_\uparrow n_\downarrow \right\} \right].$$

If we transform the first term into Fourier space, substituting $f_\sigma(\tau) = \beta^{-1/2} \sum_n f_{\sigma n} e^{-i\omega_n \tau}$, $\tilde{f}_\sigma(\tau) = \beta^{-1/2} \sum_n \tilde{f}_{\sigma n} e^{i\omega_n \tau}$ so that $\partial_\tau \rightarrow -i\omega_n$, the action can be written

$$S_F = \sum_{\sigma, i\omega_n} \tilde{f}_{\sigma n} \left\{ \underbrace{-i\omega_n + E_f + \sum_{\mathbf{k}} \frac{V^2}{i\omega_n - \epsilon_{\mathbf{k}}}}_{-G_f^{-1}(i\omega_n)} \right\} f_{\sigma n} + \int_0^\beta d\tau U n_\uparrow n_\downarrow \quad (17.42)$$

The quadratic coefficient of the f-electrons is the inverse f-electron propagator of the non-interacting resonance. We immediately recognize the self-energy term $\Sigma_c(i\omega_n) = -i\Delta \text{sgn}(\omega_n)$ introduced in (17.20). From this path integral derivation, we can see that this term accounts for the effect of the conduction bath electrons, even in the presence of interactions. If we now use the large band-width approximation $\Sigma(i\omega_n) = -i\Delta \text{sgn}\omega_n$ introduced in the (17.26), the action can be compactly written

$$S_F = \sum_{\sigma, i\omega_n} \tilde{f}_{\sigma n} \left\{ -i\omega_n + E_f - i\Delta \text{sgn}(\omega_n) \right\} f_{\sigma n} + \int_0^\beta d\tau U n_\uparrow n_\downarrow. \quad (17.43)$$

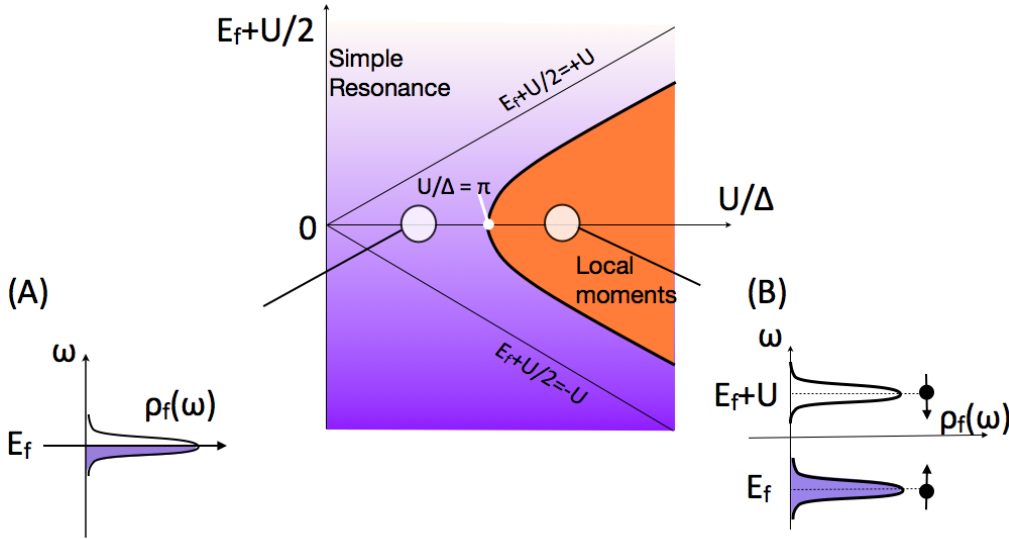


Fig. 17.6

Mean field phase diagram of the Anderson model, illustrating how the f-electron resonance splits to form a local moment. A) $U < \pi\Delta$, single half-filled resonance. B) $U > \pi\Delta$, up and down components of the resonance are split by an energy U .

17.2.5 Mean-field theory

In the Anderson model, the Coulomb interaction and hybridization compete with one-another. Crudely speaking, we expect that when the Coulomb interaction exceeds the hybridization, local moments will develop. To gain an first insight into the effect of hybridization on local moment formation, Anderson[11] carried out a

Hartree mean-field treatment of the repulsive U interaction, decoupling

$$Un_{\uparrow}n_{\downarrow} \rightarrow Un_{\uparrow}\langle n_{\downarrow} \rangle + U\langle n_{\uparrow} \rangle n_{\downarrow} - U\langle n_{\uparrow} \rangle \langle n_{\downarrow} \rangle + O(\delta n^2). \quad (17.44)$$

We can understand this factorization as the result of a saddle point description of the path integral, treated in more detail in the following exercise Ex 17.3. Using this mean-field approximation, Anderson concluded that for the symmetric Anderson model, local moments would develop provided

$$U \gtrsim U_c = \pi\Delta. \quad (17.45)$$

Let us now rederive this mean-field result. From (17.44), the mean-field effect of the interactions is to shift the f-level position,

$$E_f \rightarrow E_{f\sigma} = E_f + U\langle n_{f-\sigma} \rangle \quad (17.46)$$

which, using (17.34) implies that the scattering phase shift for the up and down channels

$$\delta_{f\sigma} = \cot^{-1} \left(\frac{E_{f\sigma}}{\Delta} \right) \quad (17.47)$$

are no-longer equal. Using the “Friedel sum rule” (17.34), we then obtain the mean-field equations

$$\langle n_{f\sigma} \rangle = \frac{\delta_{f\sigma}}{\pi} = \frac{1}{\pi} \cot^{-1} \left(\frac{E_f + U\langle n_{f-\sigma} \rangle}{\Delta} \right) \quad (17.48)$$

It is convenient to introduce an occupancy $n_f = \sum_{\sigma} \langle n_{f\sigma} \rangle$ and magnetization $M = \langle n_{f\uparrow} \rangle - \langle n_{f\downarrow} \rangle$, so that $\langle n_{f\sigma} \rangle = \frac{1}{2}(n_f + \sigma M)$ ($\sigma = \pm 1$). The mean-field equation for the occupancy and magnetization are then

$$n_f = \frac{1}{\pi} \sum_{\sigma=\pm 1} \cot^{-1} \left(\frac{E_f + U/2(n_f - \sigma M)}{\Delta} \right) \quad (17.49)$$

$$M = \frac{1}{\pi} \sum_{\sigma=\pm 1} \sigma \cot^{-1} \left(\frac{E_f + U/2(n_f - \sigma M)}{\Delta} \right) \quad (17.50)$$

To find the critical size of the interaction strength where a local moment develops, we set $M \rightarrow 0^+$ in (17.49) to obtain $\frac{E_f + U n_f / 2}{\Delta} = \cot \left(\frac{\pi n_f}{2} \right)$. Linearizing (17.50) in M , we obtain

$$1 = \frac{U_c}{\pi\Delta} \frac{1}{1 + \left(\frac{E_f + U n_f / 2}{\Delta} \right)^2} = \frac{U_c}{\pi\Delta} \sin^2 \left(\frac{\pi n_f}{2} \right). \quad (17.51)$$

so that for $n_f = 1$,

$$U_c = \pi\Delta \quad (17.52)$$

For larger values of $U > U_c$, there are two solutions, corresponding to an “up” or “down” spin polarization of the f-state. We will see that this is an over-simplified description of the local moment, but it gives us a approximate picture of the physics. The total density of states now contains two Lorentzian peaks, located at $E_f \pm UM$:

$$\rho_f(\omega) = \frac{1}{\pi} \left[\frac{\Delta}{(\omega - E_f - UM)^2 + \Delta^2} + \frac{\Delta}{(\omega - E_f + UM)^2 + \Delta^2} \right]$$

The critical curve obtained by plotting U_c and E_f as a parametric function of n_f is shown in Fig. 17.6.

The Anderson mean-field theory allows a qualitatively understand the experimentally observed formation of local moments. When dilute magnetic ions are dissolved in a metal to form an alloy, the formation of

a local moment is dependent on whether the ratio $U/\pi\Delta$ is larger than, or smaller than one. When iron is dissolved in pure niobium, the failure of the moment to form reflects the higher density of states and larger value of Δ in this alloy. When iron is dissolved in molybdenum, the lower density of states causes $U > U_c$, and local moments form. [12]

Example 17.3: Factorizing the interaction in the Anderson model

- a) Show that the interaction in the Anderson model can be decoupled via a Hubbard Stratonovich decoupling to yield

$$\int_0^\beta d\tau U n_\uparrow n_\downarrow \rightarrow \int_0^\beta d\tau \left[\phi_\uparrow n_\uparrow + \phi_\downarrow n_\downarrow - \frac{\phi_\uparrow \phi_\downarrow}{U} \right] \quad (17.53)$$

where $\phi_\sigma = \phi_0 + i\lambda(\tau) - \sigma h(\tau)$ is the sum of a real and an imaginary field.

- b) Derive the mean-field partition function obtained by assuming that the path-integral over ϕ can be approximated by the saddle point configuration where ϕ_σ is independent of time, given by

$$\begin{aligned} Z_{MF} &= \int \mathcal{D}[f] e^{-S_{MF}[\phi_\sigma, f]} \\ S_{MF} &= \sum_{\sigma, i\omega_n} \bar{f}_{\sigma n} [-G_{f\sigma}^{-1}(i\omega_n)] f_{\sigma n} + \frac{\beta}{U} \phi_\uparrow \phi_\downarrow. \end{aligned} \quad (17.54)$$

where

$$G_{f\sigma}^{-1}(i\omega_n) = i\omega_n - E_f - \phi_\sigma + i\Delta \text{sgn}(\omega_n)$$

is the inverse mean-field f-propagator

- c) Carry out the Gaussian integral in (17.54) to show that the mean-field free energy is

$$F_{MF} = -k_B T \sum_{\sigma, i\omega_n} \ln [-G_{f\sigma}^{-1}(i\omega_n)] - \frac{1}{U} \phi_\uparrow \phi_\downarrow.$$

and by setting $\partial F / \partial \phi_\sigma = 0$, derive the mean-field equations

$$\phi_{-\sigma} = U \langle n_{f\sigma} \rangle = U \int_{-\infty}^{\infty} \frac{d\omega}{\pi} f(\omega) \frac{\Delta}{(\omega - E_f - \phi_\sigma)^2 + \Delta^2}.$$

Solution:

- a) The interaction in the Anderson model can be rewritten as a sum of two terms,

$$U n_\uparrow n_\downarrow = \overbrace{\frac{U}{4} (n_\uparrow + n_\downarrow)^2}^{\text{“charge”}} - \overbrace{\frac{U}{4} (n_\uparrow - n_\downarrow)^2}^{\text{“spin”}}$$

that we can loosely interpret as a repulsion between charge fluctuations and an attraction between spin fluctuations. Following the results of Section ??, inside the path integral, the attractive magnetic interaction can be decoupled in terms of a fluctuating Weiss $h(\tau)$ field, while the repulsive charge interaction can be decoupled in terms of a fluctuating potential field $\phi(\tau) = \phi_0 + i\lambda(\tau)$, as follows

$$\begin{aligned} -\frac{1}{2} \times \frac{U}{2} (n_\downarrow - n_\uparrow)^2 &\rightarrow -h(n_\uparrow - n_\downarrow) + \frac{h^2}{2 \times (U/2)}, \\ +\frac{1}{2} \times \frac{U}{2} (n_\uparrow + n_\downarrow)^2 &\rightarrow \phi(n_\uparrow + n_\downarrow) - \frac{\phi^2}{2 \times (U/2)}, \end{aligned} \quad (17.55)$$

with the understanding that for repulsive $U > 0$, fluctuations of $\phi(\tau)$ are integrated along the imaginary axis, $\phi(\tau) = \phi_0 + i\lambda(\tau)$. Adding these terms gives

$$\int_0^\beta d\tau U n_\uparrow n_\downarrow \rightarrow \int_0^\beta d\tau \left[(\phi - \sigma h) n_\sigma + \frac{h^2 - \phi^2}{U} \right] = \int_0^\beta d\tau \left[\phi_\uparrow n_\uparrow + \phi_\downarrow n_\downarrow + \frac{\phi_\uparrow \phi_\downarrow}{U} \right] \quad (17.56)$$

where $\phi_\sigma = \phi - \sigma h$. The decoupled path integral then takes the form

$$Z_F = \int \mathcal{D}[\phi_\sigma] \int \mathcal{D}[f] e^{-S_F[\phi_\sigma, f]}$$

$$S_F = \int d\tau \left\{ \bar{f}_\sigma \left(\partial_\tau + E_f + \phi_\sigma - \sum_{\mathbf{k}} \frac{V^2}{\partial_\tau + \epsilon_{\mathbf{k}}} \right) f_\sigma - \frac{1}{U} \phi_\uparrow \phi_\downarrow \right\}. \quad (17.57)$$

Note how the Weiss fields ϕ_σ shift the f-level position: $E_f \rightarrow E_f + \phi_\sigma(\tau)$. In this way, the Anderson model can be regarded as a resonant level immersed in a white noise magnetic field that modulates the splitting between the up and down spin resonances.

- b) Anderson's mean-field treatment corresponds to a saddle point approximation to the integral over the ϕ_σ fields. At the saddle point, $\langle \delta S / \delta \phi_\sigma \rangle = 0$. From (17.57), we obtain

$$\frac{\delta S_F}{\delta \phi_\sigma} = \bar{f}_\sigma f_\sigma - \frac{1}{U} \phi_{-\sigma}$$

so the saddle point condition $\langle \delta S_F / \delta \phi_\sigma \rangle = 0$ implies $\phi_{-\sigma} = U \langle n_{f\sigma} \rangle$, recovering the Hartree mean field theory. We can clearly seek solutions in which $\phi_\sigma(\tau) = \phi_\sigma^{(0)}$ is a constant. With this understanding, the saddle point approximation is

$$Z_F \approx Z_{MF} = \int \mathcal{D}[f] e^{-S_F[\phi_\sigma^{(0)}, f]} \quad (17.58)$$

where

$$S_{MF} = \int d\tau \left\{ \bar{f}_\sigma \left(\partial_\tau + E_f + \phi_\sigma^{(0)} - \sum_{\mathbf{k}} \frac{V^2}{\partial_\tau + \epsilon_{\mathbf{k}}} \right) f_\sigma - \frac{\beta}{U} \phi_\uparrow^{(0)} \phi_\downarrow^{(0)} \right\}. \quad (17.59)$$

Now since $\phi^{(0)}$ is a constant, we can Fourier transform the first term in this expression, replacing $\partial_\tau \rightarrow -i\omega_n$, to obtain

$$S_{MF} = \sum_{\sigma, i\omega_n} \bar{f}_{\sigma n} \overbrace{\left(-i\omega_n + E_f + \phi_\sigma^{(0)} - \sum_{\mathbf{k}} \frac{V^2}{-i\omega_n + \epsilon_{\mathbf{k}}} \right)}^{-G_{f\sigma}^{-1}(i\omega_n)} f_{\sigma n} - \frac{\beta}{U} \phi_\uparrow^{(0)} \phi_\downarrow^{(0)}, \quad (17.60)$$

$-i\text{sgn}(\omega_n)\Delta$

where in the broad-band width limit, we can replace

$$G_{f\sigma}^{-1}(i\omega_n) = i\omega_n - E_f - \phi_\sigma^{(0)} + i\text{sgn}(\omega_n)\Delta. \quad (17.61)$$

- c) Carrying out the Gaussian integral in (17.58), we obtain

$$Z_{MF} = \det[-G_{f\sigma}^{-1}(i\omega_n)] e^{\frac{\beta}{U} \phi_\uparrow \phi_\downarrow} = \prod_{\sigma, i\omega_n} [-G_{f\sigma}^{-1}(i\omega_n)] e^{\frac{\beta}{U} \phi_\uparrow \phi_\downarrow},$$

or

$$F_{MF} = -k_B T \ln Z_{MF} = -k_B T \sum_{\sigma, i\omega_n} \ln [-G_{f\sigma}^{-1}(i\omega_n)] e^{i\omega_n 0^+} - \frac{1}{U} \phi_\uparrow \phi_\downarrow. \quad (17.62)$$

where we have included the convergence factor $e^{i\omega_n 0^+}$. By (17.61), $\frac{\partial G_{f\sigma}^{-1}(i\omega_n)}{\partial \phi_\sigma} = -1$, so differentiating (17.62) with respect to ϕ_σ , we obtain

$$0 = k_B T \sum_{i\omega_n} G_{f\sigma}(i\omega_n) e^{i\omega_n 0^+} - \frac{1}{U} \phi_{-\sigma}, \quad (17.63)$$

or

$$\phi_{-\sigma} = U \langle n_{f\sigma} \rangle = U k_B T \sum_{i\omega_n} G_{f\sigma}(i\omega_n) e^{i\omega_n 0^+}.$$

Carrying out the sum over the Matsubara frequencies by the standard contour integral method, we obtain

$$\begin{aligned}
 \phi_{-\sigma} &= -U \oint_{\text{Im axis}} \frac{dz}{2\pi i} f(z) G_{f\sigma}(z) = U \oint_{\text{Re axis}} \frac{dz}{2\pi i} f(z) G_{f\sigma}(z) \\
 &= U \int_{-\infty}^{\infty} \frac{d\omega}{\pi} f(\omega) \text{Im} G_{f\sigma}(\omega - i\delta) \\
 &= U \int_{-\infty}^{\infty} \frac{d\omega}{\pi} f(\omega) \frac{\Delta}{(\omega - E_f - \phi_{0\sigma})^2 + \Delta^2}.
 \end{aligned} \tag{17.64}$$

17.3 The Coulomb Blockade: local moments in quantum dots

A modern realization of the physics of local moments is found within quantum dots. Quantum dots are a tiny electron pools in a doped semi-conductor, small enough so that the electron states inside the dot are quantized, loosely resembling the electronic states of an atom. Quantum dot behavior also occurs in nanotubes. Unlike a conventional atom, the separation of the electronic states in quantum dot is of the order of milli-electron volts, rather than volts. The overall position of the quantum dot energy levels can be changed by applying a gate voltage to the dot. It is then possible to pass a small current through the dot by placing it between two leads. The differential conductance $G = dI/dV$ is directly proportional to the density of states $\rho(\omega)$ inside the dot $G \propto \rho(0)$. Experimentally, when G is measured as a function of gate voltage V_g , the differential conductance is observed to develop a periodic structure, with a period of a few milli-electron volts. [13]

This phenomenon is known as the ‘‘Coulomb blockade’’[14, 15] and it results from precisely the same physics that is responsible for moment formation. A simple model for a quantum dot considers it as a sequence of single particle levels at energies ϵ_λ , interacting via a single Coulomb potential U , according to the model

$$H_{dot} = \sum_{\lambda} (\epsilon_{\lambda} + eV_g) n_{\lambda\sigma} + \frac{U}{2} N(N-1) \tag{17.65}$$

where $n_{\lambda\sigma}$ is the occupancy of the spin σ state of the λ level, $N = \sum_{\lambda\sigma} n_{\lambda\sigma}$ is the total number of electrons in the dot and V_g the gate voltage. This is a simple generalization of the single atom part of the Anderson model. Notice that the capacitance of the dot is $C = e^2/U$.

The energy difference between the n electron and $n+1$ electron state of the dot is given by

$$E(n+1) - E(n) = nU + \epsilon_{\lambda_n} - |e|V_g,$$

where λ_n is the one-particle state into which the n -th electron is being added. As the gate voltage is raised, the quantum dot fills each level sequentially, as illustrated in Fig. 17.7, and when $|e|V_g = nU + \epsilon_{\lambda_n}$, the n -th level becomes degenerate with the Fermi energy of each lead. At this point, electrons can pass coherently through the resonance giving rise to a sharp peak in the conductance. At maximum conductance, the transmission and reflection of electrons is unitary, and the conductance of the quantum dot will reach a substantial fraction of the quantum of conductance, e^2/h per spin. A calculation of the zero-temperature conductance through a single non-interacting resonance coupled symmetrically to two leads gives

$$G(V_g) = \frac{2e^2}{h} \frac{\Delta^2}{(\epsilon_{\lambda} - |e|V_g)^2 + \Delta^2} \tag{17.66}$$

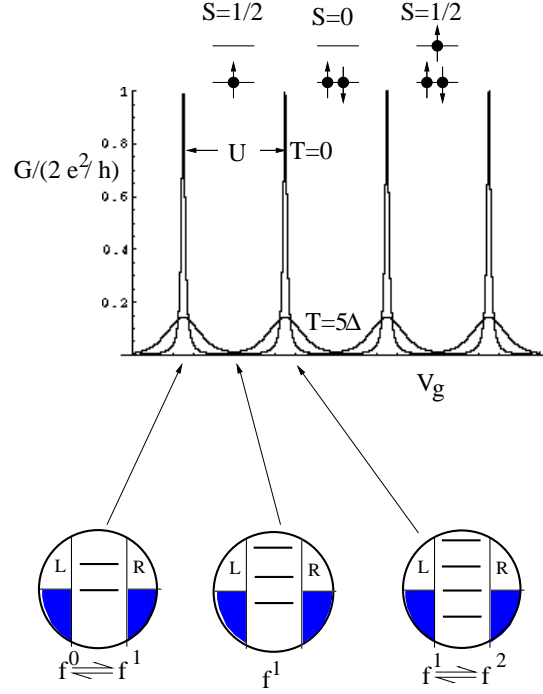


Fig. 17.7

Variation of zero bias conductance $G = dI/dV$ with gate voltage in a quantum dot. Coulomb interactions mean that for each additional electron in the dot, the energy to add one electron increases by U . When the charge on the dot is integral, the Coulomb interaction blocks the addition of electrons and the conductance is suppressed. When the energy to add an electron is degenerate with the Fermi energy of the leads, unitary transmission occurs, and for symmetric leads, $G = 2e^2/h$.

where the factor of two derives from two spin channels. This gives rise to a conductance peak when the gate voltage $|e|V_g = \epsilon_\lambda$. At a finite temperature, the Fermi distribution of the electrons in the leads is thermally broadened, and the conductance involves a thermal average about the Fermi energy

$$G(V_g, T) = \frac{2e^2}{h} \int d\epsilon \left(-\frac{\partial f}{\partial \epsilon} \right) \frac{\Delta^2}{(\epsilon_\lambda - |e|V_g - \epsilon)^2 + \Delta^2} \quad (17.67)$$

where $f(\epsilon) = 1/(e^{\beta\epsilon} + 1)$ is the Fermi function. When there are multiple levels, the each successive level contributes to the conductance, to give

$$G(V_g, T) = \sum_{n \geq 0} \frac{2e^2}{h} \int d\epsilon \left(-\frac{\partial f}{\partial \epsilon} \right) \frac{\Delta^2}{(nU + \epsilon_{\lambda_n} - |e|V_g - \epsilon)^2 + \Delta^2}$$

where the n -th level is shifted by the Coulomb blockade.

The effect of a bias voltage on these results is interesting. In this situation, the energy distribution function of the two leads are now shifted relative to one-another. A crude model for the effect of a voltage is obtained replacing the Fermi function by an average over both leads, so that $f'(\epsilon) \rightarrow \frac{1}{2} \sum_{\pm} f'(\epsilon \pm \frac{eV_{sd}}{2})$, which has the

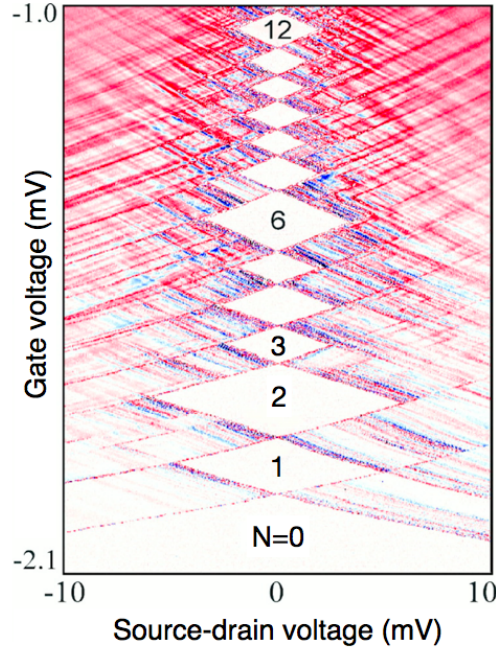


Fig. 17.8

Experimentally measured conductance for a voltage-biased quantum dot after [16], showing the splitting of the Coulomb blockade into two components, shifted up and down by the voltage bias, $\pm eV_{sd}/2$. In the white diamond-shaped regions, $G(V_{sd}) \approx 0$ as a result of Coulomb blockade. The number of particles N is fixed in each of the diamond regions. The lines outside the diamonds, running parallel to the sides, identify excited states.

effect of splitting the conductance peaks into two, peaked at voltages

$$|e|V_g = \epsilon_{\lambda_n} + nU \pm |e|V_{sd}/2 \quad (17.68)$$

as shown in Fig. 17.8.

It is remarkable that the physics of moment formation and the “Coulomb blockade” operate in both artificial mesoscopic devices and naturally occurring magnetic ions.

17.4 The Kondo Effect

Although Anderson’s mean-field theory provides a mechanism for moment formation, it raises new questions. While the mean-field treatment of the local moment would be appropriate for an ordered magnet involving a macroscopic number of spins, rigidly locked together, for a single magnetic impurity there will always be a finite quantum mechanical amplitude for the spin to tunnel between an up and down configuration.

$$e_{\downarrow}^- + f_{\uparrow}^{\uparrow} \rightleftharpoons e_{\uparrow}^- + f_{\downarrow}^{\uparrow}$$

This tunneling rate τ_{sf}^{-1} defines a temperature scale

$$k_B T_K = \frac{\hbar}{\tau_{sf}}$$

called the Kondo temperature, which sets the cross-over between local moment behavior, where the spin is free, and the low temperature physics, where the spin and conduction electrons are entangled. Historically, the physics of this cross-over posed a major problem for the theoretical physics community that took about a decade to resolve. It turns out that the process by which a local moment disappears or “quenches” at low temperatures is analogous to the physics of quark confinement. Today we name it the “Kondo effect” after the Japanese physicist Jun Kondo who calculated the leading logarithmic contribution that signals this unusual behavior[17].

The Kondo effect has a many manifestations in condensed matter physics: not only does it govern the quenching of magnetic moments in a magnetic alloy or a quantum dot[13], it is responsible for the formation of heavy fermions in dense Kondo lattice materials (heavy fermion compounds) where the local moments transform into composite quasiparticles with masses sometimes in excess of a thousand bare electron masses.[18] We will see that the Kondo temperature depends exponentially on the strength of the Anderson interaction parameter U . In the symmetric Anderson model, where $E_f = -U/2$,

$$T_K = \sqrt{\frac{2U\Delta}{\pi}} \exp\left(-\frac{\pi U}{8\Delta}\right). \quad (17.69)$$

We will derive the key elements of this basic result using perturbative renormalization group reasoning [19], but it is also obtained from the exact Bethe ansatz solution of the Anderson model [20, 21, 22].

One can view the physics of local moments from two complimentary perspectives (see Fig. (17.9)):

- an “adiabatic picture” which starts with the non-interacting resonant ground-state ($U = 0$) of the Anderson model, and then considers the effect of dialing up the interaction term U .
- a “scaling approach”, which starts with the interacting, but isolated atom ($V(k) = 0$), and considers the effect of immersing it in an electron sea, gradually “integrating out” lower and lower energy electrons.

The adiabatic approach involves dialing up the interaction, as shown by the horizontal arrow in figure (17.9). From the adiabatic perspective, the ground-state remains in a Fermi liquid. In principle, one might imagine the possibility of a phase transition at some finite interaction strength U , but in a single impurity model, with a finite number of local degrees of freedom, we don’t expect any symmetry breaking phase transitions. In the scaling approach, we follow the physics as a function of ever-decreasing energy scale, is loosely equivalent to dialing down the temperature, as shown by the vertical arrow in figure (17.9) The scaling approach starts from an atomic perspective: it allows us to understand the formation of local moments, and at lower temperatures, how a Fermi liquid can develop through the interaction of an isolated magnetic moment with a electron sea.

We shall first discuss one of the most basic manifestations of the Kondo effect: the appearance of a Kondo resonance in the spectral function of the localized electron. This part of our analysis will involve rather qualitative reasoning based on the ideas of adiabaticity introduced in earlier chapters. Afterwards we adopt the scaling approach, first deriving the Kondo model, describing low-energy coupling between the local moments and conduction electrons by using a “Schrieffer Wolff” transformation of the Anderson model. Finally, we shall discuss the concept of renormalization and apply it to the Kondo model, following the evolution of the physics from the local moment to the Fermi liquid.

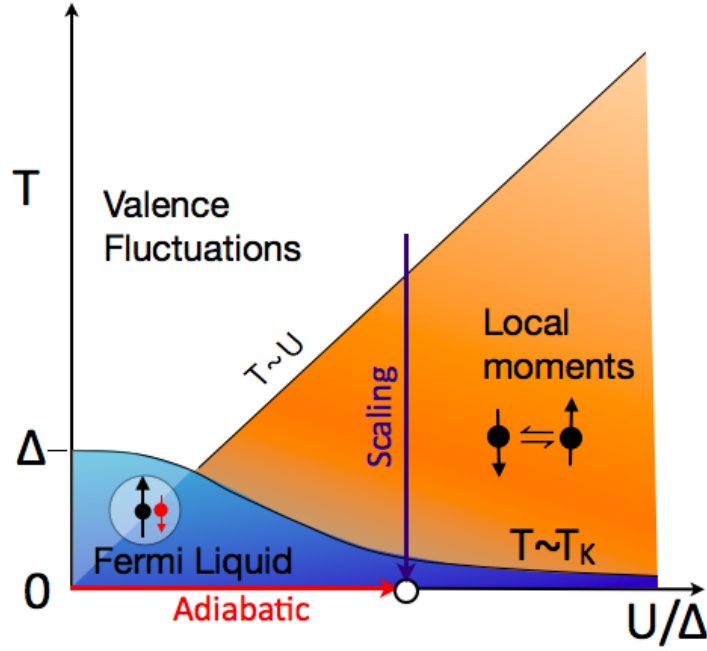


Fig. 17.9

The phase diagram of the symmetric Anderson model. Below a scale $T \sim U$ local moments develop. The Kondo temperature T_K plays the role of the renormalized resonant level width. Below a temperature $T \sim T_K$, the local moments become screened by the conduction sea via the Kondo effect, to form a Fermi liquid.

17.4.1 Adiabaticity and the Kondo resonance

The adiabatic approach allows us to qualitatively understand the emergence of a remarkable resonance in the excitation spectrum of the localized f-electron - the “Kondo resonance”. This resonance is simply the adiabatic renormalization of the Friedel-Anderson resonance seen in the non-interacting Anderson model. Its existence was first inferred by Abrikosov and Suhl [23, 24], but today it is colloquially referred to as the “Kondo resonance”.

To understand the Kondo resonance we shall study the effects of interactions on the f-spectral function

$$A_f(\omega) = \frac{1}{\pi} \text{Im} G_f(\omega + i\eta) \quad (17.70)$$

where $G_f(\omega - i\delta)$ is the advanced f-Green’s function. From a spectral decomposition (??) we know that:

$$A_f(\omega) = \begin{cases} \text{Energy distribution for adding one f-electron.} \\ \sum_{\lambda} |\langle \lambda | f_{\sigma}^{\dagger} | \phi_0 \rangle|^2 \delta(\omega - [E_{\lambda} - E_0]), & (\omega > 0) \\ \sum_{\lambda} |\langle \lambda | f_{\sigma} | \phi_0 \rangle|^2 \delta(\omega - [E_0 - E_{\lambda}]), & (\omega < 0) \\ \text{Energy distribution for removing f-electron} \end{cases} \quad (17.71)$$

where E_λ and E_0 are the excited and ground-state energies. For negative energies $\omega < 0$, this spectrum corresponds to the energy spectrum of electrons emitted in X-ray photo-emission, while for positive energies ($\omega > 0$), the spectral function can be measured from inverse X-ray photo-emission [25, 26]. The weight beneath the Fermi energy determines the f-charge of the ion

$$\langle n_f \rangle = 2 \int_{-\infty}^0 d\omega A_f(\omega) \quad (17.72)$$

In a magnetic ion, such as a Cerium atom in a $4f^1$ state, this quantity is just a little below unity.

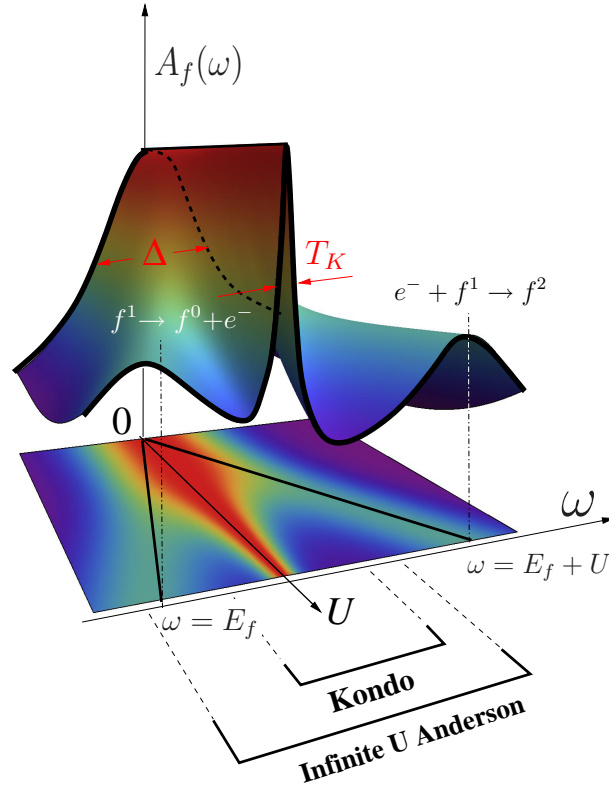


Fig. 17.10 Schematic illustrating the formation of a Kondo resonance in the f-spectral function $A_f(\omega)$ as interaction strength U is turned on. Here, the interaction is turned on while maintaining a constant f-occupancy, by shifting the bare f-level position beneath the Fermi energy. The lower part of diagram is the density plot of f-spectral function, showing how the non-interacting resonance at $U = 0$ splits into an upper and lower atomic peak at $\omega = E_f$ and $\omega = E_f + U$.

Fig. (17.16.) illustrates the effect of the interaction on the f-spectral function. In the non-interacting limit ($U = 0$), the f-spectral function is a Lorentzian of width Δ . If we turn on the interaction U , being careful to shifting the f-level position beneath the Fermi energy to maintain a constant occupancy, the resonance splits into three peaks, two at energies $\omega = E_f$ and $\omega = E_f + U$ corresponding to the energies for a valence

fluctuation, plus an additional central “Kondo resonance” associated with the spin-fluctuations of the local moment.

When the interaction is much larger than the hybridization width, $U \gg \Delta$, one might expect no spectral weight left at low energies. But it turns out that the spectral function at the Fermi energy is an adiabatic invariant determined by the scattering phase shift δ_f :

$$A_f(\omega = 0) = \frac{\sin^2 \delta_f}{\pi \Delta}. \quad (17.73)$$

This result, due to Langreth[27, 28], guarantees that a “Kondo resonance” is always present at the Fermi energy. Now the total spectral weight $\int_{-\infty}^{\infty} d\omega A_f(\omega) = 1$ is conserved, so if $|E_f|$ and U are both large compared with Δ , most of this weight will be lie far from the Fermi energy, leaving a small residue $Z \ll 1$ in the Kondo resonance. If the area under the Kondo resonance is Z , since the height of Kondo resonance is fixed $\sim 1/\Delta$, the renormalized hybridization width Δ^* must be of order $Z\Delta$. This scale is set by the Kondo temperature, so that $Z\Delta \sim T_K$.

The Langreth relation (17.73) follows from the analytic form of the f-Green’s function near the Fermi energy. For a single magnetic ion, we expect that the interactions between electrons can be increased continuously, without any risk of instabilities, so that the excitations of the strongly interacting case remain in one-to-one correspondence with the excitations of the non-interacting case $U = 0$, forming a “local Fermi liquid”. In this local Fermi liquid, the interactions give rise to an f-electron self-energy, which at zero temperature, takes the form

$$\Sigma_f(\omega - i\eta) = \Sigma_f(0) + (1 - Z^{-1})\omega + iA\omega^2, \quad (17.74)$$

at low energies. As discussed in chapter 8, The quadratic energy dependence of $\Sigma_f(\omega) \sim \omega^2$ follows from the Pauli exclusion principle, which forces a quadratic energy dependence of the phase space for the emission of a particle-hole pair. The “wavefunction” renormalization Z , representing the overlap with the state containing one additional f-quasiparticle, is less than unity, $Z < 1$. Using this result (17.74), the low energy form of the f-electron propagator is

$$\begin{aligned} G_f^{-1}(\omega - i\eta) &= \omega - E_f - i\Delta - \Sigma_f(\omega) = Z^{-1}[\omega - \overbrace{Z(E_f + \Sigma_f(0))}^{E_f^*} - i \overbrace{\frac{\Delta^*}{Z\Delta}}^{\Delta^*} - iO(\omega^2)] \\ G_f(\omega - i\eta) &= \frac{Z}{\omega - E_f^* - i\Delta^* - iO(\omega^2)}. \end{aligned} \quad (17.75)$$

This corresponds to a renormalized resonance of reduced weight $Z < 1$, located at position E_f^* with renormalized width $\Delta^* = Z\Delta$. Now by (17.29) and (17.31), the f-Green’s function determines the t-matrix of the conduction electrons $t(\omega + i\eta) = V^2 G_f(\omega + i\eta) = -(\pi\rho)^{-1} e^{i\delta(\omega)} \sin \delta(\omega)$, so the phase of the f-Green’s function at the Fermi energy determines the scattering phase shift, δ_f , hence $G_f(0 + i\eta) = (G_f(0 - i\eta))^* = -|G_f(0)|e^{i\delta_f}$. This implies that the scattering phase shift at the Fermi energy is

$$\delta_f = \text{Im} \left(\ln[-G_f^{-1}(\omega - i\eta)] \right) \Big|_{\omega=0} = \tan^{-1} \left(\frac{\Delta^*}{E_f^*} \right). \quad (17.76)$$

Eliminating $E_f^* = \Delta^* \cot \delta_f$ from (17.75), we obtain

$$G_f(0 + i\eta) = -\frac{Z}{\Delta^*} e^{-i\delta_f} \sin \delta_f = -\frac{1}{\Delta} e^{-i\delta_f} \sin \delta_f, \quad (17.77)$$

so that

$$A_f(0) = \frac{1}{\pi} \text{Im} G_f(0 - i\eta) = \frac{\sin^2 \delta_f}{\pi \Delta}. \quad (17.78)$$

is an adiabatic invariant.

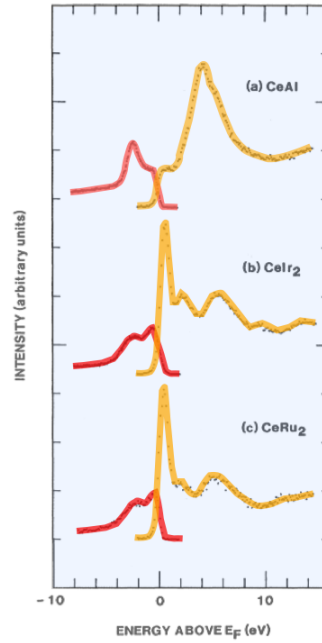


Fig. 17.11 Spectral functions for three different Cerium f-electron materials, measured using X-ray photoemission (below the Fermi energy) and inverse X-ray photoemission (above the Fermi energy) after [26]. *CeAl* is an antiferromagnet and does not display a Kondo resonance.

Photo-emission studies do reveal the three-peaked structure characteristic of the Anderson model in many *Ce* systems, such as *CeIr₂* and *CeRu₂* [26] (see Fig. 17.11). Materials in which the Kondo resonance is wide enough to be resolved are more “mixed valent” materials in which the f- valence departs significantly from unity. Three peaked structures have also been observed in certain *U* 5f materials such as *UPt₃* and *UAl₂* [29] materials, but it has not yet been resolved in *UBe₁₃*. A three peaked structure has recently been observed in 4f *Yb* materials, such as *YbPd₃*, where the $4f^{13}$ configuration contains a single *f* hole, so that the positions of the three peaks are reversed relative to *Ce* [30].

17.5 Renormalization concept

The Anderson model illustrates a central theme of condensed matter physics - the existence of physics on several widely spaced energy scales. In particular, the scale at which local moments form in f electron sys-

terms is of order the Coulomb energy U , a scale of order $10eV$, while the Kondo effect occurs at a scale a thousand times smaller, of order $10K \sim 1meV$. When energy scales are well-separated like this, we use the “renormalization group” to fold the key effects of the high energy physics into a small set of parameters that control the low energy physics. [31, 32, 33, 34]

Renormalization is built on the idea that the low energy physics of a system only depend on certain gross features of the high energy physics. The family of systems with the same low energy excitation spectrum constitute a “universality class” of models. (Fig. 17.12) We need the concept of universality, for without it we would be lost, for we could not hope to capture the physics of real-world systems with our simplified Hamiltonian models. The Anderson model, is itself a renormalized Hamiltonian, notionally derived from the elimination of high energy excitations from “the” microscopic Hamiltonian.

To carry out renormalization, the Hamiltonian of interest $H(D)$ is parameterized by its cutoff energy scale, D , the energy of the largest excitations. Renormalization involves reducing the cutoff to a slightly smaller value $D \rightarrow D' = D/b$ where $b > 1$. The excitations in the energy window $E \in [D', D]$ that are removed by this process, are said to have been integrated out of the Hilbert space, and in so doing they give rise to a new “effective” Hamiltonian \tilde{H}_L that continues to faithfully describe the remaining low-energy degrees of freedom. The energy scales are then rescaled, to obtain a new $H(D') = b\tilde{H}_L$ and the whole process is repeated.

Generically, the Hamiltonian can be divided into a block-diagonal form

$$H = \begin{bmatrix} H_L & V^\dagger \\ V & H_H \end{bmatrix} \quad (17.79)$$

where H_L and H_H act on states in the low-energy and high-energy subspaces respectively, and V and V^\dagger provide the matrix elements between them. The high energy degrees of freedom may be “integrated out”⁶ by carrying out a canonical transformation that eliminates the off-diagonal elements in this Hamiltonian \tilde{H}_L

$$H(D) \rightarrow \tilde{H} = UH(D)U^\dagger = \begin{bmatrix} \tilde{H}_L & 0 \\ 0 & \tilde{H}_H \end{bmatrix} \quad (17.80)$$

One then projects out the low energy component of the block-diagonalized Hamiltonian $\tilde{H}_L = P\tilde{H}P$. Finally, by rescaling

$$H(D') = b\tilde{H}_L \quad (17.81)$$

one arrives at a new Hamiltonian describing the physics on the reduced scale. The transformation from $H(D)$ to $H(D')$ is referred to as a “renormalization group” (RG) transformation. This term was coined long ago, even though the transformation does not form a real group, since there is no inverse transformation.

Repeated application of the RG procedure leads to a family of Hamiltonians $H(D)$. By taking the limit $b \rightarrow 1$, these Hamiltonians evolve, or “flow” continuously with D . Typically, H will contain a series of dimensionless parameters (coupling constants) $\{g_i\}$ which denote the strength of various interaction terms in the Hamiltonian. The evolution of these parameters with cut-off is given by a scaling equation. In the simplest case

$$\frac{\partial g_j}{\partial \ln D} = \beta_j(\{g_i\})$$

A negative β function denotes a “relevant” parameter which grows as the cut-off is reduced. A positive β

⁶ The term “integrating out” is originally derived from the path integral formulation of the renormalization group, in which high energy degrees of freedom are removed by integrating over these variables inside the path integral.

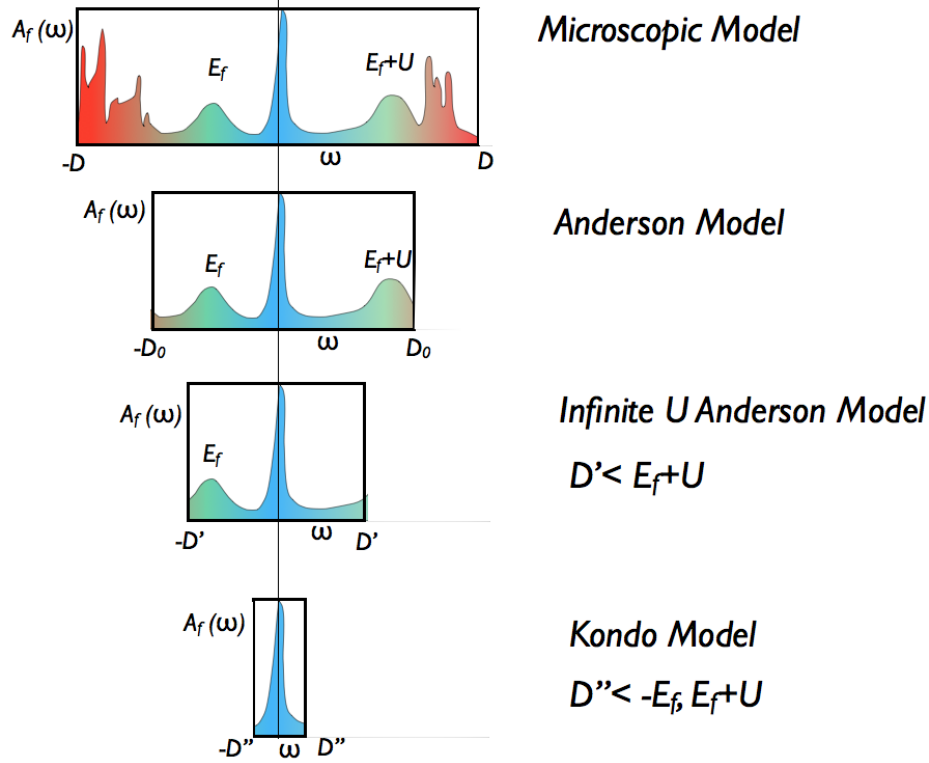


Fig. 17.12 Scaling concept. Low energy model Hamiltonians are obtained from the detailed original model by integrating out the high energy degrees of freedom. At each stage, the physics described by the model spans a successively lower frequency window in the excitation spectrum.

function denotes an “irrelevant” parameter constant which shrinks towards zero as the cut-off is reduced. There are two types of event that can occur in such a scaling procedure (Fig. 17.14):

- A *crossover*. When the cut-off energy scale D passes the characteristic energy scale of a particular class of high frequency excitations, then at lower energies, these excitations may only occur via a virtual process. When the effects of the virtual fluctuations associated with these high energy process are included into the Hamiltonian, it changes its structure.
- *Fixed Point*. If the cut-off energy scale drops below the lowest energy scale in the problem, then there are no further changes to occur in the Hamiltonian, which will now remain invariant under the scaling procedure (so that the β function of all remaining parameters in the Hamiltonian must vanish). This “*Fixed Point Hamiltonian*” describes the essence of the low energy physics.

Local moment physics involves a sequence of such cross-overs (Fig. 17.12.). The highest energy scales in the Anderson model, are associated with “valence fluctuations” into the empty and doubly occupied states

$$\begin{aligned} f^1 &\rightleftharpoons f^2 & \Delta E_I &= U + E_f > 0 \\ f^1 &\rightleftharpoons f^0 & \Delta E_{II} &= -E_f > 0 \end{aligned} \quad (17.82)$$

The successive elimination of these processes leads to two cross-overs. Suppose ΔE_I is the largest scale, then once $D < \Delta E_I$, charge fluctuations into the doubly occupied state are eliminated and the remaining low energy Hilbert space of the atom is

$$D < E_f + U : \quad |f^0\rangle, \quad |f^1, \sigma\rangle \quad (\sigma = \pm 1/2) \quad (17.83)$$

The operators that span this space are called ‘‘Hubbard operators’’[35], and they are denoted as follows

$$\begin{aligned} X_{\sigma 0} &= |f^1, \sigma\rangle\langle f^0| = P f^\dagger_\sigma, & X_{0\sigma} &= |f^0\rangle\langle f^1, \sigma| = f^\dagger_\sigma P, \\ X_{\sigma\sigma'} &= |f^1, \sigma\rangle\langle f^1, \sigma'| \end{aligned} \quad (17.84)$$

where $P = (1 - n_{f\uparrow}n_{f\downarrow})$ projects out doubly occupied states. (Note that the Hubbard operators $X_{\sigma 0} = P f^\dagger_\sigma$, can not be treated as simple creation operators, for they do not satisfy the canonical anticommutation algebra.) The corresponding renormalized Hamiltonian is the ‘‘Infinite U Anderson model’’,

$$H = \sum_{\mathbf{k}, \sigma} \epsilon_{\mathbf{k}} n_{\mathbf{k}\sigma} + [V(\mathbf{k}) c^\dagger_{\mathbf{k}\sigma} X_{0\sigma} + V(\mathbf{k})^* X_{\sigma 0} c_{\mathbf{k}\sigma}] + E_f \sum_{\sigma} X_{\sigma\sigma}. \quad (17.85)$$

Infinite U Anderson model

In this model, all the interactions are hidden inside the Hubbard operators.

Finally, once $D < \Delta E_{II}$, the low-energy Hilbert space no longer involves the f^2 or f^0 , states. The object left behind is a quantum top - a quantum mechanical object with purely spin degrees of freedom and a two dimensional⁷ Hilbert space

$$|f^1, \sigma\rangle, \quad (\sigma = \pm 1/2).$$

Now the residual spin degrees of freedom still interact with the surrounding conduction sea, for virtual charge fluctuations, in which an electron temporarily migrates off, or onto the ion lead, to spin-exchange between the local moment and the conduction sea. There are two such virtual processes:

$$\begin{aligned} e_\uparrow + f_\downarrow^1 &\leftrightarrow f^2 \leftrightarrow e_\downarrow + f_\uparrow^1 & \Delta E_I &\sim U + E_f \\ e_\uparrow + f_\downarrow^1 &\leftrightarrow e_\uparrow + e_\downarrow \leftrightarrow e_\downarrow + f_\uparrow^1 & \Delta E_{II} &\sim -E_f \end{aligned} \quad (17.86)$$

In both cases, spin exchange only takes place in the singlet channel, $S = 0$ state. From second-order perturbation theory, we know that these virtual charge fluctuations will selectively lower the energy of the singlet configurations by an amount of order $\Delta E = -J$, where

$$J \sim V^2 \left[\frac{1}{\Delta E_1} + \frac{1}{\Delta E_2} \right] = V^2 \left[\frac{1}{-E_f} + \frac{1}{E_f + U} \right]. \quad (17.87)$$

Here V is the size of the hybridization matrix element near the Fermi surface. The selective reduction in the energy of the singlet channel constitutes an effective antiferromagnetic interaction between the conduction electrons and the local moment. If we introduce $\vec{\sigma}(0) = \sum_{k,k'} c^\dagger_{k\alpha} \vec{\sigma}_{\alpha\beta} c_{k'\beta}$, measuring the the electron spin at the origin, then the effective interaction that lowers the energy of singlet combinations of conduction and

⁷ In the simplest version of the Anderson model, the local moment is a $S = 1/2$, but in more realistic atoms much large moments can be produced. For example, an electron in a Cerium Ce^{3+} ion atom lives in a $4f^1$ state. Here spin-orbit coupling combines orbital and spin angular momentum into a total angular momentum $j = l - 1/2 = 5/2$. The Cerium ion that forms thus has a spin $j = 5/2$ with a spin degeneracy of $2j + 1 = 6$. In multi-electron atoms, the situation can become still more complex, involving Hund’s coupling between atoms.

f-electrons will have the form $H_{eff} \sim J\vec{\sigma}(0) \cdot \vec{S}_f$. The resulting low-energy Hamiltonian that describes the interaction of a spin with a conduction sea is the deceptively simple “Kondo model”

$$H = \sum_{k\sigma} \epsilon_k c_{k\sigma}^\dagger c_{k\sigma} + \overbrace{J\psi^\dagger(0)\vec{\sigma}\psi(0)}^{\Delta H} \cdot \vec{S}_f. \quad (17.88)$$

Kondo model

This heuristic argument was ventured in Anderson’s paper on local moment formation in 1961. At the time, the antiferromagnetic sign in this interaction was entirely unexpected, for it had long been that exchange forces always induce a ferromagnetic interaction between the conduction sea and local moments. The innocuous-looking sign difference has deep consequences for the physics of local moments at low temperatures, giving rise to an interaction that grows as the temperature is lowered ultimately leading to a final cross-over into a low-energy Fermi liquid fixed point. The remaining sections of the chapter are devoted to following this process in detail.

17.6 Schrieffer-Wolff transformation

We now carry out the transformation that links the Anderson and Kondo models via a canonical transformation, first introduced by Schrieffer and Wolff[36, 37]. This transformation is a kind of one-step renormalization process in which the valence fluctuations are integrated out of the Anderson model. When a local moment forms, hybridization with the conduction sea induces virtual charge fluctuations. It’s useful to consider dividing the Hamiltonian into two terms

$$H = H_1 + \lambda \mathcal{V}$$

where λ is an expansion parameter. Here,

$$H_1 = H_{band} + H_{atomic} = \left[\begin{array}{c|c} H_L & 0 \\ \hline 0 & H_H \end{array} \right]$$

is diagonal in the low energy f^1 (H_L) and the high energy f^2 or f^0 (H_H) subspaces, whereas the hybridization term

$$\mathcal{V} = H_{mix} = \sum_{k\sigma} [V_k c_{k\sigma}^\dagger f_\sigma + \text{H.c.}] = \left[\begin{array}{c|c} 0 & V^\dagger \\ \hline V & 0 \end{array} \right]$$

provides the off-diagonal matrix elements between these two subspaces. The idea of the Schrieffer Wolff transformation is to carry out a canonical transformation that returns the Hamiltonian to block-diagonal form:

$$\mathcal{U} \left[\begin{array}{c|c} H_L & \lambda V^\dagger \\ \hline \lambda V & H_H \end{array} \right] \mathcal{U}^\dagger = \left[\begin{array}{c|c} H^* & 0 \\ \hline 0 & H' \end{array} \right]. \quad (17.89)$$

This is a “renormalized” Hamiltonian, and the block-diagonal part of this matrix $H^* = P_L H' P_L$ in the low energy subspace provides an *effective* Hamiltonian for the low energy physics. We now set $\mathcal{U} = e^S$, referring

to “ S ” as the “action operator”. Now since $\mathcal{U}^\dagger = \mathcal{U}^{-1} = e^{-S}$, this implies that the action operator $S^\dagger = -S$ is anti-hermitian. Writing S as a power series in λ ,

$$S = \lambda S_1 + \lambda^2 S_2 + \dots,$$

then by using the identity, $e^A B e^{-A} = B + [A, B] + \frac{1}{2!}[A, [A, B]] \dots$, (17.89) can also be expanded in powers of λ as follows

$$e^S (H_1 + \lambda \mathcal{V}) e^{-S} = H_1 + \lambda (\mathcal{V} + [S_1, H_1]) + \lambda^2 \left(\frac{1}{2} [S_1, [S_1, H_1]] + [S_1, \mathcal{V}] + [S_2, H_1] \right) + \dots$$

Since \mathcal{V} is not diagonal, by requiring

$$[S_1, H_1] = -\mathcal{V}, \quad (17.90)$$

we can eliminate all off-diagonal components to leading order in λ . To second order

$$e^S (H_1 + \lambda \mathcal{V}) e^{-S} = H_1 + \lambda^2 \left(\frac{1}{2} [S_1, \mathcal{V}] + [S_2, H_1] \right) + \dots \quad (17.91)$$

Since $[S_1, \mathcal{V}]$ is block-diagonal, we can satisfy (17.89) to second order by requiring $S_2 = 0$, so that to this order, the renormalized Hamiltonian has the form

$$H^* = H_L + \lambda^2 \Delta H \quad (17.92)$$

where

$$\Delta H = \frac{1}{2} P_L [S_1, \mathcal{V}] P_L + \dots \quad (17.93)$$

is an interaction term induced by virtual fluctuations into the high-energy manifold. Writing the action operator in matrix form,

$$S = \begin{bmatrix} 0 & -s^\dagger \\ s & 0 \end{bmatrix} \quad (17.94)$$

and substituting into (17.90), we obtain $V = -s H_L + H_H s$. Now since $(H_L)_{ab} = E_a^L \delta_{ab}$ and $(H_H)_{ab} = E_a^H \delta_{ab}$ are diagonal, it follows that

$$s_{ab} = \frac{V_{ab}}{E_a^H - E_b^L}, \quad -s_{ab}^\dagger = \frac{V_{ab}^\dagger}{E_a^L - E_b^H}, \quad , \quad (17.95)$$

or more schematically

$$S = \sum_{H,L} \left(|H\rangle \frac{\langle H|V|L\rangle}{E_H - E_L} \langle L| - \text{H.c.} \right) + O(V^3) \quad (17.96)$$

From (17.95), we obtain

$$\Delta H_{LL'} = -\frac{1}{2} (V^\dagger s + s^\dagger V)_{LL'} = -\frac{1}{2} \sum_H (V_{LH}^\dagger V_{HL'}) \left[\frac{1}{E_H - E_L} + \frac{1}{E_H - E_{L'}} \right] \quad (17.97)$$

Some important points about this result

- We recognize (17.97) as a simple generalization of second-order perturbation theory, including off-diagonal matrix elements by averaging over initial and final-state energy denominators.
- ΔH can also be written

$$\Delta H_{LL'} = \frac{1}{2}[T(E_L) + T(E_{L'})]$$

where

$$\begin{aligned} \hat{T}(E) &= P_L \mathcal{V} \frac{P_H}{E - H_1} \mathcal{V} P_L, \\ T_{LL'}(E) &= \sum_{|H\rangle} \left[\frac{V_{LH}^\dagger V_{HL'}}{E - E_H} \right] \end{aligned} \quad (17.98)$$

is the leading order expression for the many-body scattering T-matrix induced by scattering off \mathcal{V} . We can thus relate ΔH to a scattering amplitude, and schematically represent it by a Feynman diagram, illustrated in Fig. 17.13.

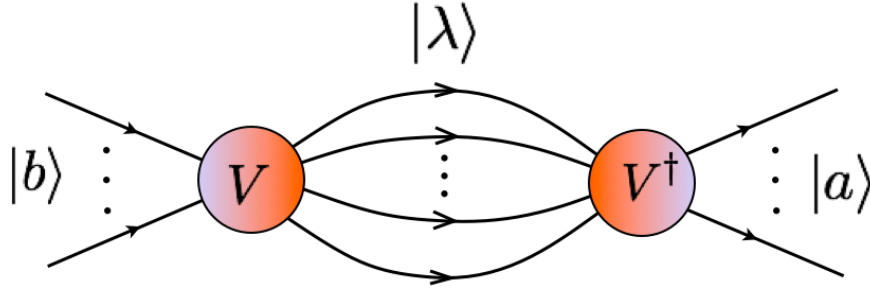


Fig. 17.13 T-matrix representation of interaction induced between states $|b\rangle$ and $|a\rangle$ by integrating out the virtual fluctuations into the high-energy states $|\lambda\rangle$.

- If the separation of the low and high energy subspaces is large, we can take $E_L \sim E_{L'}$, so that

$$\Delta H = T(E_L) = -\frac{1}{\Delta E_{HL}} (\mathcal{V} P_H \mathcal{V}) \quad (17.99)$$

where $\Delta E_{HL} = E_H - E_L$ is the energy of excitation into the high energy subspace and $P_H = \sum_{|H\rangle} |H\rangle \langle H|$.

We now apply this method to the Anderson model for which the atomic ground-state is a local moment f^1 configuration. In this case, there are two high-energy intermediate states corresponding to f^0 and f^2 configurations. When a conduction electron or hole is excited into the localized f-state to create these excited state configurations, the corresponding excitation energies are $\Delta E(f^1 \rightarrow f^0) = -E_f$ and $\Delta E(f^1 \rightarrow f^2) = E_f + U$. The hybridization $\mathcal{V} = \sum_{\mathbf{k}\sigma} [V(\mathbf{k}) c_{\mathbf{k}\sigma}^\dagger f_\sigma + \text{H.c.}]$ generates virtual fluctuations into these excited states. Using (17.99), the interaction induced by these fluctuations is given by

$$\Delta H = -\frac{VP[f^2]V}{E_f + U} - \frac{VP[f^0]V}{-E_f}$$

$$= - \sum_{k\alpha, k'\beta} V_{k'}^* V_k \left[\overbrace{\frac{(c_{k\alpha}^\dagger f_\alpha)(f_{\beta k'}^\dagger c_{k'\beta})}{E_f + U}}^{f^1 + e^- \leftrightarrow f^2} + \overbrace{\frac{(f_{\beta k'}^\dagger c_{k'\beta})(c_{k\alpha}^\dagger f_\alpha)}{-E_f}}^{f^1 \leftrightarrow f^0 + e^-} \right] P_{n_f=1} \quad (17.100)$$

where $P_{n_f=1} = (n_{f\uparrow} - n_{f\downarrow})^2$ projects into the subspace of unit occupancy. Using the Fierz identity⁸ $2\delta_{\alpha\gamma}\delta_{\eta\beta} = \delta_{\alpha\beta}\delta_{\eta\gamma} + \vec{\sigma}_{\alpha\beta} \cdot \vec{\sigma}_{\eta\gamma}$ we may recast the spin exchange terms in terms of Pauli matrices as follows

$$\begin{aligned} (c_{k\alpha}^\dagger f_\alpha)(f_{\beta k'}^\dagger c_{k'\beta}) &= (c_{k\alpha}^\dagger f_\gamma)(f_{\eta k'}^\dagger c_{k'\beta}) \times \overbrace{(\delta_{\alpha\gamma}\delta_{\eta\beta})}^{\frac{1}{2}(\delta_{\alpha\beta}\delta_{\eta\gamma} + \vec{\sigma}_{\alpha\beta} \cdot \vec{\sigma}_{\eta\gamma})} \\ &= \frac{1}{2} c_{k\alpha}^\dagger c_{k'\alpha} - (c_{k\alpha}^\dagger \vec{\sigma}_{\alpha\beta} c_{k'\beta}) \cdot \vec{S}_f, \end{aligned} \quad (17.101)$$

and similarly

$$(f_{\beta k'}^\dagger c_{k'\beta})(c_{k\alpha}^\dagger f_\alpha) = -\frac{1}{2} c_{k\alpha}^\dagger c_{k'\alpha} - (c_{k\alpha}^\dagger \vec{\sigma}_{\alpha\beta} c_{k'\beta}) \cdot \vec{S}_f. \quad (17.102)$$

(where we have replaced $n_f = 1$ and dropped residual constants in both cases). The operator

$$\vec{S}_f \equiv f^\dagger_\sigma \left(\frac{\vec{\sigma}_{\alpha\beta}}{2} \right) f_\beta, \quad (n_f = 1) \quad (17.103)$$

describes the spin of the f-electron. The induced interaction is then

$$\Delta H = \sum_{k\alpha, k'\beta} J_{k,k'} c_{k\alpha}^\dagger \vec{\sigma}_{\alpha\beta} c_{k'\beta} \cdot \vec{S}_f + H' \quad (17.104)$$

where

$$J_{k,k'} = V_{k'}^* V_k \left[\overbrace{\frac{1}{E_f + U}}^{f^1 + e^- \leftrightarrow f^2} + \overbrace{\frac{1}{-E_f}}^{f^1 \leftrightarrow f^0 + e^-} \right] \quad (17.105)$$

is the Kondo coupling constant.

Notice how, in the low energy subspace, the occupancy of the f-state is constrained to $n_f = 1$. This fermionic representation (17.103) of the spin operator proves to be very useful. Apart from a constant, the second term

$$H' = -\frac{1}{2} \sum_{k,k'\sigma} V_{k'}^* V_k \left[\frac{1}{E_f + U} + \frac{1}{E_f} \right] c_{k\sigma}^\dagger c_{k'\sigma}$$

is a residual potential scattering term. This term vanishes for the particle-hole symmetric case $E_f = -(E_f + U)$ and will be dropped, since it does not involve the internal dynamics of the local moment. Summarizing, the effect of the high-frequency valence fluctuations is to induce an antiferromagnetic coupling between the local spin density of the conduction electrons and the local moment:

⁸ This identity is obtained by expanding an arbitrary two dimensional matrix A in terms of Pauli matrices. If we write $A_{\alpha\beta} = \frac{1}{2} \text{Tr}[A \underline{1}] \delta_{\alpha\beta} + \frac{1}{2} \text{Tr}[A \vec{\sigma}] \cdot \vec{\sigma}_{\alpha\beta}$ and read off the coefficients of A inside the traces, we obtain the inequality.

$$H = \sum_{k\sigma} \epsilon_k c_{k\sigma}^\dagger c_{k\sigma} + \sum_{k,k'} J_{k,k'} c_{k\sigma}^\dagger \vec{\sigma} c_{k'\sigma} \cdot \vec{S}_f \quad (17.106)$$

This is the famous “Kondo model”. For many purposes, the k dependence of the coupling constant can be dropped, so that the Kondo model takes the deceptively simple form

$$H = \sum_{k\sigma} \epsilon_k c_{k\sigma}^\dagger c_{k\sigma} + \overbrace{J \vec{\sigma}(0) \cdot \vec{S}_f}^{\Delta H}. \quad (17.107)$$

Kondo model

where $\psi_\alpha(0) = \sum_k c_{k\alpha}$ is the electron operator at the origin and $\vec{\sigma}(0) = \psi^\dagger(0) \vec{\sigma} \psi(0)$ is the spin density at the origin. In other words, there is a simple point-interaction between the spin density of the metal at the origin and the local moment.

Example 17.4: Details of the Schrieffer Wolff Transformation

Show that the “action operator” S for the canonical transformation transformation $H \rightarrow H^* = e^S H e^{-S}$ that effects the Schrieffer Wolff transformation from the Anderson model (17.2) to the Kondo model (17.107), is given by [36, 37]

$$S = \sum_{\mathbf{k}, \sigma} \left[V_{\mathbf{k}} c_{\mathbf{k}\sigma}^\dagger f_{\sigma} \left(\frac{1 - n_{f-\sigma}}{\epsilon_{\mathbf{k}} - E_f} + \frac{n_{f\sigma}}{\epsilon_{\mathbf{k}} - (E_f + U)} \right) - \text{H.c.} \right] + O(V^3) \quad (17.108)$$

Solution:

Using (17.95), we may write the “action operator” S as

$$S = \sum_{H,L} \left[|H\rangle \frac{\langle H|V|L\rangle}{E_H - E_L} \langle L| - \text{H.c.} \right] + O(V^3) \quad (17.109)$$

where, “L” and “H” denote the low and high energy subspaces respectively. For the Anderson model, $\hat{V} = \sum_{\mathbf{k}, \sigma} (V_{\mathbf{k}} c_{\mathbf{k}\sigma}^\dagger f_{\sigma} + \text{H.c.})$ is the hybridization, while the low-energy Hilbert space are the states with $n_f = 1$. The projector into the low energy subspace H is $P_L = (n_{f\uparrow} - n_{f\downarrow})^2$, so we may write $\langle H|V|L\rangle = \langle H|VP_L|L\rangle$, so that

$$S = \sum_{H,L, \mathbf{k}\sigma} \left(|H\rangle \langle H| \frac{(V_{\mathbf{k}} c_{\mathbf{k}\sigma}^\dagger f_{\sigma} + V_{\mathbf{k}}^* f_{\sigma}^\dagger c_{\mathbf{k}\sigma}) (n_{f\uparrow} - n_{f\downarrow})^2}{E_H - E_L} |L\rangle \langle L| - \text{H.c.} \right) + O(V^3). \quad (17.110)$$

Now the initial state has energy E_f while the excited state is either a state with one conduction electron, no f-electrons, energy $\epsilon_{\mathbf{k}}$, or a state with two f-electrons, one conduction hole, energy $2E_f + U - \epsilon_{\mathbf{k}}$, so we may write

$$S = \sum_{\mathbf{k}\sigma} \left[V_{\mathbf{k}} \frac{c_{\mathbf{k}\sigma}^\dagger f_{\sigma} (1 - n_{f-\sigma})}{\epsilon_{\mathbf{k}} - E_f} + V_{\mathbf{k}}^* \frac{f_{\sigma}^\dagger c_{\mathbf{k}\sigma} n_{f-\sigma}}{E_f + U - \epsilon_{\mathbf{k}}} - \text{H.c.} \right] + O(V^3) \quad (17.111)$$

where we have replaced $f_{\sigma}(n_{f\uparrow} - n_{f\downarrow})^2 = f_{\sigma}(1 - n_{f-\sigma})^2 = f_{\sigma}(1 - n_{f-\sigma})$ and $f_{\sigma}^\dagger (n_{f\uparrow} - n_{f\downarrow})^2 =$

$f^\dagger_\sigma n_{f-\sigma}^2 = f^\dagger_\sigma n_{f-\sigma}$. Rearranging this a little, we obtain

$$S = \sum_{\mathbf{k}, \sigma} \left[V_{\mathbf{k}} \left((1 - n_{f-\sigma}) \frac{c^\dagger_{\mathbf{k}\sigma} f_\sigma}{\epsilon_{\mathbf{k}} - E_f} + n_{f-\sigma} \frac{c^\dagger_{\mathbf{k}\sigma} f_\sigma}{\epsilon_{\mathbf{k}} - (E_f + U)} \right) - \text{H.c.} \right] + O(V^3), \quad (17.112)$$

Example 17.5: Composite nature of the f-electron

The Kondo model only involves the spin of the f-electron, and the f-creation and annihilation operators have apparently, completely disappeared. To find out what has happened to them, consider adding a source term for the f-electrons

$$H_S = \sum_{\sigma} (f^\dagger_\sigma \eta_\sigma + \bar{\eta}_\sigma f)_\sigma \quad (17.113)$$

into the Anderson impurity model, so that now $H \rightarrow H[\bar{\eta}, \eta] = H + H_S$, so that the functional derivatives of the partition function

$$Z[\eta_\sigma, \eta_\sigma] = Z_0 \langle T \exp \left[- \int_0^\beta d\tau f^\dagger_\sigma(\tau) \eta_\sigma(\tau) + \bar{\eta}_\sigma(\tau) f_\sigma(\tau) \right] \rangle \quad (17.114)$$

generate correlation functions of the fermion operators,

$$\frac{\delta}{\delta \bar{\eta}_\sigma} \rightarrow f_\sigma(\tau), \quad \frac{\delta}{\delta \eta_\sigma} \rightarrow f^\dagger_\sigma(\tau), \quad (17.115)$$

- (a) Repeat the a Schrieffer Wolff transformation the case of constant hybridization $V_{\mathbf{k}} = V$ and particle-hole symmetry to show that the Kondo model with source terms now becoems

$$H_K[\bar{\eta}, \eta] = \sum_{\mathbf{k}\sigma} \epsilon_{\mathbf{k}} c^\dagger_{\mathbf{k}\sigma} c_\sigma + J \left(\psi^\dagger(0) + V^{-1} \bar{\eta} \right) \vec{\sigma} \left(\psi(0) + V^{-1} \eta \right) \cdot \mathbf{S} \quad (17.116)$$

- (b) By differentiating this expression with respect to $\bar{\eta}_\sigma$, show that in the Kondo model, the original f-electron operator has now become a “composite operator” involving a combined conduction electron and a spin-flip as follows

$$f_\sigma \equiv \frac{\delta H_K[\bar{\eta}, \eta]}{\delta \bar{\eta}_\sigma} = \frac{J}{V} \left(\sigma_{\alpha\beta} \cdot \vec{S} \right) \psi(0)_\beta. \quad (17.117)$$

When a Fermi liqui develops, it is this object that behaves like a resonant bound-state fermion.

Solution:

- (a) In the Anderson model, we can absorb the source term into the hybridization, writing it in the form

$$\mathcal{V} = \sum_{\sigma} (V \psi^\dagger_\sigma(0) + \bar{\eta}_\sigma) f_\sigma + \text{H.c.} \quad (17.118)$$

so that in the hybridization, we have replaced $\psi_\sigma(0) \rightarrow \psi_\sigma(0) + \frac{1}{V} \eta_\sigma$. If we now repeat the Schrieffer Wolff transformation, the spin exchange term in the Kondo model takes the form

$$H_K[\bar{\eta}, \eta] = \sum_{\mathbf{k}\sigma} \epsilon_{\mathbf{k}} c^\dagger_{\mathbf{k}\sigma} c_\sigma + J \left(\psi^\dagger(0) + V^{-1} \bar{\eta} \right) \vec{\sigma} \left(\psi(0) + V^{-1} \eta \right) \cdot \mathbf{S} \quad (17.119)$$

- (b) If we now differentiate H_K with respect to $\bar{\eta}$, we obtain

$$f_\sigma \equiv \left. \frac{\delta H_K[\bar{\eta}, \eta]}{\delta \eta_\sigma} \right|_{\eta, \bar{\eta}=0} = \frac{J}{V} [(\vec{\sigma} \cdot \mathbf{S}) \psi(0)]_\sigma. \quad (17.120)$$

17.7 “Poor Man” Scaling

We now apply the scaling concept to the Kondo model. This was originally carried out by Anderson and Yuval[31, 38, 39] using a method formulated in the time, rather than energy domain. The method presented here follows Anderson’s “Poor Man’s” scaling approach[32, 40], in which the evolution of the coupling constant is followed as the band-width of the conduction sea is reduced. The Kondo model is written

$$H = \sum_{|\epsilon_k| < D} \epsilon_k c_{k\sigma}^\dagger c_{k\sigma} + H^{(I)}$$

$$H^{(I)} = J(D) \sum_{|\epsilon_k|, |\epsilon_{k'}| < D} c_{k\alpha}^\dagger \vec{\sigma}_{\alpha\beta} c_{k'\beta} \cdot \vec{S}_f \quad (17.121)$$

where the density of conduction electron states $\rho(\epsilon)$ is taken to be constant. The Poor Man’s renormalization procedure follows the evolution of $J(D)$ that results from reducing D by progressively integrating out the electron states at the edge of the conduction band. In the Poor Man’s procedure, the band-width is not rescaled to its original size after each renormalization, which avoids the need to renormalize the electron operators so that instead of Eq. (17.81), $H(D') = \tilde{H}_L$.

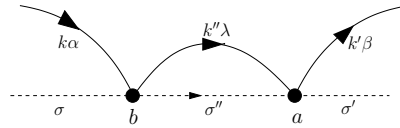
To carry out the renormalization procedure, we integrate out the high-energy spin fluctuations using the t-matrix formulation for the induced interaction ΔH , derived in the last section. Formally, the induced interaction is given by

$$\Delta H_{ab} = \frac{1}{2} [T_{ab}(E_a) + T_{ab}(E_b)]$$

where

$$T_{ab}(E) = \sum_{\lambda \in [H]} \left[\frac{H_{a\lambda}^{(I)} H_{\lambda b}^{(I)}}{E - E_\lambda^H} \right]$$

where the energy of state $|\lambda\rangle$ lies in the range $[D', D]$. There are two possible intermediate states that can be produced by the action of $H^{(I)}$ on a one-electron state: (I) either the electron state is scattered directly, or (II) a virtual electron hole-pair is created in the intermediate state. In process (I), the T-matrix can be represented by the Feynman diagram

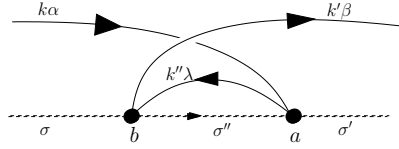


for which the T-matrix for scattering into a high energy electron state is

$$T^{(I)}(E)_{k'\beta\sigma'; k\alpha\sigma} = \sum_{\epsilon_{k''} \in [D-\delta D, D]} \left[\frac{1}{E - \epsilon_{k''}} \right] J^2 (\sigma^a \sigma^b)_{\beta\alpha} (S^a S^b)_{\sigma'\sigma}$$

$$\approx J^2 \rho \delta D \left[\frac{1}{E - D} \right] (\sigma^a \sigma^b)_{\beta\alpha} (S^a S^b)_{\sigma'\sigma} \quad (17.122)$$

In process (II),



the formation of a particle-hole pair involves a conduction electron line that crosses itself, leading to a negative sign. Notice how the spin operators of the conduction sea and antiferromagnet reverse their relative order in process II, so that the T-matrix for scattering into a high-energy hole-state is given by

$$\begin{aligned} T^{(II)}(E)_{k'\beta\sigma';k\alpha\sigma} &= - \sum_{\epsilon_{k''} \in [-D, -D+\delta D]} \left[\frac{1}{E - (\epsilon_k + \epsilon_{k'} - \epsilon_{k''})} \right] J^2 (\sigma^b \sigma^a)_{\beta\alpha} (S^a S^b)_{\sigma'\sigma} \\ &= -J^2 \rho \delta D \left[\frac{1}{E - D} \right] (\sigma^b \sigma^a)_{\beta\alpha} (S^a S^b)_{\sigma'\sigma} \end{aligned} \quad (17.123)$$

where we have assumed that the energies ϵ_k and $\epsilon_{k'}$ are negligible compared with D . Adding (Eq. 17.122) and (Eq. 17.123) gives

$$\begin{aligned} \delta H_{k'\beta\sigma';k\alpha\sigma}^{int} &= \hat{T}^I + \hat{T}^{II} = -\frac{J^2 \rho |\delta D|}{D} [\sigma^a, \sigma^b]_{\beta\alpha} S^a S^b \\ &= \frac{J^2 \rho |\delta D|}{D} \vec{\sigma}_{\beta\alpha} \cdot \vec{S}_{\sigma'\sigma}. \end{aligned} \quad (17.124)$$

In this way we see that the virtual emission of a high energy electron and hole generates an antiferromagnetic correction to the original Kondo coupling constant

$$J(D - |\delta D|) = J(D) + 2J^2 \rho \frac{|\delta D|}{D} = J(D) - 2J^2 \rho \frac{\delta D}{D}, \quad (17.125)$$

since we have reduced the band-width, $\delta D = -|\delta D|$. In other words,

$$\frac{\partial J \rho}{\partial \ln D} = -2(J\rho)^2 \quad (17.126)$$

or in terms of the dimensionless coupling constant $g = \rho J$,

$$\frac{\partial g}{\partial \ln D} = \beta(g) = -2g^2 + O(g^3). \quad (17.127)$$

Now since $\beta(g = 0) = 0$ at $g = 0$ scaling comes to halt: we say that $g = 0$ is a “fixed point”. It is instructive to rewrite the scaling equation in the form

$$\frac{\partial \ln g}{\partial \ln(D_0/D)} = 2g + O(g^2) \quad (17.128)$$

where D_0 is the initial band-width. From this form, we see that as the cutoff is reduced, (see Fig. 17.14.),

- for antiferromagnetic $J > 0$, the magnitude of g grows. We say that the fixed point is *repulsive*. In other words, spin fluctuations antiscreen the antiferromagnetic interaction causing it to grow at low energies.
- for ferromagnetic ($J < 0$), scaling reduces the magnitude of g , driving one ever closer to the weak coupling fixed point at $g = 0$. In this case, the fixed point is attractive and interaction weakens at low energies, causing J to scale slowly to zero.

To examine these two cases in more detail, we integrate the scaling equation between the initial band-width D_0 and D' , writing

$$\int_{g_0}^{g(D)} \frac{dg'}{g'^2} = -2 \int_{\ln D_0}^{\ln D'} d \ln D' \quad (17.129)$$

or

$$\left(\frac{1}{g_0} - \frac{1}{g(D')} \right) = -2 \ln(D'/D_0) \quad (17.130)$$

where $g_0 = J\rho = g(D_0)$ is the unrenormalized coupling constant at the original band-width D_0 . In this case,

$$g(D') = \frac{g_0}{1 - 2g_0 \ln \frac{D_0}{D'}} \quad (17.131)$$

Let us look at the ferromagnetic and antiferromagnetic cases separately.

Ferromagnetic Interaction $g_0 < 0$

In this case

$$g(D') = -\frac{|g_o|}{1 + 2|g_o| \ln(D_0/D')} \quad (17.132)$$

which corresponds to a very gradual decoupling of the local moment from the surrounding conduction sea. The interaction is said to marginally irrelevant, because it scales logarithmically to zero, and at all scales, the problem remains perturbative.

Antiferromagnetic Interaction $g > 0$

For the antiferromagnetic case ($g > 0$), the the solution to the scaling equation is

$$g(D') = \frac{g_o}{1 - 2g_o \ln(D/D')} = \frac{1}{2} \frac{1}{\ln(D'/D_0) + \frac{1}{2g_o}} = \frac{1}{2} \frac{1}{\ln \left[\frac{D'}{D_0 \exp(-1/(2g_o))} \right]} \quad (17.133)$$

where we have divided numerator and denominator by $2g_o$. It follows that

$$2g(D') = \frac{1}{\ln(D'/T_K)},$$

where we have introduced the Kondo temperature

$$T_K = D_0 \exp \left[-\frac{1}{2g_o} \right] \quad (17.134)$$

The “Kondo temperature” T_K is an example of a dynamically generated scale.

Were we to take this equation literally, we would say that g diverges at the scale $D' = T_K$. This interpretation is too literal, because the scaling has only been calculated to order g^2 , nevertheless it does show that the Kondo interaction can only be treated perturbatively at energies large compared with the Kondo temperature. We also see that once we have written the coupling constant in terms of the Kondo temperature, all reference to the original cut-off energy scale vanishes from the expression. This cut-off independence of the problem is an indication that the physics of the Kondo problem does not depend on the high energy details of the model: there is only one relevant energy scale, the Kondo temperature.

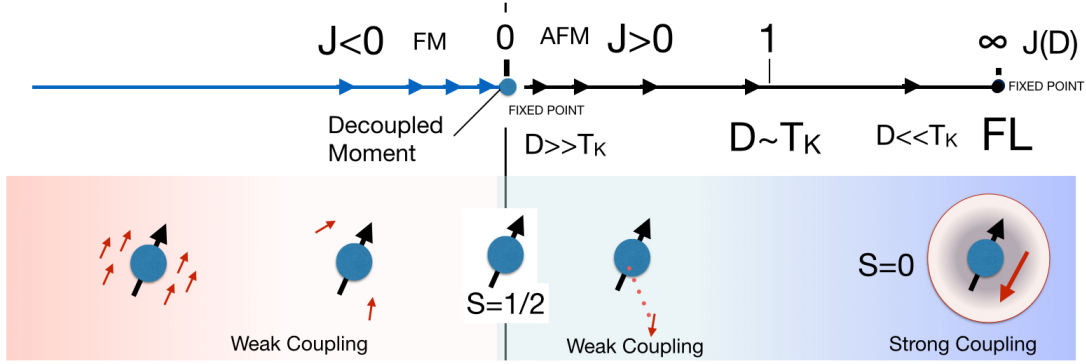


Fig. 17.14 Schematic illustration of renormalization group flow in the Kondo model. For $J < 0$ (ferromagnetic) the coupling constant scales to an attractive fixed point at $J = 0$, forming a decoupled local moment. For $J > 0$ (antiferromagnetic), scaling proceeds from a repulsive “weak coupling” fixed point, via a crossover to an attractive strong coupling fixed point in which the local moment is screened by the conduction electrons, removing its internal degrees of freedom to form a Fermi liquid.

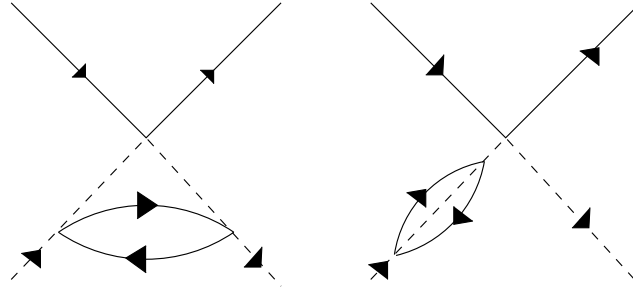


Fig. 17.15 Diagrams contributing to the third-order term in the beta function. See Ex. 17.8.

By calculating the higher order diagrams shown in fig 17.15, it is straightforward, though somewhat technical (see Ex. 17.8), to show that the beta-function to order g^3 is given by

$$\frac{\partial g}{\partial \ln D} = \beta(g) = -2g^2 + 2g^3 + O(g^4) \quad (17.135)$$

One can integrate this equation to obtain

$$\ln\left(\frac{D'}{D}\right) = \int_{g_0}^g \frac{dg'}{\beta(g')} = -\frac{1}{2} \int_{g_0}^g dg' \left[\frac{1}{g'^2} + \frac{1}{g'} + O(1) \right] \quad (17.136)$$

where we have expanded the numerator in $\frac{1}{\beta(g)} \approx -\frac{1}{g^2(1-g)} - \frac{1}{g^2}(1+g) + O(1)$. A better estimate of the temperature T_K where the system scales to strong coupling is obtained by setting $D' = T_K$ and $g = 1$ in this

equation, which gives

$$\ln\left(\frac{T_K}{D}\right) = -\frac{1}{2} \int_{g_0}^1 dg' \left[\frac{1}{g'^2} + \frac{1}{g'} \right] = -\frac{1}{2g_0} + \frac{1}{2} \ln 2g_0 + O(1), \quad (17.137)$$

where we have dropped the terms of order unity on the right hand side. Thus, up to a pre-factor, the dependence of the Kondo temperature on the bare coupling constant is given by

$$T_K = D_0 \sqrt{2g_0} e^{-\frac{1}{2g_0}}. \quad (17.138)$$

The square-root $\sqrt{g_0}$ dependence on the coupling constant is often dropped in qualitative discussion, but it is important for more quantitative comparison.

17.7.1 Abrikosov Pseudo Fermions and the Popov Fedatov method

One tool that is particularly useful for detailed Kondo model calculations, is the Abrikosov pseudo-fermion representation[23], in which the spin operator, is factorized in terms of a spin 1/2 fermion field f^\dagger_σ , as follows

$$\vec{S} = f^\dagger_\alpha \left(\frac{\vec{\sigma}}{2} \right)_{\alpha\beta} f_\beta. \quad (17.139)$$

This has the advantage that one can now take advantage of Wick’s theorem. In Abrikosov’s representation, the up and down states of the spin are now represented by the states

$$|\sigma\rangle = f^\dagger_\sigma |0\rangle, \quad (\sigma = \uparrow, \downarrow). \quad (17.140)$$

However, by using the f-electron, one has inadvertently expanded the Hilbert space, introducing two unphysical states- the empty state $|0\rangle$ and the doubly occupied state $|\uparrow\downarrow\rangle = f^\dagger_\downarrow f^\dagger_\uparrow |0\rangle$ which need to be eliminated by requiring that

$$n_f = 1. \quad (17.141)$$

One way to impose this constraint, is to use the “Popov-Fedotov trick”[41], which introduces a complex chemical potential for the f-electrons

$$\mu = -i\pi \frac{T}{2}$$

The partition function of the Hamiltonian is written as an unconstrained trace over the conduction and pseudo-fermion Fock spaces,

$$Z = \text{Tr} \left[e^{-\beta(H + i\pi \frac{T}{2} (n_f - 1))} \right] \quad (17.142)$$

Now since the Hamiltonian conserves n_f , we can divide this trace up into contributions from the d^0 , d^1 and d^2 subspaces, as follows:

$$Z = e^{i\pi/2} Z(f^0) + Z(f^1) + e^{-i\pi/2} Z(f^2)$$

But since $S_f = 0$ in the f^2 and d^0 subspaces, $Z(f^0) = Z(f^2)$ so that the contributions to the partition function from these two unwanted subspaces exactly cancel. You can test this method by applying it to a free spin in a magnetic field. (see example 17.6)

Example 17.6: Test the Popov-Fedotov trick[41]. Consider the magnetization of a free electron with Hamiltonian

$$H = \epsilon_\sigma f_\sigma^\dagger f_\sigma. \quad (17.143)$$

Show that with $\epsilon_\sigma = -\sigma B$ you obtain the wrong field dependence of the magnetization $M = \tanh\left(\frac{B}{2T}\right)$, but that with the Popov-Fedotov form $\epsilon_\sigma = -\sigma B + \frac{i\pi T}{2}$, you recover the Brillouin formula for a free spin,

$$M = \tanh\left(\frac{B}{T}\right). \quad (17.144)$$

Solution: If we write

$$F = -T \sum_{\sigma=\pm} \ln[1 + e^{-\beta\epsilon_\sigma}] \quad (17.145)$$

then the magnetization is given by

$$M = -\frac{\partial F}{\partial B} = \sum_{\sigma} \sigma f(\epsilon_\sigma) \quad (17.146)$$

If we evaluate this expression with $\epsilon_\sigma = -\sigma B$ we obtain the wrong form for the magnetization

$$M = \frac{1}{e^{-\beta B} + 1} - \frac{1}{e^{\beta B} + 1} = \frac{(e^{\beta B} - e^{-\beta B})}{2 + 2 \cosh \beta B} \quad (17.147)$$

We can see the problem: the extra contribution to the partition function from the empty and doubly occupied sites gives $Z = 2 + 2 \cosh \beta B$ rather than $Z = 2 \cosh \beta B$. If we simplify this expression, we obtain

$$M = \frac{\sinh \beta B}{1 + \cosh \beta B} = \frac{2 \sinh(\beta B/2) \cosh(\beta B/2)}{2 \cosh^2(\beta B/2)} = \tanh\left(\frac{B}{2T}\right)$$

which has the wrong field dependence. By contrast, if we use $\epsilon_\sigma = -\sigma B + \frac{i\pi T}{2}$, we obtain

$$M = \frac{1}{ie^{-\beta B} + 1} - \frac{1}{ie^{\beta B} + 1} = \frac{(e^{\beta B} - e^{-\beta B})}{2 \cosh \beta B} = \tanh\left(\frac{B}{T}\right) \quad (17.148)$$

recovering the Brillouin function.

Example 17.7: Consider the symmetric Anderson model. At energy scales greater than $U/2$ the impurity is mixed valent. However, once the cut-off $D \sim U/2$ one must carry out a Schrieffer Wolff transformation.

- (i) Show that the Kondo coupling constant of the symmetric Anderson model is $g_0 = J\rho = 4\Delta/(\pi U)$, where $\Delta = \pi\rho V^2$ is the bare resonant level width of the Anderson model
- (ii) Using expression (17.138), with a cut-off $D = U/2$, derive the following form (17.69) for the Kondo temperature of the symmetric Anderson model

$$T_K = \sqrt{\frac{2U\Delta}{\pi}} \exp\left(-\frac{\pi U}{8\Delta}\right).$$

Solution:

- (i) In the symmetric Anderson model, $E_f = -U/2$. Assuming that the hybridization $V_k = V$ is constant, then from (17.105), the Kondo coupling constant is given by

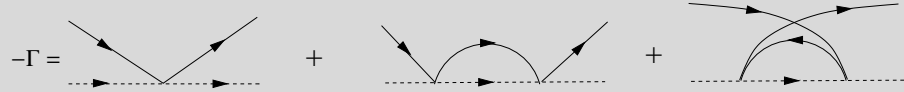
$$g_0 = J\rho = V^2\rho \left[\frac{1}{E_f + U/2} + \frac{1}{-E_f} \right] = 4 \frac{V^2\rho}{U} = \frac{4\Delta}{\pi U} \quad (17.149)$$

where $\Delta = \pi\rho V^2$.

(ii) Using (17.138) $T_K = D \sqrt{2g_o} e^{-\frac{1}{2g_o}}$, with $D = U/2$, we obtain

$$T_K = \frac{U}{2} \sqrt{\frac{8\Delta}{\pi U}} \exp\left(-\frac{8\Delta}{\pi U}\right) = \sqrt{\frac{2U\Delta}{\pi}} \exp\left(-\frac{\pi U}{8\Delta}\right). \quad (17.150)$$

Example 17.8: Explicitly calculate the Kondo scattering amplitude



to second order in J , using the Popov-Fedotov scheme. By examining the scattering amplitude on the Fermi surface, show that the Kondo coupling constant is logarithmically enhanced according to the formula

$$J\rho \rightarrow J\rho + 2(J\rho)^2 \ln \left[\frac{De^{\pi/2 - \psi(\frac{1}{2})}}{2\pi T} \right] \quad (17.151)$$

where $\psi(x)$ is the digamma function.

Solution:

We represent the conduction electron and f-electron propagators by the diagrams

$$\begin{aligned} \text{---} \blacktriangleright \text{---} &= G_c(i\omega_n, \mathbf{k}) = \frac{1}{i\omega_n - \epsilon_{\mathbf{k}}} \\ \text{---} \blacktriangleright \text{---} &= G_f(i\omega_n) = \frac{1}{i\omega_n - \lambda_f} \end{aligned} \quad (17.152)$$

where $\lambda_f \equiv i\frac{\pi T}{2}$ is the imaginary chemical potential that cancels the doubly occupied and empty states. The first order Kondo scattering amplitude is given by

$$\Gamma_0 = \begin{array}{c} \alpha \\ \swarrow \\ \text{---} \blacktriangleright \text{---} \\ \searrow \\ \beta \\ \sigma \end{array} = -J (\vec{\sigma}_{\beta\alpha} \cdot \vec{S}_{\sigma'\sigma}) \quad \left(\vec{S}_{\sigma'\sigma} \equiv \left(\frac{\vec{\sigma}}{2} \right)_{\sigma'\sigma} \right). \quad (17.153)$$

Here the minus sign derives from the Feynman rules for an interaction vertex and we have used the shorthand $\vec{S} \equiv \frac{\vec{\sigma}}{2}$ for the f-electron spin matrix elements.

The second-order scattering processes are given by

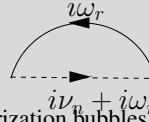
$$\Gamma_I = \begin{array}{c} \alpha \\ \swarrow \\ \text{---} \blacktriangleright \text{---} \\ \searrow \\ \beta \\ \sigma \end{array} = J^2 (\sigma^b \sigma^a)_{\beta\alpha} (S^b S^a)_{\sigma'\sigma} \pi_1(i\nu_n) \quad (17.154)$$

$$\Gamma_{II} = \begin{array}{c} \alpha \\ \swarrow \\ \text{---} \blacktriangleright \text{---} \\ \searrow \\ \beta \\ \sigma \end{array} = -J^2 (\sigma^a \sigma^b)_{\beta\alpha} (S^b S^a)_{\sigma'\sigma} \pi_2(i\nu_n) \quad (17.155)$$

where $i\nu_n$ is the total energy in the particle-particle and particle-hole channels respectively. Note the -1 prefactor in Γ_{II} and the inversion of the order of the conduction electron Pauli matrices which both derive from the crossing of the incoming and outgoing conduction electron lines Here

$$\begin{array}{c} i\omega_r \\ \uparrow \\ \text{---} \blacktriangleright \text{---} \\ \downarrow \\ i\nu_n - i\omega_r \end{array} = \pi_1(i\nu_n) = T \sum_{i\omega_r, \mathbf{k}} \frac{1}{i\omega_r - \epsilon_{\mathbf{k}}} \frac{1}{i\nu_n - i\omega_r - \lambda_f}, \quad (17.156)$$

and

$$\pi_2(i\nu_n) = -T \sum_{i\omega_r, \mathbf{k}} \frac{1}{i\omega_r - \epsilon_{\mathbf{k}}} \frac{1}{i\nu_n + i\omega_r - \lambda_f}, \quad (17.157)$$


are the Kondo polarization bubbles in the particle-particle and particle-hole channels, respectively

Now let us calculate the polarization bubbles (17.156) and (17.157). If we reverse the sign of $i\omega_r \rightarrow -i\omega_r$ in the internal summation in (17.156) we obtain

$$\pi_1(i\nu_n) = -T \sum_{i\omega_r, \mathbf{k}} \frac{1}{i\omega_r + \epsilon_{\mathbf{k}}} \frac{1}{i\nu_n + i\omega_r - \lambda_f}, \quad (17.158)$$

and assuming a particle-hole symmetric conduction electron density of states, we can replace $\epsilon_{\mathbf{k}} \rightarrow -\epsilon_{\mathbf{k}}$, so that

$$\pi_1(i\nu_n) = \pi_2(i\nu_n) = -T \sum_{i\omega_r, \mathbf{k}} \frac{1}{i\omega_r - \epsilon_{\mathbf{k}}} \frac{1}{i\nu_n + i\omega_r - \lambda_f}, \quad (17.159)$$

Now this is a well-known fermion bubble, and we can use our standard method of contour integration to carry out the summation over the internal Matsubara frequency $i\omega_r$, to obtain

$$\pi_2(i\nu_n) = \sum_{\mathbf{k}} \frac{f(\lambda) - f(\epsilon_{\mathbf{k}})}{i\nu_n - (\lambda_f - \epsilon_{\mathbf{k}})} = \int d\epsilon \rho(\epsilon) \frac{f(\lambda) - f(\epsilon)}{i\nu_n - (\lambda_f - \epsilon)}, \quad (17.160)$$

where $\rho(\epsilon)$ is the density of states per spin. The summation over energy in this integral is a bit tricky. If we use a flat density of states, then at zero temperature

$$\pi_2(i\nu_n) = \frac{\rho}{2} \int_{-D}^D \frac{\text{sgn}(\epsilon)}{i\nu_n + \epsilon} = \rho \ln \left(\frac{D}{|\nu_n|} \right)$$

so the frequency provides the lower logarithmic cut-off. When we do the calculation at a finite temperature, we expect that if $T \gg |\nu_n|$, then the temperature becomes the cutoff, so that our back-of-the-envelope estimate of this integral is

$$\pi_2(i\nu_n) \sim \rho \ln \left(\frac{D}{\max(|\nu_n|, T)} \right)$$

To calculate the precise form of the integral takes more work, but can be done for a Lorentzian density of states, $\rho(\epsilon) = \rho \Phi(\epsilon)$ where $\Phi(x) = D^2/(\epsilon^2 + D^2)$. Here we quote the result, giving the derivation at the end of this solution,

$$\int d\epsilon \Phi(\epsilon) \left(\frac{f(\lambda_f) - f(\epsilon)}{\epsilon - \xi} \right) = \ln \frac{D}{2\pi T} - \psi \left(\frac{1}{2} + \frac{\xi\beta}{2\pi i} \right) - i \frac{\pi}{2} \tanh(\beta\lambda_f/2) \quad (17.161)$$

provided $\text{Im}(\xi) > 0$ (for the opposite sign, one takes the complex conjugate of the above). Putting in $\lambda_f = i\pi T/2$, $\xi = i(\pi T/2 - \nu_n)$ we then obtain

$$\begin{aligned} \pi_2(i\nu_n) &= \rho \int d\epsilon \Phi(\epsilon) \left[\frac{f(\lambda_f) - f(\epsilon)}{\epsilon - (\lambda_f - i\nu_n)} \right] = \rho \left[\ln \frac{D}{2\pi T} - \psi \left(\frac{1}{2} + \frac{\pi T/2 - \nu_n}{2\pi T} \right) + \frac{\pi}{2} \right] \\ &= \rho \left[\ln \frac{De^{\pi/2}}{2\pi T} - \psi \left(\frac{1}{2} + \frac{\pi T/2 - \nu_n}{2\pi T} \right) \right], \quad (\pi T/2 - \nu_n > 0) \end{aligned} \quad (17.162)$$

Strictly speaking, our result only holds for $\text{Im}\xi > 0$, i.e when $\pi/2 - \nu_n = |A| > 0$. The other sign where $\pi/2 - \nu_n = -|A| < 0$ is obtained by taking the complex conjugate of the result for positive $\pi/2 - \nu_n = |A|$. But since the right-hand side is real, taking the complex conjugate has no effect, so we see that the result only depends on the magnitude $|\pi T/2 - \nu_n|$, enabling us to write

$$\pi_2(i\nu_n) = \rho \left[\ln \frac{De^{\pi/2}}{2\pi T} - \psi \left(\frac{1}{2} + \frac{|\nu_n - \pi T/2|}{2\pi T} \right) \right]. \quad (17.163)$$

Notice that the analytic continuation of this expression contains a branch cut along the line $Im[z] = i\pi T/2$, a consequence of using a non-Hermitian Hamiltonian (this can be fixed by using a shifted Matsubara frequency for the f-lines). It follows that

$$\pi_2(z) = \begin{cases} \rho \left[\ln \frac{De^{\pi/2}}{2\pi T} - \psi \left(\frac{1}{2} + \frac{z - i\pi T/2}{2\pi i T} \right) \right], & (Im(z) > \pi T/2) \\ \rho \left[\ln \frac{De^{\pi/2}}{2\pi T} - \psi \left(\frac{1}{2} - \frac{z^* + i\pi T/2}{2\pi i T} \right) \right], & (Im(z) < \pi T/2) \end{cases} \quad (17.164)$$

Adding up the second-order amplitudes we obtain

$$-\Gamma(z_{pp}, z_{ph})_{\beta\sigma';\alpha\sigma} = -J(\vec{\sigma}_{\beta\alpha} \cdot \vec{S}_{\sigma'\sigma}) + J^2 \rho [\pi_2(z_{pp})(\sigma^b \sigma^a)_{\beta\alpha} - \pi_2(z_{ph})(\sigma^b \sigma^a)_{\beta\alpha}] (S^b S^a)_{\sigma'\sigma} \quad (17.165)$$

Notice that the logarithmically divergent parts of the particle hole and particle-particle scattering are the same, while the low energy parts differ by finite amounts. However, if we examine the onshell scattering on the Fermi surface, i.e with $z_{ph} = z_{pp} = i\pi T/2$, then we obtain

$$\begin{aligned} -\Gamma &= -J(\vec{\sigma}_{\beta\alpha} \cdot \vec{S}_{\sigma'\sigma}) + J^2 \rho \ln \frac{De^{\pi/2 - \psi(1/2)}}{2\pi T} [\sigma^b, \sigma^a]_{\beta\alpha} (S^b S^a)_{\sigma'\sigma} \\ &= -J(\vec{\sigma}_{\beta\alpha} \cdot \vec{S}_{\sigma'\sigma}) + J^2 \rho \ln \frac{De^{\pi/2 - \psi(1/2)}}{2\pi T} 2i\sigma_{\beta\alpha}^c \overbrace{\epsilon_{bac} (S^b S^a)_{\sigma'\sigma}}^{iS^c} \\ &= - \left[J + 2J^2 \rho \ln \frac{De^{\pi/2 - \psi(1/2)}}{2\pi T} \right] (\vec{\sigma}_{\beta\alpha} \cdot \vec{S}_{\sigma'\sigma}) \end{aligned} \quad (17.166)$$

explicitly demonstrating the logarithmic renormalization of the coupling constant.

Derivation of integral: We wish to derive the result

$$I = \int d\epsilon \Phi(\epsilon) \left(\frac{f(\lambda_f) - f(\epsilon)}{\epsilon - \xi} \right) = \ln \frac{D}{2\pi T} - \psi \left(\frac{1}{2} + \frac{\xi\beta}{2\pi i} \right) - i \frac{\pi}{2} \tanh(\beta\lambda_f/2) \quad (17.167)$$

where $\Phi(\epsilon) = D^2/(D^2 + \epsilon^2)$ imposes the high-energy cut-off and $Im\xi > 0$. First, let us separate the integral into two, $I = I_1 - I_2$ where

$$\begin{aligned} I_1 &= \int d\epsilon \Phi(\epsilon) \frac{f(\lambda_f)}{\epsilon - \xi} \\ I_2 &= \int d\epsilon \Phi(\epsilon) \frac{f(\epsilon)}{\epsilon - \xi} \end{aligned} \quad (17.168)$$

These integrals can be carried out using contour integration. Now $\Phi(z) = D^2/((z + iD)(z - iD))$, so if we complete the first integral with a contour in the lower-half plane, there there is only a single pole at $z = -iD$, which gives

$$I_1 = -2\pi i \left(\frac{iD}{2} \right) \frac{f_\lambda}{-iD - \xi} \rightarrow i\pi f_\lambda \quad (17.169)$$

in the large D limit. To do the second term, We begin by writing

$$\begin{aligned} \frac{D^2}{D^2 + z^2} \frac{1}{z - \xi} &= \frac{1}{2} \left(\frac{-iD}{z - iD} + \{D \rightarrow -D\} \right) \frac{1}{z - \xi} \\ &= \frac{1}{2} \left(\frac{1}{z - \xi} - \frac{1}{z - iD} \right) + \{D \rightarrow -De^{i0^+}\}, \end{aligned} \quad (17.170)$$

so we can calculate the answer for positive D , change the sign of D and average over the two results. (In practice, we need to give D an infinitesimal phase $D \rightarrow De^{i0^+}$ so that the pole at $z = -iDe^{i0}$ is $f(-iD + D0^+) \rightarrow 0$.) If we now integrate the first term of this expression with $f(z)$, closing the

contour in the lower half plane, then the only poles we pick up are the poles in $f(z)$ of strength $-T$ at $z = -i\omega_n = -i(2n+1)2\pi T$, leading to

$$\begin{aligned} I_2 &= \oint dz \frac{1}{2} \left(\frac{1}{z-\xi} - \frac{1}{z-iD} \right) f(z) + \{D \rightarrow -De^{i0^+}\} \\ &= \frac{1}{2} (-2\pi i) (-T) \sum_{n=0}^{\infty} \left(-\frac{1}{i\omega_n + \xi} + \frac{1}{i\omega_n + iD} \right) + \{D \rightarrow -De^{i0^+}\} \end{aligned} \quad (17.171)$$

(where the $-2\pi i$ line derives from the left-handed contour in the lower-half plane and the $-T$ from the pole strength of $f(z)$ at $z = -i\omega_n$). Simplifying this result,

$$I_2 = \frac{1}{2} \sum_{n=0}^{\infty} \left(\frac{1}{n + \frac{1}{2} + \frac{D}{2\pi T}} - \frac{1}{n + \frac{1}{2} + \frac{\xi}{2\pi i T}} \right) + \{D \rightarrow -De^{i0^+}\}. \quad (17.172)$$

Now at this point, we use the series form of the digamma function $\psi(z) = d \ln \Gamma(z)/dz$,

$$\psi(z) = \sum_{n=0}^{\infty} \left(\frac{1}{n+1} - \frac{1}{n+z} \right) - \zeta \quad (17.173)$$

where $\zeta = 0.577216 = -\psi(1)$ is Euler's constant. From this relation, we deduce that

$$\psi(z) - \psi(a) = \sum_{n=0}^{\infty} \left(\frac{1}{n+a} - \frac{1}{n+z} \right) \quad (17.174)$$

so that

$$I_2 = \frac{1}{2} \left[\psi \left(\frac{1}{2} + \frac{\xi}{2\pi i T} \right) - \psi \left(\frac{1}{2} + \frac{D}{2\pi T} \right) \right] + \{D \rightarrow -De^{i0^+}\} \quad (17.175)$$

Now for large z , $\psi(z) \rightarrow \ln z$, so that for a large cut-off,

$$\begin{aligned} I_2 &= \frac{1}{2} \left[\psi \left(\frac{1}{2} + \frac{\xi}{2\pi i T} \right) - \ln \left(\frac{D}{2\pi T} \right) \right] + \{D \rightarrow -De^{i0^+}\} \\ &= \psi \left(\frac{1}{2} + \frac{\xi}{2\pi i T} \right) - \ln \left(\frac{D}{2\pi T} \right) + i\frac{\pi}{2} \end{aligned} \quad (17.176)$$

where the remainder term derives from $-\frac{1}{2} \ln -e^{i0^+} = i\frac{\pi}{2}$. Adding I_1 (17.169) and $-I_2$ (17.176) together then gives

$$\begin{aligned} I &= I_1 - I_2 = \ln \left(\frac{D}{2\pi T} \right) - \psi \left(\frac{1}{2} + \frac{\xi}{2\pi i T} \right) - i\frac{\pi}{2} (1 - 2f_\lambda) \\ &= \ln \left(\frac{D}{2\pi T} \right) - \psi \left(\frac{1}{2} + \frac{\xi}{2\pi i T} \right) - i\frac{\pi}{2} \tanh \left[\frac{\beta \lambda_f}{2T} \right] \end{aligned} \quad (17.177)$$

17.7.2 Universality and the resistance minimum

Provided the Kondo temperature is far smaller than the cut-off, then at low energies it is the only scale governing the physics of the Kondo effect. For this reason, we expect all physical quantities to be expressed in terms of universal functions involving the ratio of the temperature or field to the Kondo scale. For example, the susceptibility

$$\chi(T) = \frac{1}{T} F\left(\frac{T}{T_K}\right), \quad (17.178)$$

and the quasiparticle scattering rate

$$\frac{1}{\tau(T)} = \frac{1}{\tau_o} \mathcal{G}\left(\frac{T}{T_K}\right) \quad (17.179)$$

both display universal behavior. If we change the cut-off of the model, adjusting the bare coupling constant g_0 so that T_K is fixed, the physical quantities will be unchanged. If we replace $g_0 \rightarrow g(D)$ in equation (17.137), then all models with $J(D)\rho = g(D)$, where

$$\ln\left(\frac{T_K}{D}\right) = -\frac{1}{2g(D)} + \frac{1}{2} \ln 2g(D) \quad (17.180)$$

will have the same Kondo temperature and thus the same low temperature behavior. However, we can view this another way: as the temperature is lowered, quantum processes become coherent at increasingly lower energies, and the effective cutoff for quantum processes is T . Thus, as the temperature is lowered, the coupling constant g_0 is renormalized to a new value,

$$g_0 \rightarrow g(T) \quad (17.181)$$

where

$$\ln\left(\frac{T_K}{T}\right) = -\frac{1}{2g(T)} + \frac{1}{2} \ln 2g(T) \quad (17.182)$$

In this way, lowering the temperature drives the system along the renormalization trajectory from weak to strong coupling.

We can check the existence of universality by examining these properties in the weak coupling limit, where $T \gg T_K$. Here, we find

$$\frac{1}{\tau(T)} = 2\pi J^2 \rho S(S+1)n_i = \frac{2\pi}{\rho} S(S+1)n_i g_0^2 \quad (S = \frac{1}{2}) \quad (17.183)$$

$$\chi(T) = \frac{n_i}{T} [1 - 2J\rho] = \frac{n_i}{T} [1 - 2g_0] \quad (17.184)$$

where n_i is the density of impurities.

Now scaling, it is correct, implies that at lower temperatures $J\rho \rightarrow J\rho + 2(J\rho)^2 \ln \frac{D}{T}$, so that to next leading order we expect

$$\frac{1}{\tau} = n_i \frac{2\pi}{\rho} S(S+1) [J\rho + 2(J\rho)^2 \ln \frac{D}{T}]^2 \quad (17.185)$$

$$\chi(T) = \frac{n_i}{T} \left[1 - 2J\rho - 4(J\rho)^2 \ln \frac{D}{T} + O((J\rho)^3) \right]. \quad (17.186)$$

These results are readily confirmed in second-order perturbation theory as the result of adding in the one-loop corrections to the scattering vertices. The first result was obtained by Jun Kondo. Kondo was looking for a consequence of the antiferromagnetic interaction predicted by the Anderson model, so he computed the electron scattering rate to third order in the magnetic coupling. The logarithm which appears in the electron scattering rate means that as the temperature is lowered, the rate at which electrons scatter off magnetic impurities rises. It is this phenomenon that gives rise to the famous Kondo “resistance minimum”.

But we can use universality to go much further, and actually deduce the form of the universal functions $F[x]$ and $\mathcal{G}[x]$ in (17.178) and (17.179), at least in weak coupling when the temperature is large compared with the Kondo temperature $T/T_K \gg 1$. Let us rearrange (17.182) into

$$g(T) = \frac{1}{2 \ln\left(\frac{T}{T_K}\right) + \ln 2g(T)}. \quad (17.187)$$

which we may iterate to obtain

$$2g(T) = \frac{1}{\ln\left(\frac{T}{T_K}\right) + \frac{1}{2} \ln\left(\frac{1}{\ln\frac{T}{T_K} + \ln 2g}\right)} = \frac{1}{\ln\left(\frac{T}{T_K}\right)} + \frac{\ln(\ln(T/T_K))}{2 \ln^2\left(\frac{T}{T_K}\right)} + \dots \quad (17.188)$$

where the expansion has been made assuming $\ln T/T_K \gg \ln g$. At high temperature, by substituting $T_K = De^{-1/2J\rho}$ we can check that the leading order term is simply

$$2g(T) = \frac{1}{\ln\left(\frac{T}{T_K}\right)} = \frac{1}{\frac{1}{2J\rho} + \ln T/D} = \frac{2J\rho}{1 + 2J\rho \ln T/D} = 2 \left[J\rho + 2(J\rho)^2 \ln\left(\frac{D}{T}\right) \right] + O[(J\rho)^3] \quad (17.189)$$

the leading logarithmic correction to $g(T)$. By using scaling we are thus able to resum diagrams far beyond leading perturbation theory. Using this expression to make the replacement $J\rho \rightarrow g(T)$ in the leading perturbation theory (17.183), we obtain

$$\chi(T) = \frac{n_i}{T} \left[1 - \frac{1}{\ln(T/T_K)} - \frac{1}{2} \frac{\ln(\ln(T/T_K))}{\ln^2(T/T_K)} + \dots \right] \quad (17.190)$$

$$\frac{1}{\tau(T)} = n_i \frac{\pi S(S+1)}{2\rho} \left[\frac{1}{\ln^2(T/T_K)} + \frac{\ln(\ln(T/T_K))}{\ln^3(T/T_K)} + \dots \right] \quad (17.191)$$

From the second result, we see that the electron scattering rate has the scale-invariant form in (??)

$$\frac{1}{\tau(T)} = \frac{1}{\tau_0} \mathcal{G}(T/T_K). \quad (17.192)$$

where $\frac{1}{\tau_0} \propto \frac{n_i}{\rho}$ represents the intrinsic scattering rate off the Kondo impurity. The quantity $1/\rho$ is essentially the Fermi energy of the electron gas; and $1/\tau_0 \sim \frac{n_i}{\rho}$ is the “unitary scattering” rate, the maximum possible scattering rate that is obtained when an electron experiences a resonant $\pi/2$ scattering phase shift. From this result, we see that at absolute zero, the electron scattering rate will rise to the value $\frac{1}{\tau(T)}|_{T=0} = \frac{n_i}{\rho} \mathcal{G}(0)$, indicating that at strong coupling, the scattering rate is of the same order as the unitary scattering limit. We shall now see how this same result comes naturally out of a strong coupling analysis.

Example 17.9:

- a) Use the Popov-Fedotov scheme to compute the leading correction to the impurity magnetic susceptibility, given by the diagrams

$$\begin{aligned} \chi &= \text{[diagram 1]} + \text{[diagram 2]} + \text{[diagram 3]} \\ &= \frac{\mu_B^2}{T} [1 - 2J\rho + O(J^2)] \end{aligned} \quad (17.193)$$

- b) Based on scaling arguments, what is the form of the J^2 correction to the susceptibility?
c) What diagrams are responsible for the logarithmic correction to the susceptibility?

Solution:

- a) For these calculations, let us set $\mu_B = 1$ temporarily. We need to calculate the f-electron susceptibility, given by

$$\chi_f \delta^{ab} = \sigma^a \text{---} \text{---} \sigma^b = -T \sum_{i\omega_n} \text{Tr}[\sigma^a G_f(i\omega_n) \sigma^b G_f(i\omega_n)] = \chi_f \delta^{ab}. \quad (17.194)$$

So

$$\begin{aligned} \chi_f &= -2T \sum_{i\omega_n} \frac{1}{(i\omega_n - \lambda_f)^2} = \frac{\partial}{\partial \lambda_f} \overbrace{2T \sum_{i\omega_n} \frac{1}{i\omega_n - \lambda_f}}^{-f(\lambda_f)} \\ &= 2 \left(-\frac{\partial f(\lambda_f)}{\partial \lambda_f} \right) = \frac{2f_\lambda(1 - f_\lambda)}{T} = \frac{1}{T} \end{aligned} \quad (17.195)$$

where the factor of two derives from the trace over the spin degrees of freedom and we have used $f_\lambda(1 - f_\lambda) = 1/[(i+1)(-i+1)] = 1/2$. Similarly, the conduction electron susceptibility given by

$$\begin{aligned} \chi_c \delta^{ab} &= \sigma^a \text{---} \text{---} \sigma^b = -T \sum_{\mathbf{k}, i\omega_n} \text{Tr}[\sigma^a G_{\mathbf{k}}(i\omega_n) \sigma^b G_{\mathbf{k}}(i\omega_n)] \\ &= -2\delta^{ab} T \sum_{\mathbf{k}, i\omega_n} \frac{1}{(i\omega_n - \epsilon_{\mathbf{k}})^2} = 2\delta^{ab} \sum_{\mathbf{k}} \frac{\partial}{\partial \epsilon_{\mathbf{k}}} \overbrace{T \sum_{i\omega_n} \frac{1}{i\omega_n - \epsilon_{\mathbf{k}}}}^{-f(\epsilon_{\mathbf{k}})} \\ &= 2\delta^{ab} \sum_{\mathbf{k}} \left(-\frac{\partial f(\epsilon_{\mathbf{k}})}{\partial \epsilon_{\mathbf{k}}} \right) = 2\rho \delta^{ab}. \end{aligned} \quad (17.196)$$

Now the first order diagrams are given by

$$\chi_A \delta^{ab} = \sigma^a \text{---} \text{---} \text{---} \sigma^b = (\chi_f \delta^{ac}) \left(-\frac{J}{2} \right) (\chi_c \delta^{cb}) = -\frac{J\rho}{T} \quad (17.197)$$

and

$$\chi_B \delta^{ab} = \sigma^a \text{---} \text{---} \text{---} \sigma^b = (\chi_c \delta^{ac}) \left(-\frac{J}{2} \right) (\chi_f \delta^{cb}) = -\frac{J\rho}{T} \quad (17.198)$$

Adding the results together, the first order correction to the impurity susceptibility is given by

$$\chi = \frac{\mu_B^2}{T} (1 - 2J\rho) + O((J\rho)^2) \quad (17.199)$$

where we have reinstated μ_B

- b) We expect the second order corrections to the susceptibility to be obtained by renormalizing the coupling constant. Following the results of example 17.7, the renormalization is given by

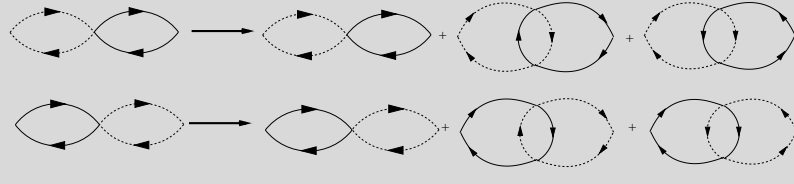
$$J\rho \rightarrow J\rho + 2(J\rho)^2 \ln \left[\frac{D}{T} \right] \quad (17.200)$$

Since the renormalization group only provides leading logarithmic accuracy, we have dropped the dimensionless constants inside the logarithm. We therefore expect that the second-order corrections to the susceptibility will take the form

$$\chi(T) = \frac{\mu_B^2}{T} \left[1 - 2 \left(J\rho + 2(J\rho)^2 \ln \left[\frac{D}{T} \right] \right) \right]$$

$$= \frac{\mu_B^2}{T} \left[1 - 2J\rho + 4(J\rho)^2 \ln \left[\frac{D}{T} \right] \right] + O[(J\rho)^3] \quad (17.201)$$

- c) The logarithmic corrections to the susceptibility derive from the vertex insertions into the first order diagrams, given by



$$(17.202)$$

There are other contributions to the susceptibility, such as self-energy corrections and corrections to the external magnetic vertex, but none of these will contribute logarithmically divergent corrections. Moreover, the conservation of spin will mean that many self-energy and vertex corrections will cancel one-another.

17.8 Nozières Fermi Liquid Theory

The weak-coupling analysis tells us that somewhere around the Kondo temperature, the running Kondo coupling constant g becomes of order one, $O(1)$. Although perturbative renormalization group methods can not go past this point, Anderson and Yuval[31, 38, 39] argued that it is not unreasonable to suppose that the coupling constant continues scaling to infinity. This is the simplest possibility and if true, it means that the strong-coupling limit is an attractive fixed point, a fixed point that is stable under the renormalization group. Anderson and Yuval conjectured that the Kondo singlet would be paramagnetic, with a temperature independent magnetic susceptibility and a universal linear specific heat given by $C_V = \gamma_K \frac{T}{T_K}$ at low temperatures.

The first controlled treatment of this cross-over regime was carried out by Wilson using the numerical renormalization group method that he invented[33]. Wilson's numerical renormalization method was able to confirm the conjectured renormalization of the Kondo coupling constant to infinity. This limit is called the "strong coupling" limit of the Kondo problem. Wilson carried out an analysis of the strong-coupling limit, and was able to show that the specific heat would be a linear function of temperature, like a Fermi liquid. Wilson showed that the linear specific heat could be written in a universal form

$$C_V = \gamma T, \quad \gamma = \frac{\pi^2}{3} \frac{0.4128 \pm 0.002}{8T_K} \quad (17.203)$$

Wilson also compared the ratio between the magnetic susceptibility and the linear specific heat with the corresponding value in a non-interacting system, computing

$$W = \frac{\chi/\chi^0}{\gamma/\gamma^0} = \frac{\chi}{\gamma} \left(\frac{\pi^2 k_B^2}{3(\mu_B)^2} \right) = 2 \quad (17.204)$$

within the accuracy of the numerical calculation.

17.8.1 Strong Coupling Expansion

Remarkably, the second result of Wilson's can be re-derived using an exceptionally elegant set of arguments due to Nozières[34] that leads to an explicit form for the strong coupling fixed point Hamiltonian. Nozières began by considering a local moment coupled via a strong antiferromagnetic Kondo coupling to an electron sea. Wilson had previously shown that the local moment only couples to the s-wave scattering channel so that the Kondo model can be mapped onto a spin coupled to one-dimensional a one-dimensional tight-binding chain, as illustrated in Fig. 17.16.

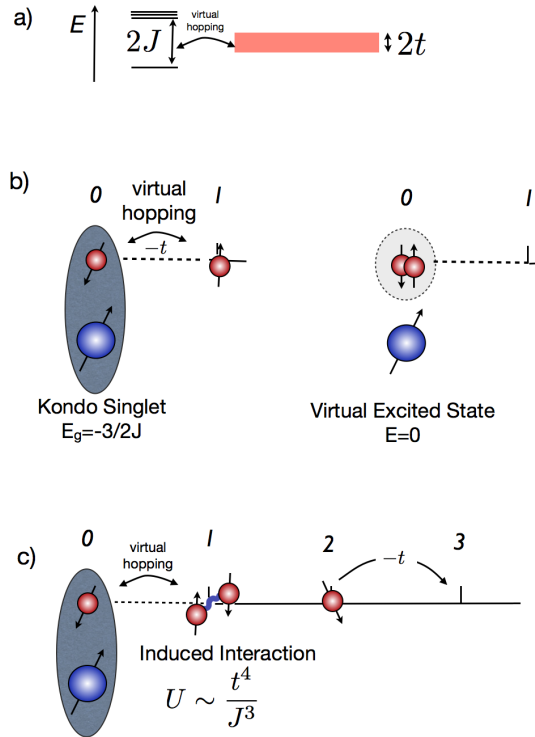


Fig. 17.16

Illustrating the strong-coupling limit of the Kondo model. (a) Singlet with bound-state energy $-3J/2$ interacts with narrow band of width $2t$. (b) Kondo singlet formed at origin because the addition or removal of electrons costs energy. (c) Virtual fluctuations of charge in and out of the Kondo singlet induces interactions between electrons at site 1.

The Hamiltonian for the one-dimensional Kondo model is

$$H_{lattice} = -t \sum_{j=0,\infty} [c_{\sigma}^{\dagger}(j+1)c_{\sigma}(j) + \text{H.c.}] + Jc_{\alpha}^{\dagger}(0)\vec{\sigma}_{\alpha\beta}c_{\beta}(0) \cdot \vec{S}_f. \quad (17.205)$$

Since the renormalization trajectories link the weak-coupling, model where $J/t \ll 1$, to the strong coupling, model where $J/t \gg 1$, Nozières reasoned that the strong coupling physics of this model could be used to

understand the low temperature physics of the Kondo model. When $J \gg t$, in the ground-state, the local moment couples to an electron at the origin, forming a “Kondo singlet” denoted by

$$|GS\rangle = \frac{1}{\sqrt{2}} (|\uparrow\downarrow\rangle - |\downarrow\uparrow\rangle), \quad (17.206)$$

where the thick arrow refers to the spin state of the local moment and the thin arrow refers to the spin state of the electron at site 0. The ground-state energy of the Kondo singlet is

$$E_g = J[S(S+1) - 3/2] = -\frac{3}{2}J. \quad (17.207)$$

The kinetic energy of the electrons in the one-dimensional band now becomes a perturbation to the Kondo singlet. Any electron which hops from site 1 to site 0 will automatically break the Kondo singlet, raising its energy by $3J/2$. This will have the effect of excluding electrons (or holes) from the origin. The fixed point Hamiltonian must then take the form

$$H_{\text{lattice}} = -t \sum_{j=1,\infty} [c^\dagger_{\sigma}(j+1)c_{\sigma}(j) + \text{H.c.}] + \text{weak interaction} \quad (17.208)$$

where the second-term refers to the weak-interactions induced by virtual fluctuations onto site 0. If the wavefunction of electrons far from the impurity has the form $\psi(x) \sim \sin(k_F x)$, where k_F is the Fermi momentum, then the exclusion of electrons from site 1 has the effect of phase-shifting the electron wavefunctions by one the lattice spacing a , so that now $\psi(x) \sim \sin(k_F x - \delta)$ where $\delta = k_F a$. But if there is one electron per site, then $2(2k_F a / (2\pi)) = 1$ by the Luttinger sum rule, so that $k_F = \pi/(2a)$ and hence the Kondo singlet acts as a spinless, elastic scattering center with scattering phase shift

$$\delta = \pi/2. \quad (17.209)$$

The appearance of $\delta = \pi/2$ can also be deduced by appeal to the Friedel sum rule, which determines the number of bound-electrons at the magnetic impurity site in terms of the phase shift $\sum_{\sigma=\uparrow,\downarrow} \frac{\delta}{\pi} = 2\delta/\pi$, so that $\delta = \pi/2$. By considering virtual fluctuations of electrons between site 1 and 0, Nozières argued that the induced interaction at site 1 must take the form

$$\Delta H = U n_{1\uparrow} n_{1\downarrow}, \quad U \sim \frac{t^4}{J^3} \quad (17.210)$$

because fourth order hopping processes lower the energy of the singly occupied state relative to the doubly occupied state. This repulsive interaction amongst the conduction electrons is actually a marginal operator under the renormalization group, leading to the conclusion that the effective Hamiltonian describes a weakly interacting “local” Landau Fermi liquid.

17.8.2 Phase shift formulation of the Local Fermi liquid

Nozières then used the results of the strong coupling expansion to formulate a local Fermi liquid description of the strong coupling fixed point of the Kondo model. He formulated this theory in terms of an occupancy-dependent phase shift as follows. In a non-interacting impurity problem, the asymptotic wavefunction’s experience a scattering phase shift, with a radial wavefunction that takes the form

$$\psi(r) \sim \frac{\sin(kr + \delta(E_k))}{r}. \quad (17.211)$$

If we put the system inside a sphere of radius R , and the boundary condition $\psi(R) = 0$, then $kR + \delta(E_k) = n\pi$ determines the allowed momenta of the quasiparticles, given by $k_n = n\frac{\pi}{R} - \frac{\delta(E_k)}{R}$. The level spacing in the absence of scattering is $\Delta\epsilon = \frac{\partial E}{\partial k} \frac{\pi}{R}$. Now in the presence of the scattering phase shift, momenta are reduced by an amount $\Delta k = -\frac{\delta(E_k)}{R}$, so the corresponding energy levels are shifted downwards by an amount

$$\begin{aligned} E_k &\rightarrow E_k - \frac{\partial E}{\partial k} \frac{\delta(E_k)}{R} \\ &= E_k - \Delta\epsilon \frac{\delta(E_k)}{\pi}. \end{aligned} \quad (17.212)$$

Now in the impurity Landau Fermi liquid, the ground-state energy will be a functional of quasiparticle occupancies $\{n_{k\sigma}\}$. As in bulk Landau Fermi liquid theory, the differential of the total energy with respect to occupancies defines a renormalized quasiparticle energy as follows

$$\frac{\delta E[\{n_{k'\sigma'}\}]}{\delta n_{k\sigma}} = E_k - \frac{\Delta\epsilon}{\pi} \delta_\sigma(\{n_{k'\sigma'}, E_k\}). \quad (17.213)$$

Now, interactions cause the phase shift, and the downward shift of the quasiparticle energies to depend on the quasiparticle occupancies $n_{k\sigma}$. Expanding to linear order in the deviation of quasiparticle occupancies about the ground state, $\delta n_{k\sigma} = n_{k\sigma} - n_{k\sigma}^{(0)}$, then

$$\delta_\sigma(\{n_{k'\sigma'}\}, E) = \frac{\pi}{2} + \alpha(E - \mu) + \Phi \sum_{k'} \delta n_{k', -\sigma}. \quad (17.214)$$

The term with coefficient Φ is the impurity analog of the Landau Fermi liquid interaction $f_{\mathbf{k}\sigma, \mathbf{k}'\sigma'}$. This term describes the onsite interaction between opposite spin states of the Fermi liquid. Nozières argued that when the chemical potential of the conduction sea is changed, the occupancy of the localized d state will not change, and because the Friedel sum rule links the $\pi/2$ phase shift to the occupancy, this implies that phase shift is invariant under changes in μ , i.e the Kondo resonance is pinned to the Fermi energy. Now under a shift $\Delta\mu$, the change in the occupancy of the quasiparticle states $\sum_k \delta n_{k-\sigma} \rightarrow \rho \Delta\mu$, so that changing the chemical potential modifies the phase shift at the Fermi surface by an amount

$$\begin{aligned} \Delta\delta_\uparrow &= \delta(\{n_{k'\sigma'}\}, \mu + \Delta\mu) - \delta(\{n_{k'\sigma'}^{(0)}\}, \mu) \\ &= \alpha\Delta\mu + \Phi \overbrace{\sum_{k'} (n_{k'\downarrow} - n_{k'\downarrow}^{(0)})}^{\rho\Delta\mu} \\ &= (\alpha + \Phi\rho)\Delta\mu = 0 \end{aligned} \quad (17.215)$$

In other words, the interaction term must compensate for the energy dependence of the phase shift, so that magnitude $\Phi = -\alpha/\rho$ is set by the density of states α .

We are now in a position to calculate the impurity contribution to the magnetic susceptibility and specific heat. First note that the density of quasiparticle states is given by

$$\rho = \frac{dN}{dE} = \rho_o + \frac{1}{\pi} \frac{\partial \delta}{\partial \epsilon} = \rho_o + \frac{\alpha}{\pi} \quad (17.216)$$

so that the low temperature specific heat is given by $C_V = (\gamma_{bulk} + \gamma)T$ where

$$\gamma = 2 \left(\frac{\pi^2 k_B^2}{3} \right) \frac{\alpha}{\pi}, \quad (17.217)$$

where the prefactor “2” is derived from the spin up and spin-down bands. It is convenient to write this in the

form

$$\gamma = \left(\frac{\pi^2 k_B^2}{3} \right) \tilde{\gamma},$$

where $\tilde{\gamma} = 2\alpha/\pi$. Now in a magnetic field, the impurity magnetization is given by

$$M = \frac{\delta_{\uparrow}}{\pi} - \frac{\delta_{\downarrow}}{\pi} \quad (17.218)$$

Since the Fermi energies of the up and down quasiparticles are shifted to $\epsilon_{F\sigma} \rightarrow \epsilon_F - \sigma B$, we have $\sum_k \delta n_{k\sigma} = \sigma \rho B$, so that the phase shift at the Fermi surface in the up and down scattering channels becomes

$$\begin{aligned} \delta_{\sigma} &= \frac{\pi}{2} + \alpha \delta \epsilon_{F\sigma} + \Phi \left(\sum_k \delta n_{k\sigma} \right) \\ &= \frac{\pi}{2} + \alpha \sigma B - \Phi \rho \sigma B \\ &= \frac{\pi}{2} + 2\alpha \sigma B \end{aligned} \quad (17.219)$$

so that the presence of the interaction term doubles the size of the change in the phase shift due to a magnetic field. The impurity magnetization then becomes

$$M_i = \chi_s B = \frac{\delta_{\uparrow}}{\pi} - \frac{\delta_{\downarrow}}{\pi} = 2 \left(\frac{2\alpha}{\pi} \right) B. \quad (17.220)$$

If we reinstate the magnetic moment μ_B of the electron, this becomes

$$\chi_s = \mu_B^2 \tilde{\chi}_s = \mu_B^2 \left(\frac{4\alpha}{\pi} \right) \quad (17.221)$$

This is twice the value expected for a “rigid” resonance, and it means that the Wilson ratio is

$$W = \frac{\chi_s}{\gamma} \left(\frac{\pi^2 k_B^2}{3(\mu_B)^2} \right) = \frac{\tilde{\chi}_s}{\tilde{\gamma}} = 2 \quad (17.222)$$

Example 17.10: Consider what happens to the Fermi liquid ground-state of the Anderson impurity model in which the change of the phase shifts $\Delta\delta_{\uparrow} = \Delta\delta_{\downarrow} = \Delta\delta$ due to a shift $\Delta\mu$ in the chemical potential is now finite, due to the finite charge susceptibility χ_c so that

$$\frac{\Delta(\delta_{\uparrow} + \delta_{\downarrow})}{\pi} = \frac{2\Delta\delta}{\pi} = \chi_c \Delta\mu \quad (17.223)$$

where $\Delta\mu$ is the change in the chemical potential.

- (a) By generalizing the Nozières Fermi liquid theory to the Anderson model, using the above result to show that equation (??) becomes

$$\Delta\delta = \frac{\pi}{2} \chi_c \Delta\mu = (\alpha + \Phi\rho) \Delta\mu, \quad (17.224)$$

in the Anderson impurity model, so that the charge susceptibility is given by

$$\chi_c = \frac{2}{\pi} (\alpha + \Phi\rho).$$

- (b) By generalizing the calculation of the susceptibility to the Anderson impurity model show that the specific heat, charge and spin susceptibility are related by the Yamada Yosida identity

$$2\tilde{\gamma} = \tilde{\chi}_s + \chi_c \quad (17.225)$$

where

$$\gamma = \left(\frac{\pi^2 k_B^2}{3} \right) \tilde{\gamma}, \quad \chi_s = \mu_B^2 \tilde{\chi}_s. \quad (17.226)$$

- (c) What happens to the charge susceptibility when U is large and negative? (This is the “charge” Kondo model).

Solution:

- (a) In the impurity Anderson model, we write

$$\delta_\sigma(\{n_{k'\sigma'}\}, \epsilon_k) = \delta_0 + \alpha(\epsilon_k - \mu) + \Phi \left(\sum_k \delta n_{k,-\sigma} \right), \quad (17.227)$$

where, by the Friedel sum rule $2\delta_0/\pi = \Delta n_e$, the number of electrons bound by the impurity. If we add extra quasiparticles to the Fermi sea, shifting the Fermi energy up by an amount $\Delta\mu$, the change in the phase shift at the Fermi energy is given by

$$\Delta\delta_\sigma = \delta_\sigma(\{n_{k'\sigma'}\}, \Delta\mu + \mu) - \delta_\sigma(\{n_{k'\sigma'}^{(0)}\}, \mu) = \alpha\Delta\mu + \Phi \left(\sum_{k'} \delta n_{k'-\sigma} \right) = (\alpha + \Phi\rho)\Delta\mu \quad (17.228)$$

But the change in the impurity charge is then given by

$$\chi_c \Delta\mu = \frac{2\Delta\delta}{\pi} = \frac{2}{\pi}(\alpha + \Phi\rho)\Delta\mu$$

so that

$$\chi_c = \frac{2}{\pi}(\alpha + \Phi\rho). \quad (17.229)$$

Now the linear specific heat is determined by the impurity density of states (17.217)

$$\gamma = \left(\frac{\pi^2 k_B^2}{3} \right) \frac{2}{\pi} \frac{\partial \delta}{\partial \epsilon} = \left(\frac{\pi^2 k_B^2}{3} \right) \overbrace{\frac{2\alpha}{\pi}}^{\equiv \tilde{\gamma}} \quad (17.230)$$

so we may write

$$\begin{aligned} \chi_c &= \tilde{\gamma} + \left(\frac{2\Phi\rho}{\pi} \right), \\ \left(\frac{2\Phi\rho}{\pi} \right) &= \chi_c - \tilde{\gamma}. \end{aligned} \quad (17.231)$$

- (b) Now setting $\mu_B = 1$, the magnetization of the impurity is given by

$$M = \chi_s B = \left(\frac{\delta_\uparrow}{\pi} - \frac{\delta_\downarrow}{\pi} \right) \quad (17.232)$$

where, in a field, the Fermi surface splits into two, with the shift in the Fermi energy given by σB , so that the changes in the phase shifts are given by

$$\begin{aligned} \delta_\sigma &= \delta_0 + \alpha\sigma B + \Phi \left(\sum_{k'} \delta n_{k'-\sigma} \right) \\ &= \delta_0 + (\alpha - \Phi\rho)\sigma B \end{aligned} \quad (17.233)$$

Using (17.231), it follows that

$$M = \tilde{\chi}_s = \frac{\delta_{\uparrow}}{\pi} - \frac{\delta_{\downarrow}}{\pi} = 2 \frac{\alpha - \Phi\rho}{\pi} = \tilde{\gamma} - (\chi_c - \tilde{\gamma}) = 2\tilde{\gamma} - \chi_c \quad (17.234)$$

from which the Yamada Yoshida identity

$$2\tilde{\gamma} = \chi_c + \chi_s \quad (17.235)$$

follows. Notice that if we restore μ_B , then $\chi_s \rightarrow \chi_s/\mu_B^2 = \tilde{\chi}_s$.

- (c) Notice that in the non-interaction impurity ($U = 0$), $\chi_c = \tilde{\chi}_s = \gamma$. In the limit that $U < 0$ is large and negative, the spin susceptibility is suppressed to zero, so that the charge Wilson ratio

$$\frac{\chi_c}{\tilde{\gamma}} = 2. \quad (17.236)$$

This is a result of the charge Kondo effect.

17.8.3 Experimental observation of Kondo effect

Experimentally, there is now a wealth of observations that confirm our understanding of the single impurity Kondo effect. Here is a brief itemization of some of the most important observations. (Fig. 17.17.)

- A resistance minimum appears when local moments develop in a material. For example, in $Nb_{1-x}Mo_x$ alloys, a local moment develops for $x > 0.4$, and the resistance is seen to develop a minimum beyond this point.[42, 2]
- Universality seen in the specific heat $C_V = \frac{n_i}{T} F(T/T_K)$ of metals doped with dilute concentrations of impurities. Thus the specific heat of $\underline{Cu} - Fe$ (iron impurities in copper) can be superimposed on the specific heat of $\underline{Cu} - Cr$, with a suitable rescaling of the temperature scale. [43]
- Universality is observed in the differential conductance of quantum dots[44, 45] and spin-fluctuation resistivity of metals with a dilute concentration of impurities.[46] Actually, both properties are dependent on the same thermal average of the imaginary part of the scattering T-matrix

$$\begin{aligned} \rho_i &= n_i \frac{ne^2}{m} \int d\omega \left(-\frac{\partial f}{\partial \omega} \right) 2\text{Im}[T(\omega)] \\ G &= \frac{2e^2}{\hbar} \int d\omega \left(-\frac{\partial f}{\partial \omega} \right) \pi \rho \text{Im}[T(\omega)]. \end{aligned} \quad (17.237)$$

Putting $\pi \rho \int d\omega \left(-\frac{\partial f}{\partial \omega} \right) \text{Im}T(\omega) = t(\omega/T_K, T/T_K)$, we see that both properties have the form

$$\begin{aligned} \rho_i &= n_i \frac{2ne^2}{\pi m \rho} t(T/T_K) \\ G &= \frac{2e^2}{\hbar} t(T/T_K) \end{aligned} \quad (17.238)$$

where $t(T/T_K)$ is a universal function. This result is born out by experiment.

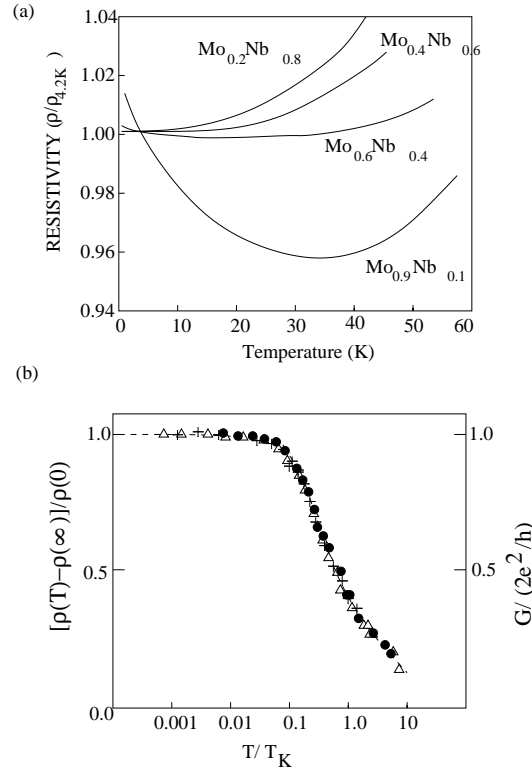


Fig. 17.17 (a) Sketch of resistance minimum in Mo_xNb_{1-x} (b) Sketch of excess resistivity associated with scattering from an impurity spin. Right hand-scale- differential conductivity of a quantum dot.

17.9 Multi-channel Kondo physics and Non-Fermi liquids

In a now famous Review Article, “Kondo effect in Real Metals”, Nozières and Blandin[?] pointed out that there are many variants of the original Kondo model: some of these are important because they describe the real-world behavior of multi-orbital and spin-orbit coupled magnetic moments in metals; others are of particular interest because they lead to new kinds of fixed point associated with “underscreening” and “overscreening” that were not realized in the original model. Remarkably, almost all of these cases can be understood qualitatively from a strong-coupling expansion of the Kondo model.

Exercises

Exercise 17.1 (a) Using the identity $n_{f\sigma}^2 = n_{f\sigma}$, show that the atomic part of the Anderson model can be written in the form

$$H_{atomic} = (E_f + \frac{U}{2})n_f + \frac{U}{2}[(n_f - 1)^2 - 1], \quad (17.239)$$

What happens when $E_f + U/2 = 0$?

(b) Using the completeness relation

$$\underbrace{|f^0\rangle\langle f^0| + |f^2\rangle\langle f^2|}_{(n_f - 1)^2} + \underbrace{|\uparrow\downarrow\rangle\langle\uparrow\downarrow|}_{\mathbf{S}^2} = 1. \quad (S = 1/2)$$

show that the interaction can also be written in the form

$$H_{atomic} = (E_f + \frac{U}{2})n_f - \frac{2U}{3}\mathbf{S}^2 \quad (17.240)$$

which makes it clear that the repulsive U term induces a “magnetic attraction” that favors formation of a local moment.

(c) Derive the Hubbard Stratonovich decoupling for (17.240).

Exercise 17.2 By expanding a plane wave state in terms of spherical harmonics:

$$\langle \mathbf{r} | \mathbf{k} \rangle = e^{i\mathbf{k} \cdot \mathbf{r}} = 4\pi \sum_{l,m} i^l j_l(kr) Y_{lm}^*(\hat{\mathbf{k}}) Y_{lm}(\hat{\mathbf{r}})$$

show that the overlap between a state $|\psi\rangle$ with wavefunction $\langle \mathbf{x} | \psi \rangle = R(r)Y_{lm}(\hat{\mathbf{r}})$ with a plane wave is given by $V(\vec{k}) = \langle \vec{k} | V | \psi \rangle = V(k)Y_{lm}(\hat{\mathbf{k}})$ where

$$V(k) = 4\pi i^{-l} \int dr r^2 V(r) R(r) j_l(kr) \quad (17.241)$$

Exercise 17.3(i) Show that $\delta = \cot^{-1}(\frac{E_d}{\Delta})$ is the scattering phase shift for scattering off a resonant level at position E_d .

(ii) Show that the energy of states in the continuum is shifted by an amount $-\Delta\epsilon\delta(\epsilon)/\pi$, where $\Delta\epsilon$ is the separation of states in the continuum.

(iii) Show that the increase in density of states is given by $\partial\delta/\partial E = \rho_d(E)$. (See chapter 3.)

Exercise 17.4 Generalize the scaling equations to the anisotropic Kondo model with an anisotropic interaction

$$H_I = J^x \sigma^x(0) S^x + J^y \sigma^y(0) S^y + J^z \sigma^z(0) S^z \quad (17.242)$$

where $\sigma^a(0) = \sum_{k,k'} c_k^\dagger \sigma^a c_{k'}$ is the local spin density of the conduction sea and $S^{x,y,z}$ are the three components of the localized magnetic moment. Show that the scaling equations take the form

$$\frac{\partial J_a}{\partial \ln D} = -2J_b J_c \rho + O(J^3),$$

where and (a, b, c) are a cyclic permutation of (x, y, z) . Show that in the special case where $J_x = J_y = J_\perp$, the scaling equations become

$$\frac{\partial J_\perp}{\partial \ln D} = -2J_z J_\perp \rho + O(J^3),$$

$$\frac{\partial J_z}{\partial \ln D} = -2(J_z)^2 \rho + O(J^3), \quad (17.243)$$

so that $J_z^2 - J_\perp^2 = \text{constant}$. Draw the corresponding scaling diagram.

Exercise 17.5 Consider the symmetric Anderson model, with a symmetric band-structure at half filling, given by

$$H = \sum_{\mathbf{k}} \epsilon_{\mathbf{k}} c_{\mathbf{k}\sigma}^\dagger c_{\mathbf{k}\sigma} + \sum_{\mathbf{k}} (V c_{\mathbf{k}\sigma}^\dagger f_\sigma + \text{H.c.}) + \frac{U}{2} (n_f - 1)^2. \quad (17.244)$$

where the density of states satisfies $\rho(\epsilon) = \rho(-\epsilon)$. In this model, the d^0 and d^2 states are degenerate and there is the possibility of a “charged Kondo effect” when the interaction U is negative. Show that under the “particle-hole” transformation

$$\begin{aligned} c_{k\uparrow} &\rightarrow c_{k\uparrow}, & d_\uparrow &\rightarrow d_\uparrow \\ c_{k\downarrow} &\rightarrow -c_{k\downarrow}^\dagger, & d_\downarrow &\rightarrow -d_\downarrow^\dagger \end{aligned} \quad (17.245)$$

the sign of U reverses, so that the positive U model is transformed to the negative U model. Show that under this transformation, spin operators of the local moment are transformed into Nambu “isospin operators” which describe the charge and pair degrees of freedom of the d-state, i.e

$$\vec{S} = f^\dagger \left(\frac{\vec{\sigma}}{2} \right) f \leftrightarrow \vec{\mathcal{T}} = \tilde{f}^\dagger \left(\frac{\vec{\tau}}{2} \right) \tilde{f} \quad (17.246)$$

where $\tilde{f}^\dagger = (f_{\uparrow}^\dagger, f_{\downarrow})$ is the Nambu spinor for the f-electrons and $\vec{\tau}$ is used to denote the Pauli (“Nambu”) matrices, acting in particle-hole space. Use this transformation to prove that when U is negative, a charged Kondo effect will occur at exactly half-filling involving quantum fluctuations between the degenerate d^0 and d^2 configurations. If the spin susceptibility is enhanced in the spin Kondo effect, what susceptibilities are enhanced in the charge Kondo effect? This negative U physics is believed to occur at Tl ions, in the doped semiconductor PbTe. If magnetic impurities like to magnetic order, what kind of order is expected for negative U impurities?

Exercise 17.6 Consider the “infinite U ” Anderson model, in which U is taken to infinity, eliminating double occupancy. The Hamiltonian for this limit is given by

$$H = \sum_{\mathbf{k}} \epsilon_{\mathbf{k}} c_{\mathbf{k}\sigma}^\dagger c_{\mathbf{k}\sigma} + \sum_{\mathbf{k}} V (c_{\mathbf{k}\sigma}^\dagger X_{0\sigma} + X_{\sigma 0} c_{\mathbf{k}\sigma}) + E_f \sum_{\sigma} X_{\sigma\sigma} \quad (17.247)$$

where $X_{0\sigma} = P_0 f_\sigma$ and $X_{\sigma 0} = f_\sigma^\dagger P_0$ where $P_0 = (1 - n_\uparrow)(1 - n_\downarrow)$ projects into the empty state, are the “Hubbard” operators linking the singly occupied f-state and the empty state, while $X_{\sigma\sigma'} = f_\sigma^\dagger P_0 f_{\sigma'} = |f^1 : \sigma\rangle \langle f^1 : \sigma'|$ is the generalized spin operator, acting on the singly occupied states.

- What happens to the Schrieffer-Wolff transformation in this infinite U limit?
- Generalize the Schrieffer-Wolff transformation in the infinite U limit to the case where the electrons have N spin components, i.e in every equation, the spin summation runs from $\sigma \in [1, N]$?

Exercise 17.7 The Kondo model, relevant to spin-orbit coupled ions with total angular momentum j , where $N = 2j + 1$ is the number of spin components, is called the “Coqblin Schrieffer model”, and takes the

$$H = \sum_{\mathbf{k}\sigma \in [-j, j]} \epsilon_{\mathbf{k}} c_{\mathbf{k}\sigma}^\dagger c_{\mathbf{k}\sigma} + J \sum_{\alpha, \beta \in [-j, j]} c_{\alpha}^\dagger c_{\beta} S_{\beta\alpha}$$

where $S_{\beta\alpha} = |\beta\rangle \langle \alpha|$ is the spin operator linking the $J_z = \alpha$ and the $J_z = \beta$ states of the local moment.

(i) Begin by generalizing 17.248 to N components to obtain

Why is the phase shift π/N for an SU (N) Kondo model?

- Exercise 17.8** This question takes you through the calculation of the two-loop corrections to the Kondo beta function. In this calculation, work at zero temperature, replacing Matsubara summations by their continuum version, $T \sum_{i\alpha_n} F(i\alpha_n) \rightarrow \int \frac{d\alpha}{2\pi} F[i\alpha]$.


- where (for $Im[z] > 0$),

Hint: you may find it useful to use the result of Example 17.7, which calculated the Kondo polarization bubble

Using this result, one can rewrite the f-electron self-energy as

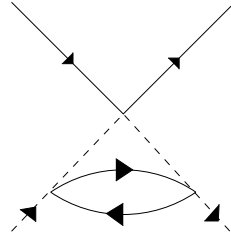
(b) Show that at low energies, the f-electron propagator acquires a wavefunction renormalization $G_f(i\omega) = Z(i\omega)/i\omega$, where

and the that the leading order corrections to the Kondo coupling coming from the f-electron self energies are then



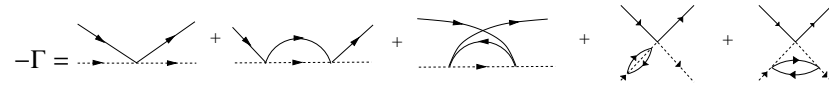
$$= (Z - 1) \left[-J \vec{\sigma} \cdot \vec{S} \right] = \left[-\frac{3}{2} (J\rho)^2 \ln \frac{D}{-i\omega} \right] (-J \vec{S} \cdot \vec{\sigma}) \quad (17.254)$$

- (c) Now consider the vertex correction to the Kondo interaction, and show that this can be re-written as a derivative of the same diagram appearing in the f-electron self energy, so that



$$= \left(\frac{\partial \sigma(i\omega)}{\partial(i\omega)} \right) \left(\frac{1}{2} \right) (-J\vec{S} \cdot \vec{\sigma}) = \left[-\frac{1}{2} (J\rho)^2 \ln \frac{D}{-i\omega} \right] (-J\vec{S} \cdot \vec{\sigma}) \quad (17.255)$$

- (d) Summing the two results of the last section and combining them with the results of exercise 17.8, show that the leading logarithmic corrections to the Kondo interaction up to two loop order are



$$-\Gamma = \dots + \dots + \dots + \dots + \dots$$

$$= (-J\vec{S} \cdot \vec{\sigma}) \times \left(1 + 2(J\rho) \ln \frac{D}{-i\omega} - 2(J\rho)^2 \ln \frac{D}{-i\omega} \right) \quad (17.256)$$

so that if we reduce the band-width from D to D' , the renormalization of $J(D)$ required to keep the low energy scattering amplitudes and physics fixed, is given by

$$J\rho(D') = J\rho + [2(J\rho)^2 - 2(J\rho)^3] \ln \left(\frac{D}{D'} \right) \quad (17.257)$$

leading to the scaling equation for $g = J\rho$,

$$\frac{\partial g}{\partial \ln D'} = \beta(g) = -2g^2 + 2g^3 + \dots \quad (17.258)$$

References

- [1] Werner Heisenberg, *Zur Theorie des Ferromagnetismus*, *Zeitschrift für Physik A*, vol. 49, pp. 619–636, 1928.
- [2] A. M. Clogston, B. T. Matthias, M. Peter, H. J. Williams, E. Corenzwit, and R. C. Sherwood, *Local Magnetic Moment Associated with an Iron Atom Dissolved in Various Transition Metal Alloys*, *Phys. Rev.*, vol. 125, pp. 541, 1962.
- [3] P. W. Anderson, *Local moments and localized states*, *Rev. Mod. Phys.*, vol. 50, pp. 191, 1978.
- [4] N. F. Mott and R. Peierls, *Discussion of the paper by de Boer and Verwey*, *Proc. Royal Society*, vol. 49, pp. 72–73, 1937.
- [5] N. F. Mott, *The Basis of the Electron Theory of Metals, with Special Reference to the Transition Metals*, *Proc. Phys. Society (London)*, vol. A62, pp. 416, 1949.
- [6] J. H. Van Vleck, *Models of Exchange Coupling in Ferromagnetic Media*, *Rev. Mod. Phys.*, vol. 25, pp. 220, 1953.
- [7] J. Friedel, *On Some Electrical and Magnetic Properties of Magnetic Solid Solutions*, *Can. J. Phys.*, vol. 34, pp. 1190, 1956.
- [8] J. Friedel, *Lecture notes on the electronic structure of alloys*, *Nuovo Cimento Suppl.*, vol. VII, pp. 287–311, 1958.
- [9] A. Blandin and J. Friedel, *J. Phys. Radium*, vol. 19, pp. 573, 1958.
- [10] D. Morandi and D. Sherrington, *Functional integral transformation of the Anderson model into the s-d exchange model*, *J. Phys. F: Met. Phys.*, vol. 4, 1974.
- [11] P. W. Anderson, *Localized Magnetic States in Metals*, *Phys. Rev.*, vol. 124, pp. 41, 1961.
- [12] A. M. Clogston, B. T. Matthias, M. Peter, H. J. Williams, E. Corenzwit, and R. C. Sherwood, *Phys. Rev. B*, vol. 125, pp. 541, 1962.
- [13] Leo Kouwenhoven and Leonid Glazman, *The revival of the Kondo effect*, *Physics World*, vol. 14, pp. 33–38, 2001.
- [14] T. E. Kopley, P. L. McEuen, and R. G. Wheeler, *Resonant Tunneling through Single Electronic States and Its Suppression in a Magnetic Field*, *Phys. Rev. Lett.*, vol. 61, no. 14, pp. 1654–1657, Oct 1988.
- [15] H. Grabert and M. H. Devoret, *Single Charge Tunneling Coulomb Blockade Phenomena in Nanostructures*, Plenum, New York, 1992.
- [16] L. P. Kouwenhoven, T. H. Oosterkamp, M. W. S. Danoesastro, M. Eto, D. G. Austing, T. Honda, and S. Tarucha, *Excitation Spectra of Circular, Few-Electron Quantum Dot*, *Science*, vol. 5, pp. 1788–1792, 1997.
- [17] J. Kondo, *g-Shift and Anomalous Hall Effect in Gadolinium Metals*, *Prog. Theor. Phys.*, vol. 28, pp. 846, 1962.
- [18] G. Stewart, *“Heavy-fermion systems”*, *Rev. Mod. Phys.*, vol. 56, pp. 755, 1984.
- [19] F. D and M. Haldane, *Scaling Theory of the Asymmetric Anderson Model*, *Phys. Rev. Lett.*, vol. 40, pp. 416, 1978.

-
- [20] P. B. Wiegmann, *Towards an exact solution of the Anderson model*, *Phys. Lett.*, vol. 80A, pp. 163, 1980.
 - [21] N. Kawakami and A. Okiji, *Exact expression of the ground-state energy for the symmetric anderson model*, *Phys. Lett.*, vol. 86A, pp. 483, 1981.
 - [22] A. Okiji and N. Kawakami, *Thermodynamic Properties of the Anderson Model*, *Phys. Rev. Lett*, vol. 50, pp. 1157, 1983.
 - [23] A. A. Abrikosov, *Electron scattering on magnetic impurities in metals and anomalous resistivity effects*, *Physics*, vol. 2, pp. 5, 1965.
 - [24] H. Suhl, *Formation of Local Magnetic Moments in Metals*, *Phys. Rev.*, vol. 38A, pp. 515, 1965.
 - [25] J.W. Allen, S.J. Oh, O. Gunnarsson, K. Schönhammer, M.B. Maple, M.S. Torikachvili, and I. Lindau, *Electronic structure of cerium and light rare-earth intermetallics*, *Advances in Physics*, vol. 35, pp. 275, 1986.
 - [26] J. W. Allen, S. J. Oh, M. B. Maple, and M. S. Torikachvili, *Large Fermi-level resonance in the electron-addition spectrum of $CeRu_2$ and $CeIr_2$* , *Phys. Rev.*, vol. 28, pp. 5347, 1983.
 - [27] D. Langreth, *Friedel Sum Rule for Anderson's Model of Localized Impurity States*, *Phys. Rev.*, vol. 150, pp. 516, 1966.
 - [28] J. S. Langer and V. Ambegaokar, *Friedel Sum Rule for a System of Interacting Electrons*, *Phys. Rev.*, vol. 121, pp. 1090, 1961.
 - [29] J. W. Allen, S. J. Oh, L. E. Cox, W. P. Ellis, S. Wire, Z. Fisk, J. L. Smith, B. B. Pate, I. Lindau, and J. Arko, *Spectroscopic Evidence for the 5f Coulomb Interaction in UAl_2 and UPt_3* , *Phys. Rev. Lett.*, vol. 2635, pp. 54, 1985.
 - [30] L. Z. Liu, J. W. Allen, C. L. Seaman, M. B. Maple, Y. Dalichaouch, J. S. Kang, M. S. Torikachvili, and M. A. Lopez de laTorre, *Kondo resonance in $Y_{1-x}U_xPd_3$* , *Phys. Rev. Lett*, vol. 68, pp. 1034, 1992.
 - [31] P. W. Anderson and G. Yuval, *Exact Results in the Kondo Problem: Equivalence to a Classical One-Dimensional Coulomb Gas*, *Phys. Rev. Lett.*, vol. 45, pp. 370, 1969.
 - [32] P. W. Anderson, *Kondo Effect IV: Out of the Wilderness*, *Comm. S. St. Phys.*, vol. 5, pp. 73, 1973.
 - [33] K. G. Wilson, *The renormalization group: Critical phenomena and the Kondo problem*, *Rev. Mod. Phys.*, vol. 47, pp. 773, 1975.
 - [34] P. Nozières, *A "Fermi Liquid" Description of the Kondo Problem at Low Tempertures*, *Journal de Physique C*, vol. 37, pp. 1, 1976.
 - [35] J. Hubbard, *Electron Correlations in Narrow Energy Bands. II. The Degenerate Band Case*, *Proc. R. Soc. London, Ser. A.*, vol. 277, pp. 237, 1964.
 - [36] J. R. Schrieffer and P. Wolff, *Relation between the Anderson and Kondo Hamiltonians*, *Phys. Rev.*, vol. 149, pp. 491, 1966.
 - [37] B. Coqblin and J. R. Schrieffer, *Exchange Interaction in Alloys with Cerium Impurities*, *Phys. Rev.*, vol. 185, pp. 847, 1969.
 - [38] P. W. Anderson and G. Yuval, *Exact Results for the Kondo Problem: One-Body Theory and Extension to Finite Temperature*, *Phys. Rev. B*, vol. 1, pp. 1522, 1970.
 - [39] P. W. Anderson and G. Yuval, *Some numerical results on the Kondo problem and the inverse square one-dimensional Ising model*, *J. Phys. C*, vol. 4, pp. 607, 1971.
 - [40] P. W. Anderson, *Poor Man's derivaton of scaling laws for the Kondo problem*, *J. Phys. C*, vol. 3, pp. 2346, 1970.
 - [41] V N Popov and S A Fedotov, *The functional-integration method and diagram technique for soub ststems*, *Zh. Eksp. Teor. Fiz.*, vol. 94, 1988.

- [42] M. Sarachik, E. Corenzwit, and L. D. Longinotti, *Resistivity of Mo-Nb and Mo-Re Alloys Containing 1% Fe*, *Phys Rev.*, vol. 135, pp. A1041, 1964.
- [43] Robert H. White and Theodore H. Geballe, "Long range order in solids", in *Solid State Physics*, H. Ehrenreich, F. Seitz, and D. Turnbull, Eds., New York, 1979, vol. 15, p. 283, Academic Press.
- [44] S. M. Cronenwett, T. H. Oosterkamp, and L. P. Kouwenhoven, *A tunable Kondo effect in Quantum Dots*, *Science*, vol. 281, pp. 540, 1998.
- [45] W. G. van der Wiel, S. De Franceschi, T. Fujisawa, J. M. Elzerman, S. Tarucha, and L. P. Kouwenhoven, *The Kondo Effect in the Unitary Limit*, *Science*, vol. 289, pp. 2105, 2000.
- [46] F. T. Hedgcock and C. Rizzuto, *Influence of Magnetic Ordering on the Low-Temperature Electrical Resistance of Dilute Cd-Mn and Zn-Mn Alloys*, *Phys. Rev.*, vol. 517, pp. 163, 1963.

References

- [1] Werner Heisenberg, *Zur Theorie des Ferromagnetismus*, *Zeitschrift für Physik A*, vol. 49, pp. 619–636, 1928.
- [2] A. M. Clogston, B. T. Matthias, M. Peter, H. J. Williams, E. Corenzwit, and R. C. Sherwood, *Local Magnetic Moment Associated with an Iron Atom Dissolved in Various Transition Metal Alloys*, *Phys. Rev.*, vol. 125, pp. 541, 1962.
- [3] P. W. Anderson, *Local moments and localized states*, *Rev. Mod. Phys.*, vol. 50, pp. 191, 1978.
- [4] N. F. Mott and R. Peierls, *Discussion of the paper by de Boer and Verwey*, *Proc. Royal Society*, vol. 49, pp. 72–73, 1937.
- [5] N. F. Mott, *The Basis of the Electron Theory of Metals, with Special Reference to the Transition Metals*, *Proc. Phys. Society (London)*, vol. A62, pp. 416, 1949.
- [6] J. H. Van Vleck, *Models of Exchange Coupling in Ferromagnetic Media*, *Rev. Mod. Phys.*, vol. 25, pp. 220, 1953.
- [7] J. Friedel, *On Some Electrical and Magnetic Properties of Magnetic Solid Solutions*, *Can. J. Phys.*, vol. 34, pp. 1190, 1956.
- [8] J. Friedel, *Lecture notes on the electronic structure of alloys*, *Nuovo Cimento Suppl.*, vol. VII, pp. 287–311, 1958.
- [9] A. Blandin and J. Friedel, *J. Phys. Radium*, vol. 19, pp. 573, 1958.
- [10] D. Morandi and D. Sherrington, *Functional integral transformation of the Anderson model into the s-d exchange model*, *J. Phys. F: Met. Phys.*, vol. 4, 1974.
- [11] P. W. Anderson, *Localized Magnetic States in Metals*, *Phys. Rev.*, vol. 124, pp. 41, 1961.
- [12] A. M. Clogston, B. T. Matthias, M. Peter, H. J. Williams, E. Corenzwit, and R. C. Sherwood, *Phys. Rev. B*, vol. 125, pp. 541, 1962.
- [13] Leo Kouwenhoven and Leonid Glazman, *The revival of the Kondo effect*, *Physics World*, vol. 14, pp. 33–38, 2001.
- [14] T. E. Kopley, P. L. McEuen, and R. G. Wheeler, *Resonant Tunneling through Single Electronic States and Its Suppression in a Magnetic Field*, *Phys. Rev. Lett.*, vol. 61, no. 14, pp. 1654–1657, Oct 1988.
- [15] H. Grabert and M. H. Devoret, *Single Charge Tunneling Coulomb Blockade Phenomena in Nanostructures*, Plenum, New York, 1992.
- [16] L. P. Kouwenhoven, T. H. Oosterkamp, M. W. S. Danoesastro, M. Eto, D. G. Austing, T. Honda, and S. Tarucha, *Excitation Spectra of Circular, Few-Electron Quantum Dot*, *Science*, vol. 5, pp. 1788–1792, 1997.
- [17] J. Kondo, *g-Shift and Anomalous Hall Effect in Gadolinium Metals*, *Prog. Theor. Phys.*, vol. 28, pp. 846, 1962.
- [18] G. Stewart, *“Heavy-fermion systems”*, *Rev. Mod. Phys.*, vol. 56, pp. 755, 1984.
- [19] F. D and M. Haldane, *Scaling Theory of the Asymmetric Anderson Model*, *Phys. Rev. Lett.*, vol. 40, pp. 416, 1978.

-
- [20] P. B. Wiegmann, *Towards an exact solution of the Anderson model*, *Phys. Lett.*, vol. 80A, pp. 163, 1980.
 - [21] N. Kawakami and A. Okiji, *Exact expression of the ground-state energy for the symmetric anderson model*, *Phys. Lett.*, vol. 86A, pp. 483, 1981.
 - [22] A. Okiji and N. Kawakami, *Thermodynamic Properties of the Anderson Model*, *Phys. Rev. Lett*, vol. 50, pp. 1157, 1983.
 - [23] A. A. Abrikosov, *Electron scattering on magnetic impurities in metals and anomalous resistivity effects*, *Physics*, vol. 2, pp. 5, 1965.
 - [24] H. Suhl, *Formation of Local Magnetic Moments in Metals*, *Phys. Rev.*, vol. 38A, pp. 515, 1965.
 - [25] J.W. Allen, S.J. Oh, O. Gunnarsson, K. Schönhammer, M.B. Maple, M.S. Torikachvili, and I. Lindau, *Electronic structure of cerium and light rare-earth intermetallics*, *Advances in Physics*, vol. 35, pp. 275, 1986.
 - [26] J. W. Allen, S. J. Oh, M. B. Maple, and M. S. Torikachvili, *Large Fermi-level resonance in the electron-addition spectrum of $CeRu_2$ and $CeIr_2$* , *Phys. Rev.*, vol. 28, pp. 5347, 1983.
 - [27] D. Langreth, *Friedel Sum Rule for Anderson's Model of Localized Impurity States*, *Phys. Rev.*, vol. 150, pp. 516, 1966.
 - [28] J. S. Langer and V. Ambegaokar, *Friedel Sum Rule for a System of Interacting Electrons*, *Phys. Rev.*, vol. 121, pp. 1090, 1961.
 - [29] J. W. Allen, S. J. Oh, L. E. Cox, W. P. Ellis, S. Wire, Z. Fisk, J. L. Smith, B. B. Pate, I. Lindau, and J. Arko, *Spectroscopic Evidence for the 5f Coulomb Interaction in UAl_2 and UPt_3* , *Phys. Rev. Lett.*, vol. 2635, pp. 54, 1985.
 - [30] L. Z. Liu, J. W. Allen, C. L. Seaman, M. B. Maple, Y. Dalichaouch, J. S. Kang, M. S. Torikachvili, and M. A. Lopez de laTorre, *Kondo resonance in $Y_{1-x}U_xPd_3$* , *Phys. Rev. Lett*, vol. 68, pp. 1034, 1992.
 - [31] P. W. Anderson and G. Yuval, *Exact Results in the Kondo Problem: Equivalence to a Classical One-Dimensional Coulomb Gas*, *Phys. Rev. Lett.*, vol. 45, pp. 370, 1969.
 - [32] P. W. Anderson, *Kondo Effect IV: Out of the Wilderness*, *Comm. S. St. Phys.*, vol. 5, pp. 73, 1973.
 - [33] K. G. Wilson, *The renormalization group: Critical phenomena and the Kondo problem*, *Rev. Mod. Phys.*, vol. 47, pp. 773, 1975.
 - [34] P. Nozières, *A "Fermi Liquid" Description of the Kondo Problem at Low Tempertures*, *Journal de Physique C*, vol. 37, pp. 1, 1976.
 - [35] J. Hubbard, *Electron Correlations in Narrow Energy Bands. II. The Degenerate Band Case*, *Proc. R. Soc. London, Ser. A.*, vol. 277, pp. 237, 1964.
 - [36] J. R. Schrieffer and P. Wolff, *Relation between the Anderson and Kondo Hamiltonians*, *Phys. Rev.*, vol. 149, pp. 491, 1966.
 - [37] B. Coqblin and J. R. Schrieffer, *Exchange Interaction in Alloys with Cerium Impurities*, *Phys. Rev.*, vol. 185, pp. 847, 1969.
 - [38] P. W. Anderson and G. Yuval, *Exact Results for the Kondo Problem: One-Body Theory and Extension to Finite Temperature*, *Phys. Rev. B*, vol. 1, pp. 1522, 1970.
 - [39] P. W. Anderson and G. Yuval, *Some numerical results on the Kondo problem and the inverse square one-dimensional Ising model*, *J. Phys. C*, vol. 4, pp. 607, 1971.
 - [40] P. W. Anderson, *Poor Man's derivaton of scaling laws for the Kondo problem*, *J. Phys. C*, vol. 3, pp. 2346, 1970.
 - [41] V N Popov and S A Fedotov, *The functional-integration method and diagram technique for soub ststems*, *Zh. Eksp. Teor. Fiz.*, vol. 94, 1988.

- [42] M. Sarachik, E. Corenzwit, and L. D. Longinotti, *Resistivity of Mo-Nb and Mo-Re Alloys Containing 1% Fe*, *Phys Rev.*, vol. 135, pp. A1041, 1964.
- [43] Robert H. White and Theodore H. Geballe, "Long range order in solids", in *Solid State Physics*, H. Ehrenreich, F. Seitz, and D. Turnbull, Eds., New York, 1979, vol. 15, p. 283, Academic Press.
- [44] S. M. Cronenwett, T. H. Oosterkamp, and L. P. Kouwenhoven, *A tunable Kondo effect in Quantum Dots*, *Science*, vol. 281, pp. 540, 1998.
- [45] W. G. van der Wiel, S. De Franceschi, T. Fujisawa, J. M. Elzerman, S. Tarucha, and L. P. Kouwenhoven, *The Kondo Effect in the Unitary Limit*, *Science*, vol. 289, pp. 2105, 2000.
- [46] F. T. Hedgcock and C. Rizzuto, *Influence of Magnetic Ordering on the Low-Temperature Electrical Resistance of Dilute Cd-Mn and Zn-Mn Alloys*, *Phys. Rev.*, vol. 517, pp. 163, 1963.